Title

Theoretical estimates of equilibrium sulfur isotope effects in aqueous sulfur systems: Highlighting the role of isomers in the sulfite and sulfoxylate systems

Authors

Eldridge, DL
Guo, W
Farquhar, J

Publication Date

2016-12-01

DOI

10.1016/j.gca.2016.09.021

Peer reviewed

Theoretical estimates of equilibrium sulfur isotope effects in aqueous sulfur systems: Highlighting the role of isomers in the sulfite and sulfoxylate systems

Author links open overlay panel D.L.Eldridge[a] W.Guo[b] J.Farquhar[a]
Show more

https://doi.org/10.1016/j.gca.2016.09.021 Get rights and content

Abstract

We present theoretical calculations for all three isotope ratios of sulfur ($^{33}S/^{32}S$, $^{34}S/^{32}S$, $^{36}S/^{32}S$) at the B3LYP/6-31+G(d,p) level of theory for aqueous sulfur compounds modeled in 30–40H_2O clusters spanning the range of sulfur oxidation state (S^n, n = −2 to +6) for estimating equilibrium fractionation factors in aqueous systems. Computed $^{34}\beta$ values based on major isotope ($^{34}S/^{32}S$) reduced partition function ratios (RPFRs) scale to a first order with sulfur oxidation state and coordination, where $^{34}\beta$ generally increase with higher oxidation state and increasing coordination of the sulfur atom. Exponents defining mass dependent relationships based on β values ($^{x/34}\kappa = \ln(^{x}\beta)/\ln(^{34}\beta)$, x = 33 or 36) conform to tight ranges over a wide range of temperature for all aqueous compounds ($^{33/34}\kappa \approx 0.5148$–$0.5159$, $^{36/34}\kappa \approx 1.89$–$1.90$ from $T \geqslant 0$ °C). The exponents converge near a singular value for all compounds at the high temperature limit ($^{33/34}\kappa_{T\rightarrow\infty} = 0.51587 \pm 0.00003$ and $^{36/34}\kappa_{T\rightarrow\infty} = 1.8905 \pm 0.0002$; 1 s.d. of all computed compounds), and typically follow trends based on oxidation state and coordination similar to those seen in $^{34}\beta$ values at lower temperatures. Theoretical equilibrium fractionation factors computed from these β-values are compared to experimental constraints for $HSO_3^-{}_{T(aq)}/SO_{2(g,\,aq)}$, $SO_{2(aq)}/SO_{2(g)}$, $H_2S_{(aq)}/H_2S_{(g)}$, $H_2S_{(aq)}/HS^-_{(aq)}$, $SO_4^{2-}{}_{(aq)}/H_2S_{T(aq)}$, $S_2O_3^{2-}{}_{(aq)}$ (intramolecular), and $S_2O_3^{2-}{}_{(aq)}/H_2S_{T(aq)}$, and generally agree within a reasonable estimation of uncertainties. We make predictions of fractionation factors where other constraints are unavailable. Isotope partitioning of the isomers of protonated compounds in the sulfite and sulfoxylate systems depend strongly on whether protons are bound to either sulfur or oxygen atoms. The magnitude of the $HSO_3^-{}_T/SO_3^{2-}$ major isotope ($^{34}S/^{32}S$) fractionation factor is predicted to increase with temperature from 0 to 70 °C due to the combined effects of the large magnitude $(HS)O_3^-/SO_3^{2-}$ fractionation factor ($1000\ln{}^{34}\alpha_{(HS)bisulfite\text{-}sulfite} = 19.9‰$, 25 °C) relative to the $(HO)SO_2^-/SO_3^{2-}$ fractionation factor ($1000\ln{}^{34}\alpha_{(HO)bisulfite–sulfite} = -2.2‰$, 25 °C), and the increased stability of the $(HS)O_3^-$ isomer with increasing temperature. We argue that isomerization phenomenon should be considered in models of the sulfur cycle,

including models that describe the overall sulfur isotope fractionations associated with microbial metabolism (e.g., microbial sulfate reduction).

- **Previous** article in issue
- **Next** article in issue

Keywords

Sulfur isotopes
Sulfite
Bisulfite
Sulfoxylate
Isotope effects
Mass dependent
Theoretical calculations

1. Introduction

1.1. Overview

Quantum mechanical electronic structure calculations of aqueous clusters complement experimental investigations of isotope effects in aqueous systems (e.g., Rustad et al., 2008, Rustad et al., 2010, Zeebe, 2009), and have been instrumental for predicting isotope effects when experimental determinations are unavailable (e.g., Li et al., 2009, Li and Liu, 2011). Theoretical approaches are especially useful for compounds like those of the sulfite and sulfoxylate systems that contain numerous compounds that are difficult to experimentally isolate and study directly. The aim of the present study is to: (1) provide an internally consistent set of constraints for equilibrium isotope fractionations among aqueous sulfur compounds relevant to low and high temperature conditions, emphasizing the poorly documented sulfite and sulfoxylate systems; (2) provide new constraints on the exponents of mass-dependence associated with equilibrium isotope fractionation in aqueous systems and their relationships to sulfur oxidation state and bonding environment; (3) compare our theoretical constraints to the available experimental datasets and make predictions where estimates are currently unavailable, and assess where future experimental work may be needed; and (4) illustrate the effects of isomerization on isotope partitioning in the sulfite system where isomerization leads to relatively large and apparently unusual effects in observable isotope fractionation behavior.

1.2. Sulfite and sulfoxylate in the sulfur cycle

The sulfite (denoted $SO_{3}^{2-}{}_{T}$) and sulfoxylate systems (denoted $SO_{2}^{2-}{}_{T}$) are the series of inorganic compounds and oxyanions that contain sulfur in the +4 and +2 oxidation states, respectively. These oxidation states are intermediate between the most common end member sulfur oxidation states of −2 as the most reduced (e.g., $H_2S/HS^-/S^{2-}$) and +6 as the most oxidized (e.g., SO_4^{2-}). Sulfite is a well-documented intermediate in a variety of settings where sulfur is cycled, and sulfoxylate species, while very rarely observed, are inferred to be a 'missing-link' oxidation state in sulfur redox processes between zero-valent sulfur compounds (e.g., generically as S^0) and those of the sulfite system.

1.2.1. Sulfite In the sulfur cycle

Sulfite *sensu lato* in natural environments is typically transient and does not comprise a significant fraction of the bulk sulfur in Earth's surface environment but nevertheless plays essential roles in the environmental cycling of sulfur and related elemental cycles. The hydrolysis and subsequent oxidation of sulfur dioxide in atmospheric water droplets is a major pathway of acid-rain formation (e.g., Brandt and van Eldik, 1995). Sulfite is a major intermediate in both the oxidative and reductive portions of the sulfur cycle, including the microbial production and subsequent oxidation of sulfide (HS^-/H_2S; Zhang and Millero, 1993, Zopfi et al., 2004). In marine sediments containing relatively high amounts of organic matter, sulfide is generated as a byproduct of anaerobic respiration (microbial sulfate reduction; MSR) and ca. 80–95% of the sulfide produced is eventually re-oxidized through intermediates like sulfite back to sulfate (Jørgensen, 1977, Jørgensen, 1982, Jørgensen et al., 1990, Canfield and Teske, 1996, Jørgensen and Nelson, 2004). Depending on the conditions and biota present, the sulfite thus produced can support or supplement a variety of metabolisms carried out by microorganisms that oxidize, reduce, and disproportionate sulfite and other intermediate sulfur compounds for overall energy conservation and metabolic function.
At the intracellular level, sulfite (*sensu lato*) is a pivotal intermediate during microbial sulfate reduction (MSR), which in general is responsible for the oxidation of much of the organic matter contained in modern marine sediments (e.g., Bowles et al., 2014). Intracellular sulfite within a sulfate reducing microorganism sits between two reversible transformations: (1) its production via the reduction of activated sulfate (adenosine-5′-phosphosulfate; cleaving an S—O bond) and (2) its reaction with the siroheme active site of dissimilatory sulfite reductase where it is reduced to eventually form the end waste product sulfide via other enzymatically-bound intermediates like sulfoxylate (S^{2+}) and zero-valent sulfur (S^0) (Parey et al., 2010). The sulfide thus produced and its subsequent cycling in the environment places primary controls on the isotopic

composition of authigenic pyrite, which in sedimentary rocks serves as a major archive of the sulfur cycle through geologic time. Isotope network models that attempt to constrain the overall sulfur isotope fractionations that occur during the step-wise reduction of sulfate have relied on estimations of fractionation factors involving sulfite compounds (e.g., Wing and Halevy, 2014), but these fractionations have yet to be determined in detail. In particular, present network models simplify the intracellular inorganic speciation of sulfite (assuming sulfite *sensu stricto* only, SO_3^{2-}) and have yet to take into consideration the influence of bisulfite compounds (generically: HSO_3^-).

1.2.2. Sulfur isotope partitioning in the sulfite system

Despite the recognized importance of sulfite in the overall cycling of sulfur, the determination of the equilibrium isotope fractionations among various sulfite species has received very little attention. To our knowledge, only one set of experimental constraints has been reported (Eriksen, 1972a, Eriksen, 1972b, Eriksen, 1972c), suggesting a fractionation factor between bulk bisulfite in solution and gaseous SO_2 ($1000\ln^{34}\alpha_{bisulfite\text{-}SO2(g)}$) of 10.9 ± 1.4‰ (1 s.d., 10 experiments) at 25 °C (Eriksen, 1972a). No resolvable change in this fractionation factor was observed over the investigated temperature range of 25–45 °C. Fractionations among aqueous sulfite species (e.g., the bisulfite compounds and sulfite) are completely unconstrained. Given that these are the dominant species under most natural conditions as well as within sulfate reducing organisms, these fractionations are key to a detailed understanding of sulfite isotope systematics in natural systems.

1.2.3. Sulfoxylate in the sulfur cycle

Sulfoxylate species are difficult to detect and analyze and their role in the (bio)geochemical cycling of sulfur is not well understood. Hoffmann and Lim (1979) were among the first to suggest sulfoxylate as a reaction intermediate of the sulfide oxidation mechanism in a scheme of hypothetical reactions known as the polar mechanism (*cf.* Zhang and Millero, 1993). In this scheme, sulfoxylate is postulated to be among the initial products of oxidation, and a key intermediate in the formation of sulfite species and thiosulfate that are commonly observed products of the reaction (e.g., Cline and Richards, 1969, Chen and Morris, 1972, Zhang and Millero, 1993). Vairavamurthy and Zhou (1995) confirmed the presence of an S^{2+}oxyanion during sulfide oxidation via sulfur k-edge X-ray Absorbance Near Edge Structure (S-XANES) spectroscopy and attributed it to the sulfoxylate (SO_2^{2-}) structure based on Fourier Transformed Infrared (FT-IR) spectroscopic analysis. Tossell (1997) later compared the spectral observations

of Vairavamurthy and Zhou (1995) and their pH dependence with calculated vibrational frequencies of sulfoxylate compounds, and revised the species identified by Vairavamurthy and Zhou (1995) to more likely be bisulfoxylate (HSO_2^-) where the proton is bound to an oxygen atom (denoted $(HO)SO^-$). To date, the study of Vairavamurthy and Zhou (1995) appears to be the only study to directly document sulfoxylate compounds in sulfur redox processes.

Sulfur in the +2 oxidation state is a hypothesized intracellular intermediate during MSR. In recent biochemically-informed models (Oliveira et al., 2008, Parey et al., 2010, Bradley et al., 2011, Wing and Halevy, 2014, Santos et al., 2015), the reduction of sulfite at the siroheme-[4Fe-4S] catalytic site in dissimilatory sulfite reductase occurs stepwise, first producing a bound S^{2+} intermediate, then a bound S^0-intermediate before eventually forming sulfide facilitated by a mechanism involving a related protein known as DsrC (Oliveira et al., 2008, Santos et al., 2015). Reactions of these enzymatically-bound intermediate moieties (S^{2+}, S^0) via nucleophilic attack by residual non-enzymatically bound sulfite species have been hypothesized pathways for the generation of polythionates (principally trithionate, $S_3O_6^{2-}$) and thiosulfate ($S_2O_3^{2-}$) that have been observed in some MSR culture experiments (Parey et al., 2010). If the hypothesized S^{2+} intermediates detach from the catalytic site and form free aqueous species, they are likely to be included within the sulfoxylate system. The speciation and isotope partitioning behavior of inorganic sulfoxylate compounds in intracellular media may play additional roles in the distribution of sulfur isotopes within the MSR framework, and remains to be investigated in detail.

2. Background: aqueous sulfur speciation

2.1. Sulfite system chemistry

Sulfite species are distributed in solution as a continuum that depends on pH, temperature, ionic strength (μ), and total S(IV) concentration (see Fig. 1). A summary of select equilibrium quotients related to sulfite speciation is included in Table S.1. At $\mu \sim 0$ *m* and 25 °C, dissolved SO_2 dominates sulfite solutions under extremely acidic conditions (pH < 1.9), bisulfite compounds dominate at 1.9 < pH < 7.2, and sulfite *sensu stricto* at pH > 7.2 (Martell and Smith, 1982, Beyad et al., 2014). The hypothetical sulfurous acid (two generic groups of isomers: $SO(OH)_2$ and $(HS)O_2OH$; collectively H_2SO_3) may be intermediary in the hydrolysisof SO_2 to form bisulfite anions, but has never been detected in solution (Gerding and Nijveld, 1936, Falk and Giguere, 1958, Zhang and Ewing, 2002, Voegele et al., 2004). Sulfurous acid (and related isomers) is therefore unlikely to be a significant component of the mass balance.

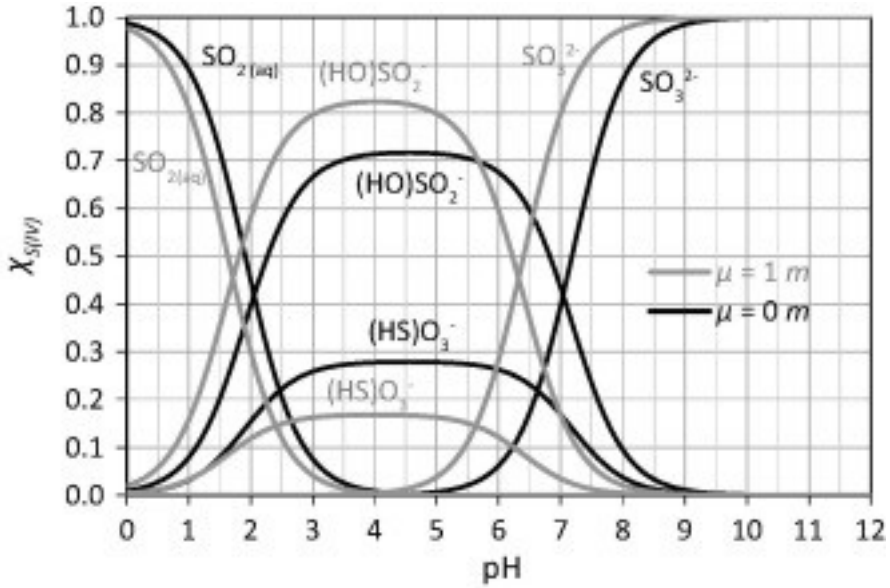

1. Download high-res image (197KB)
2. Download full-size image

Fig. 1. Mole fraction of sulfite species ($\chi_{S(IV)}$) as a function of pH at 25 °C, highlighting the isomers of bisulfite (not including bisulfite dimers for simplicity; $[S^{4+}]_T$ < ~ 0.1 M). The solid black curves are computed using dissociation and isomerization quotients determined at an ionic strength of zero (Damian Martell and Smith, 1982, Risberg et al., 2007, Beyad et al., 2014) and the gray curves at an ionic strength of 1 *m* (Horner and Connick, 1986, Millero et al., 1989).

Bisulfite exists in two isomeric forms: one tetrahedral form where the proton is bound to the sulfur—denoted herein as $(HS)O_3^-$—and another that is pyramidal where the proton is bound to one of the oxygen atoms—denoted herein as $(HO)SO_2^-$ (Golding, 1960 and references therein; Connick et al., 1982, Horner and Connick, 1986, Littlejohn et al., 1992, Risberg et al., 2007). The relative proportions of the bisulfite isomers in solution is given by the isomerization quotient (Q_i), defined as:

(1)(HS)O3-⇄(HO)SO2-Qi=[(HO)SO2-][(HS)O3-]

where brackets "[ ]" denote concentrations. Studies utilizing ^{17}O-NMR, IR-Raman, and sulfurk-edge XANES spectroscopy have shown that the OH-bonded pyramidal isomer of bisulfite is the dominant form in solution at low temperature, comprising ~72–84% of bisulfite at 25 °C depending on ionic strength (see Fig. 1; Horner and Connick, 1986, Littlejohn et al., 1992, Risberg et al., 2007).

The relative proportion of the bisulfite isomers is temperature-dependent, and the proportion of the HS-bonded isomer increases with increasing temperature (Horner and Connick, 1986, Littlejohn et al., 1992, Risberg et al., 2007). Horner and Connick (1986) and Littlejohn et al. (1992) determined the quotient in a medium of relatively high

ionic strength (μ = 1 *m*) over a total temperature range of 2–67 °C, from which the following temperature dependence is obtained (Fig. 2):

(2)ln(Qi)=1413(±119)T-3.1(±0.4)(T=275-340K;μ=1m)

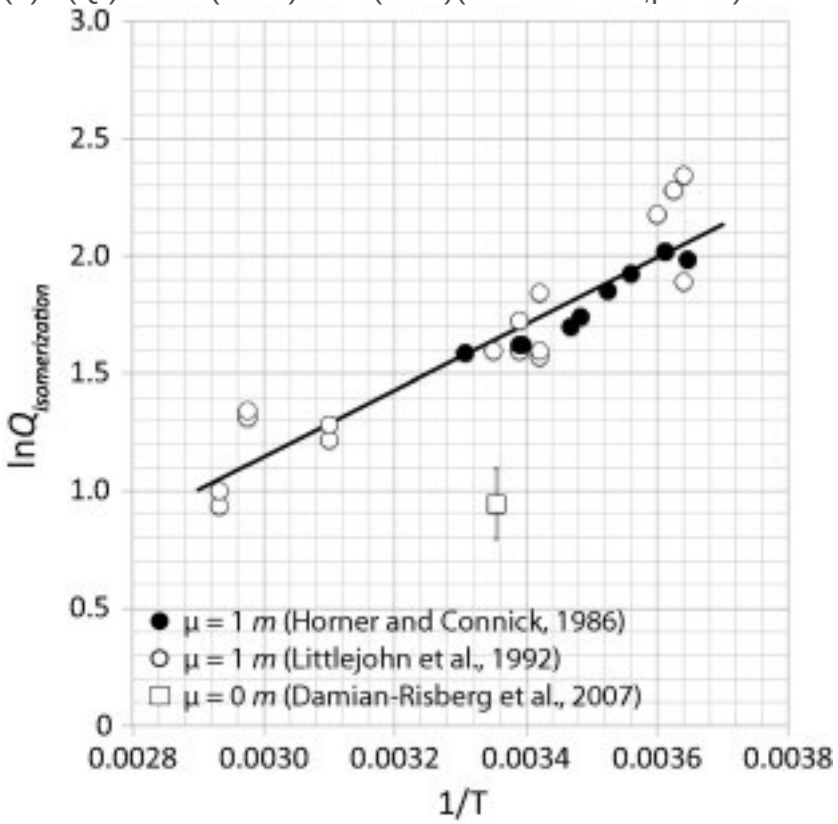

1. Download high-res image (192KB)
2. Download full-size image

Fig. 2. Experimental constraints on the bisulfite isomerization quotient as a function of temperature, defined as Q_i = [(HO)SO_2^-]/[(HS)O_3^-]. The μ = 1 *m* constraints are from Horner and Connick (1986)(black circles) and Littlejohn et al. (1992) (white circles), and the μ = 0 *m* constraint is from Risberg et al. (2007) (white square). The least-squares linear regression of the 1 *m* constraints yields: lnQ_i = 1413(±119)/T – 3.1(±0.4) (valid over ≈ 0–67 °C).

The isomerization quotient may be a strong function of ionic strength as indicated by the much lower Q_i more recently determined in a low-ionic strength medium at 25 °C (*cf.*Risberg et al., 2007; Fig. 1, Fig. 2, Table S.1). This suggests that application of the quotients of Horner and Connick (1986) and Littlejohn et al. (1992) to solutions of lower ionic strength may significantly underestimate the amount of (HS)O_3^- present in solution. However, the exact effect of ionic strength on the isomerization quotient is yet to be quantified over a wide range of temperatures relevant to many natural systems.

Bisulfite can also form dimers in solution (*cf.* Golding, 1960). The principle dimer of bisulfite is $S_2O_5^{2-}$ known as pyrosulfite or disulfite, whose structure can be schematically illustrated as: $(O_2S\text{-}SO_3)^{2-}$ (note, however, that an aqueous form with a bridging oxygen —$(O_2S\text{-}O\text{-}SO_2)^{2-}$—remains to be ruled out in solution; *cf.* Williamson and Rimstidt, 1992). The extent of dimerization varies as a function of the total bisulfite concentration and is quantified as the dimerization quotient (Q_d):
(3)2HSO3T-⇄S2O52-+H2OQd=[S2O52-][HSO3T-]2(M-1)
Studies directed at quantifying the dimerization quotient have produced varied results (see Table S.1). Some of the discrepancies may have arisen from a variety of experimental errors in the earliest determinations (see discussion in Connick et al., 1982). The existing experimental datasets indicate that total bisulfite has to reach concentrations on the order of ⩾0.1 M in order for significant conversion to the dimer to occur. For example, the dimer comprises ⩽1% of total bisulfite at $[HSO_3^-]_T$ ⩽0.12 M at μ = 1 *m* and ⩽1% of total bisulfite at $[HSO_3^-]_T$ ⩽~0.29 M at μ = 0 (using the quotients of Connick et al., 1982). Recently, Beyad et al. (2014) found evidence for a protonated dimer ($HS_2O_5^-$) via UV-spectrophotometric titrations and quantified its dissociation quotient (Table S.1).

2.2. Sulfoxylate system chemistry

The sulfoxylate system comprises aqueous sulfur compounds and oxyanions in the 2+ oxidation state (S^{2+}), including compounds of the general compositions: H_2SO_2, HSO_2^-, and SO_2^{2-}. Makarov et al. (2010) is among the few studies to report the acid dissociation quotients of H_2SO_2: H_2SO_2 dominates at pH < 7.97, bisulfoxylate species (HSO_2^-) from 7.97 < pH < 13.55, and sulfoxylate (SO_2^{2-}) at pH > 13.55 (*T* = 25 °C, μ = 0.1 *m*; Makarov et al., 2010). Electronic structure calculations have shown that the lowest energy configurations of H_2SO_2 in vacuum are rotamers of sulfoxylic acid (denoted $S(OH)_2$), where the protons are bound to each of the oxygen atoms and differ structurally in the relative orientation of the O⎯H bonds (Steiger and Steudel, 1992, Tossell, 1997, Napolion et al., 2008, Crabtree et al., 2013). Other isomers of H_2SO_2 of potential significance are those termed sulfinic acid, where one proton is bound to the sulfur atom and the other to one of the oxygen atoms (denoted: $(HS)O_2H$). The relative stabilities of these isomers in solution are not constrained, nor are the isomers of bisulfoxylate: $(HS)O_2^-$ and $(HO)SO^-$. Sulfur monoxide (SO) would be the hypothetical unhydrolyzed component of the system (analogous to SO_2 in the sulfite system), but it is extremely unstable and not known to undergo hydrolysis to form H_2SO_2(Lyons and Nickless,

1968 and references therein). Sulfur monoxide will not be considered a component of this system in this study.

2.3. Aqueous sulfide, thiosulfate, and sulfate

Aqueous sulfide compounds (H_2S, HS^-, and S^{2-}) and sulfate (SO_4^{2-}) represent the lowest and highest oxidation states of sulfur (−2 and +6, respectively), and are the most abundant forms of sulfur in natural systems, either in aqueous or mineral form. Thiosulfate ($S_2O_3^{2-}$) is also a relatively common mixed-valence intermediate in sulfur cycling processes (e.g., Jørgensen, 1990, Jørgensen and Nelson, 2004, Zopfi et al., 2004).

The first acid dissociation quotient of H_2S is very close to neutral pH at 25 °C and μ = 0 *m*($H_2S \rightleftharpoons HS^- + H^+$, pQ_{d1} = 6.98; Hershey et al., 1988). In the range of ca. 100–350 °C, pQ_{d1}increases with increasing temperature (e.g., at 300 °C, $pQ_{d1} \approx 8.2$; Ellis and Giggenbach, 1971, Ohmoto and Lasaga, 1982). The second acid dissociation quotient ($HS^- \rightleftharpoons S^{2-} + H^+$, pQ_{d2}) is not as well constrained, but likely to be on the order of $pQ_{d2} \approx 17–18$ at 25 °C (Ellis and Giggenbach, 1971, Schoonen and Barnes, 1988, Migdisov et al., 2002). Thus, S^{2-} may only comprise an appreciable component of aqueous sulfide speciation in highly alkaline solutions possibly at high temperature (Ellis and Giggenbach, 1971). Under the conditions of most natural systems, aqueous sulfide is therefore predominately in the form of H_2S or HS^-(and any ion pairs, e.g., $NaSH^0$).

Sulfuric acid (H_2SO_4) is a very strong acid and the doubly protonated form generally does not form an appreciable component of the mass balance of sulfate solutions at low temperature but may become a significant species in low pH solutions at high temperature (*cf.*Ohmoto and Lasaga, 1982 and references therein). The second acid dissociation quotient for sulfuric acid ($HSO_4^- \rightleftharpoons SO_4^{2-} + H^+$) is pQ_{d2} = 1.99 ± 0.01 at 25 °C and μ = 0 *m*(Martell and Smith, 1982) but has values as high as 6.4 at 350 °C (*cf.*Ohmoto and Lasaga, 1982 and references therein).

Thiosulfate ($S_2O_3^{2-}$, schematically: S-SO_3^{2-}) contains two sulfur atoms: one outer (“sulfanyl”) sulfur in a -1 oxidation state and another inner (“sulfonate”) sulfur in a +5 oxidation state that is four-fold coordinated with the sulfanyl sulfur and three oxygen atoms (Vairavamurthy et al., 1993). There are many hypothetical forms of protonated thiosulfate: isomeric forms of $HS_2O_3^-$ (e.g., $(HS)SO_3^-$, $S_2O_2OH^-$) and isomeric forms of $H_2S_2O_3$ (e.g., $(HS)SO_2(OH)$ and $S_2O(OH)_2$) (Steudel and Steudel, 2009). Anhydrous forms of $H_2S_2O_3$have been reported in syntheses as well as solid forms of $HS_2O_3^-$ ($[NH_4][HS_2O_3]$) (Steudel and Prenzel, 1989 and references therein) but protonated forms in the aqueous phase are unstable, and have never been directly detected in solution via

spectroscopic techniques (e.g., Steudel and Prenzel, 1989, Steudel and Steudel, 2009). Acid dissociation quotients for $H_2S_2O_3$ have been reported: $pQ_{d1} \approx 0.6$ and $pQ_{d2} = 1.6 \pm 0.1$ at 25 °C and $\mu = 0$ *m* (Martell and Smith, 1982), and these pQ_d values may increase with increasing temperature over hydrothermal ranges (*cf.* Ohmoto and Lasaga, 1982 and references therein).

3. Methods

3.1. Overview: the Bigeleisen and Mayer equation

Theoretical calculations of equilibrium fractionation factors use the principles of quantum mechanics to calculate the ground-state harmonic vibrational frequencies of molecules for use in the Bigeleisen and Mayer equation (BM-equation), also referred to as the reduced partition function ratio (RPFR; Bigeleisen and Mayer, 1947, Urey, 1947). These techniques have been widely applied since the original derivation of the BM-equation and many extensive reviews cover this approach in detail (e.g., Urey, 1947, Richet et al., 1977, Chacko et al., 2001, Wolfsberg et al., 2010, Liu et al., 2010). The BM-equation or RPFR is given by:

(4)RPFR=ss∗∏ilui∗e-ui∗/2(1-e-ui)uie-ui/2(1-e-ui∗)

where $*$ denotes terms related to the isotopically substituted molecule, s is the symmetry number, and $u_i = hc\omega_i/kT$, where: k is the Boltzmann constant, h is the Planck constant, c is the speed of light, T is temperature, and ω_i is the wave number for harmonic vibrational mode i (note vibrational frequency $\nu_i = c\omega_i$) and the product is over all harmonic vibrational modes (number of modes equal to $l = 3n - 6$ for a non-linear molecule and $l = 3n - 5$ for a linear molecule, where n is the number of atoms in the molecule). In many cases, isotopic substitution does not change the symmetry of the isotopologue and the quantity s/s^* is unity, leaving the RPFR in terms of harmonic vibrational frequencies. In all cases, symmetry numbers do not influence isotope partitioning and merely represent the relative probabilities of forming asymmetric vs. symmetric molecules (Bigeleisen and Mayer, 1947).

RPFRs can be directly related to the commonly employed β-values for computing equilibrium fractionation factors among compounds, where β-factors represent an equilibrium fractionation factor between a compound (e.g., VY_n, where V and Y are generic elements) and an ideal monoatomic gaseous reference (e.g., Y) (Richet et al., 1977). In our study, we focus on the computation of RPFRs for singly substituted isotopologues such that β = RPFR when excess factors are ignored (for a more detailed discussion of the relationship between β and RPFR, see: Richet et al., 1977, Liu et al., 2010, Cao and Liu, 2011, Cao and Liu, 2012). Equilibrium fractionation factors (denoted

α) in this study are computed between two compounds based on singly substituted isotopologues by taking the ratio of their respective β-values: ${}^{x}\alpha_{A\text{-}B} = {}^{x}\beta_{A}/{}^{x}\beta_{B}$, where x = 33, 34, or 36.

3.2. Exponents defining mass-dependence relationships

The mass dependence of an isotope effect relating a minor isotope fractionation factor and the major isotope fractionation factor is given generally by an exponential relationship (*cf.* Craig, 1957, Matsuhisa et al., 1978, Clayton and Mayeda, 1996, Miller, 2002), which yields the following for the sulfur isotope system under the condition of equilibrium:

(5)$33/34\theta = \ln(33\alpha A\text{-}B)\ln(34\alpha A\text{-}B)$

(6)$36/34\theta = \ln(36\alpha A\text{-}B)\ln(34\alpha A\text{-}B)$

The exponent is referred to as "θ" when computed from equilibrium fractionation factors between two substances (here, compound "A" and compound "B"). Generally speaking, the capital delta values commonly employed in multiple sulfur isotope studies ($\Delta^{33}S$ and $\Delta^{36}S$) are defined from such exponential relationships as deviations from a reference exponent (e.g., $\Delta^{33}S_{A\text{-}B} = {}^{33}\alpha_{A\text{-}B} - ({}^{34}\alpha_{A\text{-}B})^{0.515}$ and $\Delta^{36}S_{A\text{-}B} = {}^{36}\alpha_{A\text{-}B} - ({}^{34}\alpha_{A\text{-}B})^{1.9}$), where the reference exponents are intended to represent the approximate relationship of mass dependence for typical equilibrium isotope exchange reactions at lower temperature (i.e., well below the high temperature limit). Similar exponential relationships can be applied to β-values. Following Cao and Liu (2011), we adopt the kappa ("κ") notation to describe these relationships: ${}^{33/34}\kappa = \ln({}^{33}\beta)/\ln({}^{34}\beta)$ and ${}^{36/34}\kappa = \ln({}^{36}\beta)/\ln({}^{34}\beta)$. Analogous to the definition of β-values, κ-values describe the equilibrium exponent of mass dependence between a compound of interest and an ideal gaseous monoatomic reference (Cao and Liu, 2011).

3.3. Quantum mechanical software: Gaussian 09

We use Gaussian 09 software (Frisch et al., 2010) at the B3LYP/6-31+G(d,p) level of theory and basis set in this study to compute harmonic vibrational frequencies for use in the B–M equation. The B3LYP method is a hybrid HF/B-LYP theoretical approach (employing the Becke and Lee, Yang, & Parr 3-parameter gradient-corrected correlational functional; Lee et al., 1988, Becke, 1993, Foresman and Frisch, 1996) that includes electron correlation. The basis set is the double-zeta Pople basis set (6-31G) with diffuse functions added (+) to the non-hydrogen atoms (often required for modeling anions) and polarization functions (p functions for all atoms, d functions for all non-hydrogen atoms) for additional flexibility in the computation of molecular orbitals. Overall

it is an approach of low/moderate computational complexity and accuracy, chosen for reasons of practicality given the relatively large molecular clusters modeled in this study.

3.4. Explicit solvation model

Optimization and frequency calculations were carried out with the sulfur molecules of interest explicitly coordinated with water molecules in clusters containing up to 30–40H_2O to approximate the effects of solvation on molecular vibrations. The construction of molecular clusters involved the gradual addition of water molecules to sulfur solutes in an iterative series of optimization calculations at lower levels of theory utilizing GaussView 5.0.9 and Gaussian 09 software (Frisch et al., 2010). First, the sulfur molecules of interest were coordinated with ca. 12–15 water molecules and optimized at relatively low levels of theory and basis set (B3LYP/6-31G(d)). Following these initial optimization calculations, 2–5 water molecules were manually added to these clusters and subsequently optimized at the same theoretical level. This procedure was then repeated in a similar sequence of 2–5H_2O-addition/optimization steps until the clusters reached a maximum size of 30–40 depending on the solute and the required solvation coverage. The coordinates from the B3LYP/6-31G(d)-level optimized geometries of the 30–40H_2O solute clusters that resulted from this step-wise cluster-building procedure were then used as the basis for the optimization and frequency calculations at the B3LYP/6-31+(d,p) level that was used for computing fractionation factors in this study. The majority of the optimization and frequency calculations were performed on a desktop computer at the University of Maryland. For some of the sulfitecalculations, coordinates from lower-level B3LYP/6-31G(d) optimizations (computed at the University of Maryland) were run at the B3LYP/6-31+G(d,p) level on the high performance computation cluster (Scylla) at the Woods Hole Oceanographic Institution.

3.5. Sources of uncertainty

Uncertainties in our theoretically estimated fractionation factors can derive from three main sources: (1) errors arising from the harmonic and other approximations used in the derivation of the Bigeleisen and Mayer equation (requiring higher-order corrections, e.g., for anharmonicity), (2) inadequacies in the quantum mechanical theoretical method used to model the molecular system (i.e., choice of theoretical method and basis set size), and (3) variability arising from the water cluster geometry. All β-values and fractionation factors in this study are reported in the harmonic approximation due to the inability to apply appropriate anharmonic corrections to our cluster calculations at this time. We compute the anharmonic corrections to the ZPE (AnZPE) for a handful of

gaseous sulfur molecules (H_2S, $S(OH)_2$, $(HS)O_2H$, SO_2, SO_3) at the B3LYP/6-31+G(d,p) level to gain insight into the magnitude of these corrections for more complex systems (Section 5.1). We have additionally chosen not to apply any scaling factors (harmonic or otherwise) to our harmonic frequencies due to the potential issues associated with this practice (Section 5.1), but we do discuss the effects of harmonic scaling derived from high level gas phase calculations (CCSD/aug-cc-pVTZ) on fractionation factors for individual systems to evaluate error arising from the chosen theoretical method and basis set (following the approach of Li and Liu, 2011) (Section 5.4). Unless otherwise noted, all plotted and tabulated β-values and fractionation factors utilize un-scaled harmonic frequencies at the B3LYP/6-31+G(d,p) level. We provide harmonic vibrational frequencies for all computed clusters and compounds in a supplementary data file such that any user can scale the frequencies in specific applications. To evaluate variability associated with cluster geometry, we performed a series of at least duplicate constructions and optimizations of water clusters for a select set of 30–40H_2O clusters in the sulfite system: SO_3^{2-}, $(HS)O_3^-$, $(HO)SO_2^-$, and the bisulfite dimer, $S_2O_5^{2-}$, following the approach outlined in Section 3.4. Uncertainties derived from the above sources are discussed in more detail in Section 5.1.

4. Results

Optimized geometries of the 30–34H_2O molecular clusters of compounds in the sulfite, sulfoxylate, and other systems (sulfide, thiosulfate, sulfate) are presented in Fig. 3, Fig. 4, and Fig. 5, respectively. These geometric parameters are also provided in Table S.2.

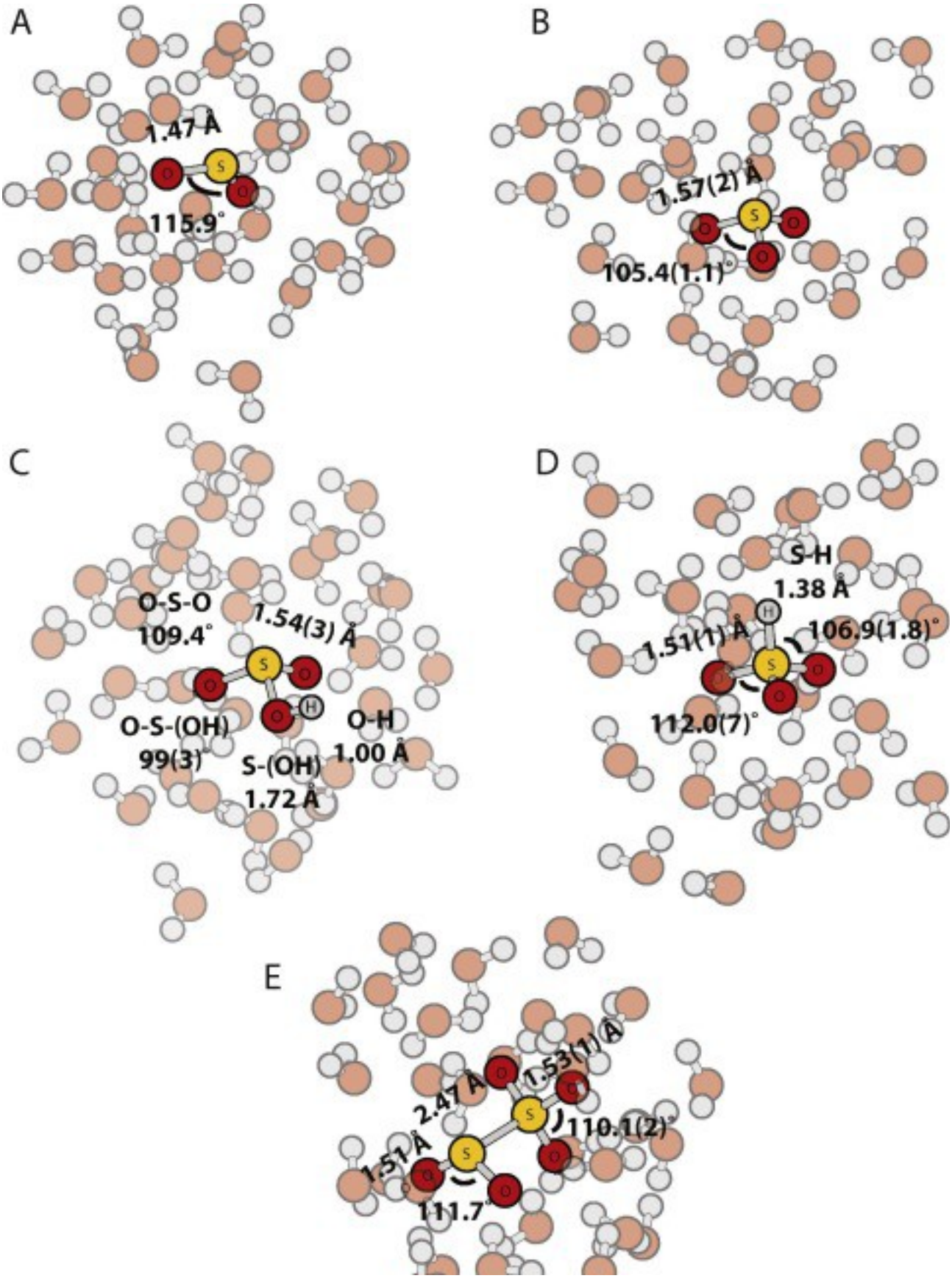
A
1.47 Å
115.9°
B
1.57(2) Å
105.4(1.1)°
C
O-S-O
109.4°
1.54(3) Å
O-S-(OH)
99(3)°
S-(OH)
1.72 Å
O-H
1.00 Å
D
S-H
1.38 Å
1.51(1) Å
106.9(1.8)°
112.0(7)°
E
2.47 Å
1.53(1) Å
110.1(2)°
1.51 Å
111.7°

1. Download high-res image (701KB)
2. Download full-size image

Fig. 3. Optimized geometries of sulfite species in $30H_2O$–$34H_2O$ clusters. (A) Sulfur dioxide($SO_{2(aq)}\cdot 30H_2O$), (B) sulfite *sensu stricto* ($SO_3^{2-}\cdot 30H_2O$), (C) OH isomer of bisulfite ($(HO)SO_2^-\cdot 34H_2O$), (D) HS isomer of bisulfite ($(HS)O_3^-\cdot 30H_2O$), and (E) the bisulfite dimer, disulfite ($S_2O_5^{2-}\cdot 30H_2O$) containing the shortest computed S⎯S bond length. Geometries can also be found in Table S.2.

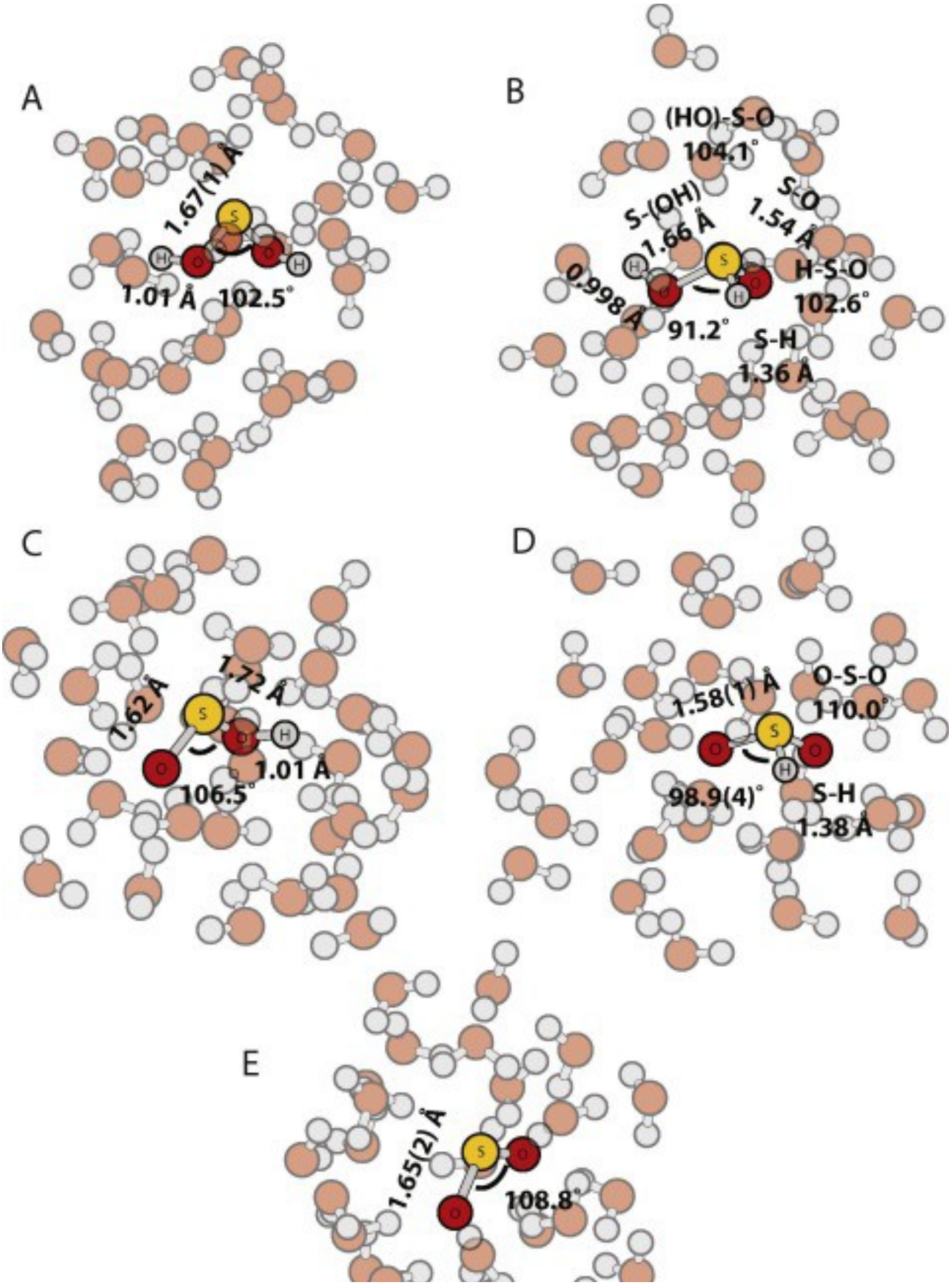
A
1.67(1) Å
1.01 Å
102.5°
B
(HO)-S-O
104.1°
S-(OH)
1.66 Å
S-O
1.54 Å
0.998 Å
91.2°
H-S-O
102.6°
S-H
1.36 Å
C
1.62 Å
1.72 Å
1.01 Å
106.5°
D
1.58(1) Å
O-S-O
110.0°
98.9(4)°
S-H
1.38 Å
E
1.65(2) Å
108.8°

1. Download high-res image (706KB)
2. Download full-size image

Fig. 4. Optimized geometries of sulfoxylate species in $30H_2O$ clusters. (A) Sulfoxylic acid ($S(OH)_2$), (B) sulfinic acid ($(HS)O_2H$), (C) OH isomer of bisulfoxylate ($(HO)SO^-$), (D) SH isomer of bisulfoxylate ($(HS)O_2^-$), and (E) sulfoxylate (SO_2^{2-}). Geometries can also be found in Table S.2.

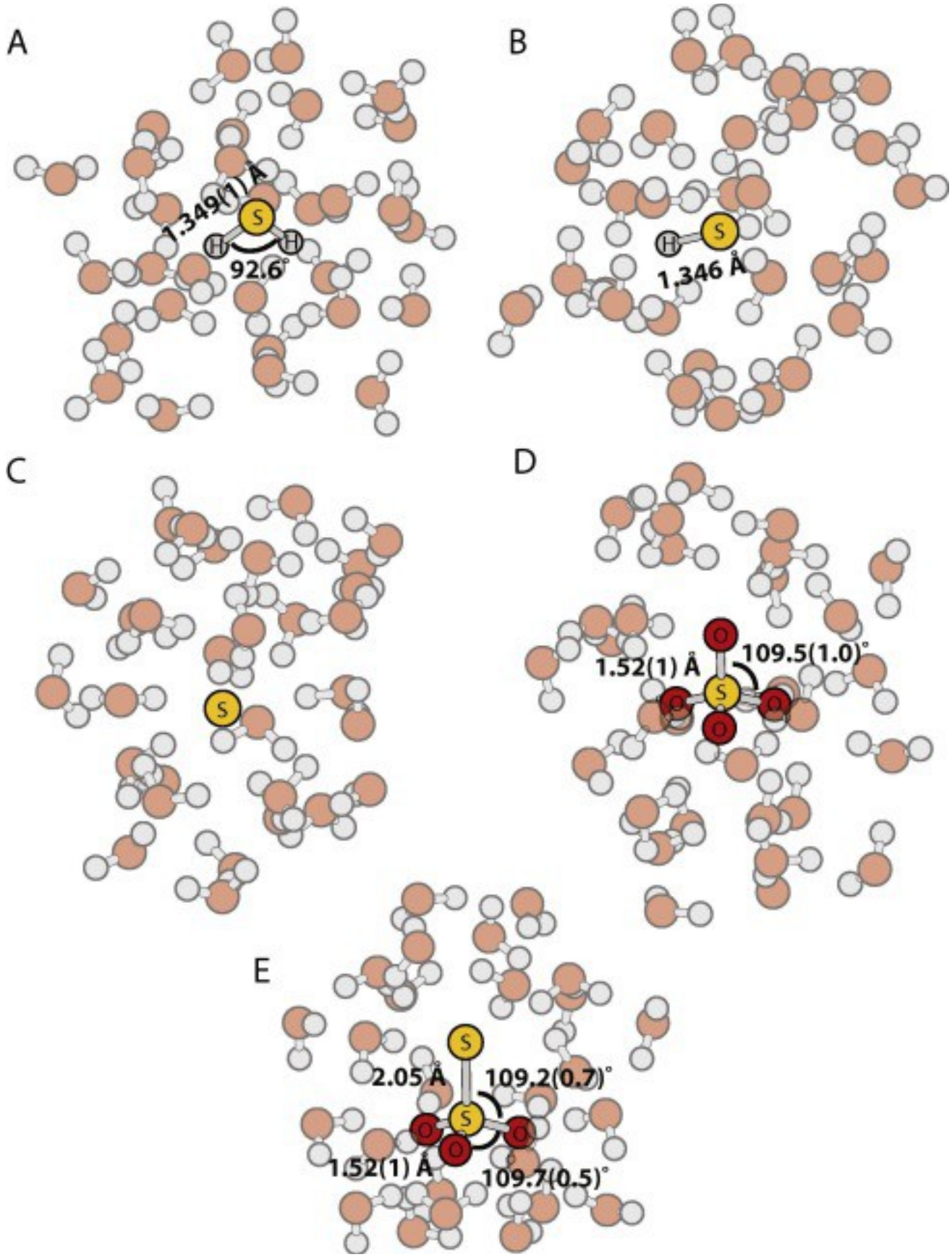
A
1.349(1) Å
92.6°
B
1.346 Å
C
D
1.52(1) Å
109.5(1.0)°
E
2.05 Å
109.2(0.7)°
1.52(1) Å
109.7(0.5)°

1. Download high-res image (660KB)
2. Download full-size image

Fig. 5. Optimized geometries of sulfide species, sulfate, and thiosulfate in 30H_2O clusters. (A) Hydrogen sulfide (H_2S), (B) bisulfide (HS^-), (C) sulfide dianion (S^{2-}), (D) sulfate (SO_4^{2-}), and (E) thiosulfate ($S_2O_3^{2-}$). Geometries can also be found in Table S.2.

4.1. $^{34}\beta$ values for aqueous sulfur compounds

The major isotope $^{34}\beta$ values calculated at the B3LYP/6-31+G(d,p) level are presented in Fig. 6 as functions of inverse absolute temperature (1000/T; 273–373 K) for aqueous cluster calculations, including the sulfite system, sulfoxylate system, sulfide system, sulfate, and thiosulfate (inner 'sulfonate' sulfur, and the outer 'sulfanyl' sulfur). A tabulation of coefficients to polynomial fits to the β values over 0–2000 °C based on all three isotope ratios of sulfur is given in Table 1 in the form of $A/T^4 + B/T^3 + C/T^2 + D/T + E$ (T in Kelvin).

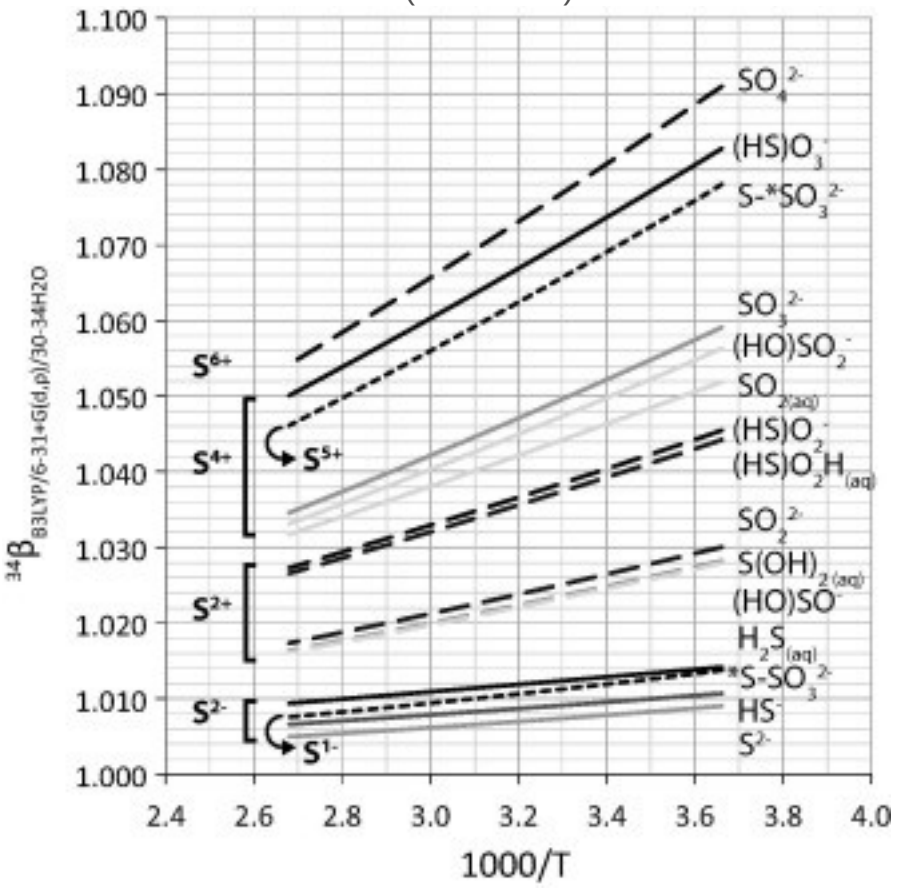

1. Download high-res image (324KB)
2. Download full-size image

Fig. 6. Computed $^{34}\beta$-values for aqueous sulfur compounds modeled in 30–34H_2O clusters at the B3LYP/6-31+G(d,p) level of theory over *T* = 0–100 °C.

Table 1. Coefficients from polynomial fits to β-values computed at the B3LYP/6-31+G(d,p) level of theory in 30–40H_2O clusters over 273.15–2273.15 K (0–2000 °C). Values are computed using the coefficients via: $^{34}\beta$ or $^{33/34}K$ or $^{36/34}K$ = $A/T^4 + B/T^3 + C/T^2 + D/T + E$, where T is in Kelvin. Extra significant figures are given to minimize rounding errors. Values for $^{33}\beta$ and $^{36}\beta$ are computed from the $^{33/34}K$ and $^{36/34}K$exponents, respectively, using: $^{33}\beta = (^{34}\beta)^{33/34K}$ and $^{36}\beta = (^{34}\beta)^{36/34K}$ at a given temperature. For the bisulfite dimer ($S_2O_5^{2-}$), the S‒‒S bond length is noted in Å and A and B refer to: $(O_2S_A\text{-}S_BO_3)^{2-}$. Note: The values of E are intercepts at the high temperature limit ($T \to \infty$) and should theoretically converge on: $^{34}\beta_{[E]} = 1$, $^{33/34}K_{[E]} = 0.51588$, and $^{36/34}K_{[E]} = 1.8904$ (Matsuhisa et al., 1978).

Compound	**nH_2O**	**$^{34}\beta$**					**$^{33/34}K$**			
		A × 10^{-5}	**B × 10^{-4}**	**C × 10^{-2}**	**D × 10^{2}**	**E**	**A × 10^{-5}**	**B × 10^{-3}**	**C × 10^{1}**	**D × 10^{3}**
SO_4^{2-}	30	590.371	−126.799	109.869	−137.516	1.000347	−30.8690	46.1900	−2194.08	48.4610
$(HS)O_3^-$ [1]	30	905.705	−147.268	105.824	−92.3176	1.000195	−36.0529	47.5396	−2038.76	40.6206
$(HS)O_3^-$ [2]	30	914.750	−148.129	106.124	−93.3723	1.000198	−37.0901	48.3512	−2051.71	35.6621
S-SO_3^{2-}(inner)	30	411.460	−96.9863	90.9001	−108.003	1.000274	−24.5634	37.7929	−1869.03	39.3817
SO_3^{2-} [1]	30	147.138	−57.1113	64.8862	−66.7662	1.000174	−12.1588	22.3335	−1256.77	5.84049
SO_3^{2-} [2]	30	131.638	−55.2533	64.0120	−65.9924	1.000172	−10.6590	21.1779	−1242.26	13.2399
$(HO)SO_2^-$[1]	34	227.691	−62.3345	63.6829	−69.8409	1.000178	−16.2693	26.2215	−1364.47	27.2021
$(HO)SO_2^-$[2]	34	243.446	−64.2295	63.9099	−72.0204	1.000184	−16.7025	26.7737	−1377.83	30.2698
$SO_{2(aq)}$	30	692.521	−108.509	71.7931	−103.029	1.000245	−48.0459	57.0980	−2177.40	55.0250
$SO_{2(g)}$	0	754.026	−114.672	71.5395	−105.747	1.000248	−55.2114	63.5980	−2337.13	44.8960
$(HS)O_2^-$	30	360.997	−67.0840	54.3488	−27.5149	1.000048	−10.6136	18.2893	−982.056	3.89045
$(HS)O_2H$	30	380.899	−66.3215	52.4857	−12.5409	1.000006	−12.2554	18.5304	−918.537	−13.8604
SO_2^{2-}	30	11.8836	−20.4170	30.3733	−24.9619	1.000066	−2.56730	9.61814	−733.960	10.4911
$S(OH)_2$	30	32.5192	−21.8550	29.2787	−26.1670	1.000068	−3.24888	10.4655	−768.717	32.7233
$(HO)SO^-$	30	19.4614	−20.0430	28.5160	−24.7943	1.000065	−3.49639	9.82567	−688.628	−6.14640
$H_2S_{(aq)}$	30	462.536	−48.3382	20.1638	77.2695	0.999749	−11.2082	8.59125	−133.040	−53.7633
S-SO_3^{2-}(outer)	30	−24.5550	−2.01175	11.3562	−2.64754	1.000007	2.58474	1.26805	−386.465	41.8080
HS^-	30	213.257	−22.4384	12.2701	42.8805	0.999864	−5.47337	3.11818	−6.41346	−53.7300
$H_2S_{(g)}$	0	470.075	−48.9645	19.2083	82.5595	0.999735	−10.7593	8.05933	−103.577	−55.2088
S^{2-}	30	2.46274	−2.30464	7.54757	−0.688045	1.000001	3.46783	−1.51862	−140.010	32.1639
$S_2O_5^{2-}$ [1A] (2.468 Å)	30	364.444	−73.0226	61.6230	−79.4550	1.000199	−26.4546	35.9415	−1591.09	34.2723
$S_2O_5^{2-}$ [1B]		380.966	−91.5445	85.5763	−103.665	1.000264	−22.1841	34.9103	−1750.48	41.3451
$S_2O_5^{2-}$ [2A] (2.505 Å)	30	397.137	−76.6766	62.5608	−82.4519	1.000205	−28.2450	38.4494	−1704.01	56.0947
$S_2O_5^{2-}$ [2B]		336.782	−85.7470	82.5440	−98.3850	1.000252	−19.6417	32.2172	−1663.53	38.7957

Compound	nH_2O	$^{34}\beta$					$^{33/34}\kappa$			
		A × 10^{-5}	**B × 10^{-4}**	**C × 10^{-2}**	**D × 10^{2}**	**E**	**A × 10^{-5}**	**B × 10^{-3}**	**C × 10^{1}**	**D × 10^{3}**
$S_2O_5^{2-}$ [3A] (2.482 Å)	31	349.189	−71.2235	60.5973	−78.5580	1.000197	−25.7908	35.3032	−1571.94	34.7375
$S_2O_5^{2-}$ [3B]		369.152	−89.9354	84.7548	−102.548	1.000262	−22.2684	34.7752	−1734.75	35.7416
$S_2O_5^{2-}$ [4A] (2.542 Å)	40	433.004	−80.4687	63.5931	−85.0203	1.000210	−30.6365	40.2622	−1719.62	44.8114
$S_2O_5^{2-}$ [4B]		316.881	−82.9536	81.0520	−95.5356	1.000245	−19.0720	31.5150	−1638.88	37.0809
Intercept (E) Average						*1.0001*				
Intercept (E) 1 s.d.						*0.0002*				

Our calculated $^{34}\beta$ values generally scale with the oxidation state of sulfur, where higher oxidation states generally have higher values than lower oxidation states, with the exception of the two sulfur atoms in thiosulfate (−1 and +5; Vairavamurthy et al., 1993). For a given temperature and oxidation state of sulfur, our calculations predict that the magnitude of the $^{34}\beta$ increases with increasing coordination of the sulfur atom. The species with the highest coordination of sulfur in each system generally have the highest $^{34}\beta$ of their respective systems, and species of lower coordination have lower $^{34}\beta$. For example, in the sulfite system, which contains the greatest diversity in bonding arrangements around sulfur of any system in this study (triatomic bent, pyramidal, and tetrahedral structures), the $^{34}\beta$ scale directly with coordination where: $^{34}\beta = (HS)O_3^- > SO_3^{2-} \approx (HO)SO_2^- > SO_{2(aq)}$. Species where protonation occurs only on the oxygen atoms (i.e., $(HO)SO_2^-$, $(HO)SO^-$, and $S(OH)_2$) typically exhibit very similar $^{34}\beta$ to their un-protonated counterparts.

The isotope partitioning behavior of the bisulfite dimer ($S_2O_5^{2-}$) warrants its own separate description due to its unusual structure; it has been omitted from Fig. 6 for simplicity of presentation and due to difficulties in constraining its structure. The bisulfite dimer contains two sulfur atoms that are coordinated differently in the molecule, where one sulfur atom (denoted “A”) is 3-fold coordinated (one S and two O) and the other sulfur atom (denoted “B”) is 4-fold coordinated (one S and three O). We optimized four independently constructed $S_2O_5^{2-}\cdot nH_2O$ clusters (two n = 30, one n = 31, and one n = 40) and found slight variability in the 4-fold coordinated site ($^{34}\beta$ = 1.0609–1.0633; 25 °C) that appears to correlate with the computed structure’s S–S bond length, where higher $^{34}\beta$ for this site corresponded to shorter S–S bond lengths (see Fig. S.1). In contrast, the 3-fold coordinated site’s computed $^{34}\beta$ was found to be much more consistent between conformers ($^{34}\beta$ = 1.0438 ± 0.0003; 25 °C; 1 s.e., all four computed conformers), and lower than any other species in the sulfite system. In all cases, the calculated S–S bond lengths for the aqueous clusters—ranging between 2.46 and

2.54 Å—are significantly longer than available experimental determinations in crystalline solids (~2.2 Å; Zachariasen, 1932). Solvation could in principle affect the bond length but we are unable to find any experimental constraints in the aqueous phase. We additionally note that the precise structure of the aqueous dimer is perhaps contentious and forms with an S⋯O⋯S linkage have yet to be ruled out (*cf.* Williamson and Rimstidt, 1992). For most discussions in this paper, we will be using the conformer with the shortest S⋯S bond length and caution that the overall $^{34}\beta$ for disulfite may be poorly constrained by our calculations due to a poorly constrained structure.

4.2. $^{33/34}\kappa$ and $^{36/34}\kappa$ values for aqueous sulfur compounds

In Fig. 7, we plot the computed $^{33/34}K = \ln(^{33}\beta)/\ln(^{34}\beta)$ and $^{36/34}K = \ln(^{36}\beta)/\ln(^{34}\beta)$ as a function of temperature for the explicitly solvated molecular water clusters and the related gaseous species, which here only includes $SO_{2(g)}$ and $H_2S_{(g)}$. The exponents converge on or near a singular value for all compounds at the high temperature limit: i.e., $^{33/34}K_{T\rightarrow\infty} = 0.51587 \pm 0.00003$ and $^{36/34}K_{T\rightarrow\infty} = 1.8905 \pm 0.0002$ (1 s.d. from averaging the intercepts of the polynomial fits; Table 1), with ranges of $^{33/34}K_{T\rightarrow\infty} = 0.51582–0.51594$ and $^{36/34}K_{T\rightarrow\infty} = 1.8903–1.8913$ (Table 1). These calculated values are in generally good agreement with the high temperature limits that have been derived based on the atomic masses of the four sulfur isotopes (*cf.* Matsuhisa et al., 1978, Young et al., 2002):

(7)1m32-1m331m32-1m34=0.51588

(8)1m32-1m361m32-1m34=1.8904

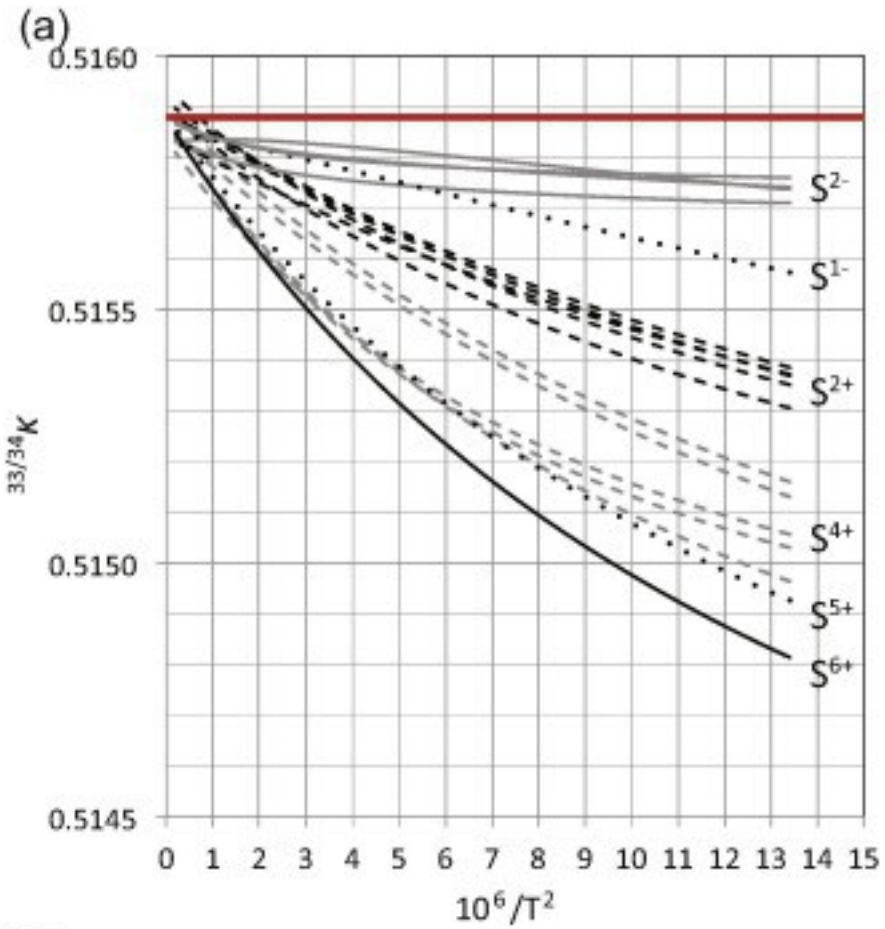
(a)
0.5160
0.5155
0.5150
0.5145
33/34K
0 1 2 3 4 5 6 7 8 9 10 11 12 13 14 15
10^6/T^2
S2-
S1-
S2+
S4+
S5+
S6+

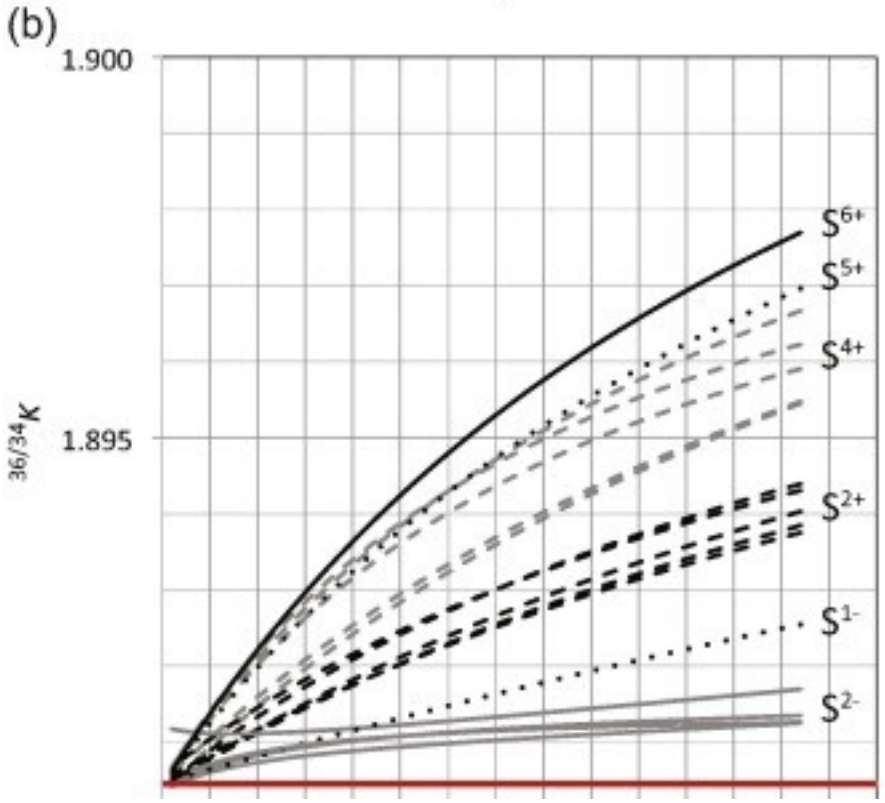
(b)
1.900
1.895
36/34K
S6+
S5+
S4+
S2+
S1-
S2-

1. Download high-res image (442KB)
2. Download full-size image

Fig. 7. Exponents of mass dependence based on β-values computed from 0–2000 °C ($^{33/34}\kappa = \ln(^{33}\beta)/\ln(^{34}\beta)$, $^{36/34}\kappa = \ln(^{36}\beta)/\ln(^{34}\beta)$). The horizontal red lines indicate the high temperature limits (as T → ∞) based on the atomic mass of the sulfur isotopes derived from RPFRs (Matsuhisa et al., 1978).

The variability (or noise) in our computed exponents as the high temperature limit is approached (*cf.* Fig. 7) is likely the result of error introduced by the cluster model and may relate specifically to the multiple vibrational modes associated with the coordinated water molecules that contribute to the overall β values. Such error may be most exemplified in the calculation of the atomic sulfide ion ($S^{2-}\cdot 30H_2O$)—a sulfur species that has no vibrational modes of its own—that displays the most unusual behavior in $^{33/34}\kappa$ and $^{36/34}\kappa$ as the high temperature limit is approached.

At temperatures well-below the high temperature limit, $^{33/34}\kappa$ and $^{36/34}\kappa$ values follow trends based on coordination and oxidation state similar to those seen in $^{34}\beta$ values as a function of temperature (Fig. 6), where the end-member oxidation states (sulfide species and sulfate) generally represent end-member values and intermediate oxidation states plot successively in between. Higher oxidation states tend to have lower $^{33/34}\kappa$ than lower oxidation states, and *vice versa* for $^{36/34}\kappa$. For a given oxidation state, the more highly coordinated sulfur bonding sites generally have lower $^{33/34}\kappa$ than lower coordinated sites and *vice versa* for $^{36/34}\kappa$, following similar relationships to those observed in the magnitude of their $^{34}\beta$, but with some exceptions. Overall, the exponents of mass dependence for sulfur compoundsspanning the entire range of available oxidation states define a narrow range of $^{33/34}\kappa$ = 0.5148–0.5159 and $^{36/34}\kappa$ = 1.890–1.898 over a wide range of temperature (T ⩾ 0 °C).

4.3. Fractionations in the sulfite system

Triple sulfur isotope fractionations ($^{33}\alpha$ vs. $^{34}\alpha$) for aqueous species in the sulfite system ($SO_{2(aq)}$, $(HO)SO_2^-$, two conformers of $(HS)O_3^-$, $S_2O_5^{2-}$, and two conformers of SO_3^{2-}) at 25 °C are summarized in Fig. 8. For purposes of illustration, fractionations are plotted relative to $SO_{2(aq)}$. Fractionations among the major sulfite species in solution ($SO_{2(aq)}$, $(HO)SO_2^-$, and SO_3^{2-}) are relatively small ($1000\ln{}^{34}\alpha < 6‰$). The fractionation between $(HO)SO_2^-$ and SO_3^{2-} at 25 °C is computed to be on the order of −2.2‰ with corresponding $^{33/34}\theta$ = 0.51519 and $^{36/34}\theta$ = 1.8972. Fractionations between the $(HS)O_3^-$ isomer and these species are much larger: at 25 °C, the $1000\ln{}^{34}\alpha$ between $(HS)O_3^-$ and $SO_{2\,(aq)}$ is on the order of 25‰ ($^{33/34}\theta$ = 0.51488 and $^{36/34}\theta$ = 1.8975), and the

1000ln$^{34}\alpha$ between $(HS)O_3^-$ and SO_3^{2-} is 20‰ at 25 °C ($^{33/34}\theta$ = 0.51456 and $^{36/34}\theta$ = 1.8993). The influence of the minor $(HS)O_3^-$ isomer on overall isotope partitioning in this system will be a major focus of the discussion (Section 5.4).

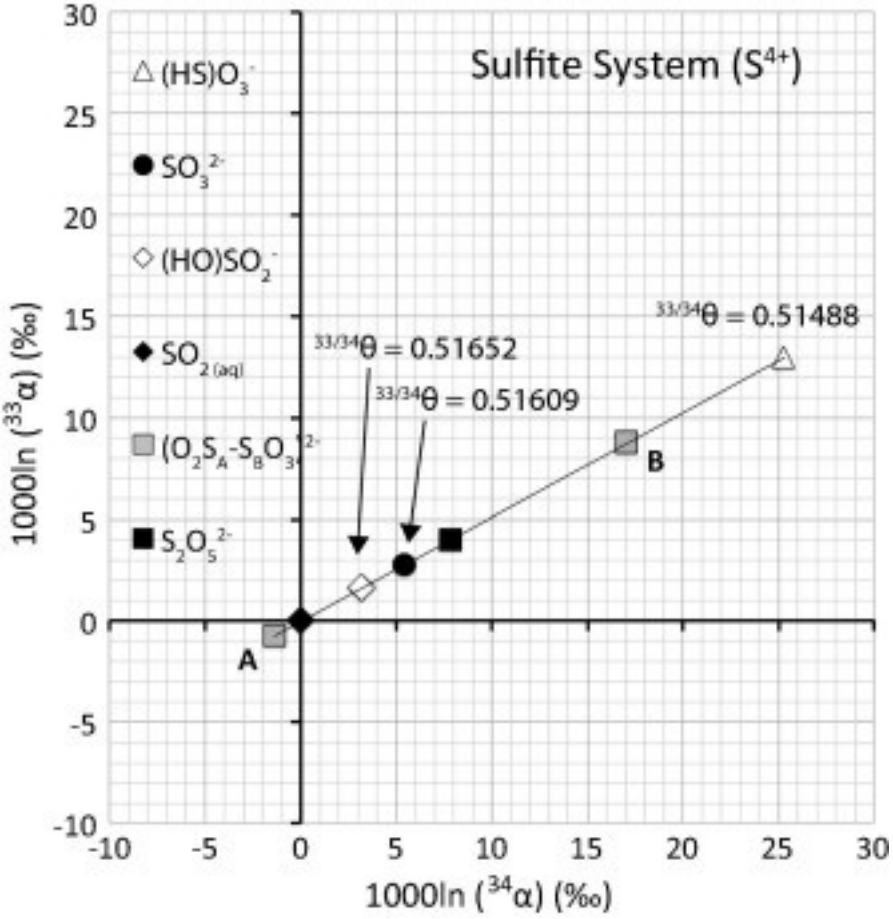

1. Download high-res image (266KB)
2. Download full-size image

Fig. 8. Triple isotope plot of theoretical fractionation factors for aqueous sulfite species relative to aqueous sulfur dioxide at 25 °C. The A and B subscripts for disulfite (conformer computed with the shortest S‾‾S bond length) refer to the 3-fold and 4-fold coordinated sites within the dimer, respectively (gray squares). The $S_2O_5^{2-}{}_T$ refers to the site-averaged fractionation factor for the dimer (black square). The exponents of mass dependence for select fractionation factors ($^{33/34}\theta$) are noted.

Fractionations involving the bisulfite dimer ($S_2O_5^{2-}$) are also presented in Fig. 8. The 3-fold coordinated site (with the most reproducible β between conformers) has a slightly lower preference for heavier isotopes than $SO_{2(aq)}$, contrary to what would be expected from simple coordination relationships. The 4-fold coordinated site has a β that is intermediary between the pyramidal and tetrahedral sulfite species. When site-averaged, the isotopic composition of the dimer is only slightly elevated from sulfite

according to the conformer plotted in Fig. 8. Given the inverse correlation that we have observed between β values (namely that of the 4-fold coordinated site) and S—S bond length, we expect this value to represent a minimum site-averaged fractionation factor for the dimer if our calculations overestimate the S—S bond length.

4.4. Fractionations in the sulfoxylate system

Triple sulfur isotope fractionations ($^{33}\alpha$ vs. $^{34}\alpha$) for aqueous species in the sulfoxylate system (two isomers of H_2SO_2, $(HS)O_2^-$, $OS(OH)^-$, and SO_2^{2-}) at 25 °C are summarized in Fig. 9. For purposes of illustration, fractionations are plotted relative to sulfoxylic acid, $S(OH)_2$. Similar to the sulfite system, sulfoxylate species with similar coordination around the sulfur atom ($S(OH)_2$, $(HO)SO^-$, SO_2^{2-}) are minimally fractionated with respect to one another ($1000\ln^{34}\alpha$ < 3‰ at 25 °C) and species where protonation occurs on the sulfur atom (increasing coordination around sulfur) are significantly fractionated from the other species. For example, the $1000\ln^{34}\alpha$ between the two-fold coordinated $(HO)SO^-$ and the two-fold coordinated $S(OH)_2$ is predicted to be −0.3‰ ($^{33/34}\theta$ = 0.51410 and $^{36/34}\theta$ = 1.8874), and the $1000\ln^{34}\alpha$ between three-fold coordinated $(HS)O_2^-$ and the two-fold coordinated $S(OH)_2$ is predicted to be 14.8‰ ($^{33/34}\theta$ = 0.51526 and $^{36/34}\theta$ = 1.8950).

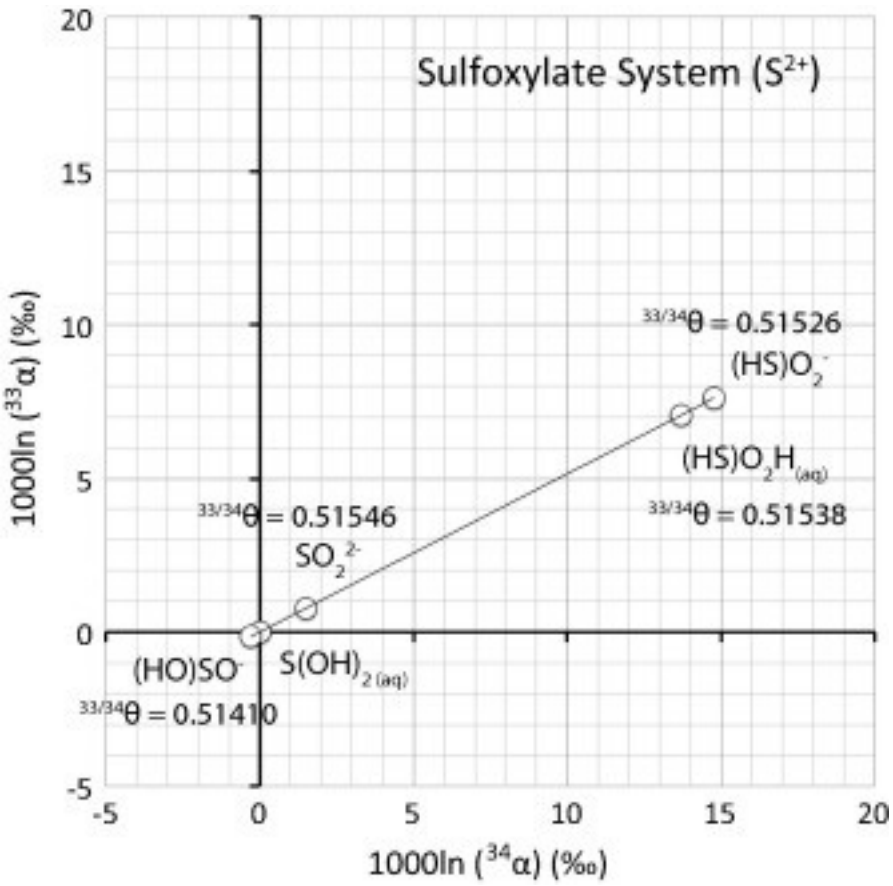

1. Download high-res image (200KB)
2. Download full-size image

Fig. 9. Triple isotope plot of theoretical fractionation factors for aqueous sulfoxylate species relative to sulfoxylic acid, $S(OH)_2$, at 25 °C. The exponents of mass dependence for individual fractionation factors ($^{33/34}\theta$) are noted.

4.5. Fractionations in the sulfide system

Triple sulfur isotope fractionations ($^{33}\alpha$ vs. $^{34}\alpha$) for aqueous species in the sulfide system (H_2S, HS^-, and S^{2-}) at 25 °C are summarized in Fig. 10. For purposes of illustration, fractionations are plotted relative to the divalent sulfide anion, S^{2-}. Similar to the sulfite and sulfoxylate systems, the magnitude of fractionation between sulfide species increases with coordination. In all cases, fractionations are predicted to be relatively small in the sulfide system: at 25 °C, the $1000\ln^{34}\alpha$ between H_2S and HS^- is estimated to be on the order of 3.3‰ ($^{33/34}\theta$ = 0.51561 and $^{36/34}\theta$ = 1.8916), and the $1000\ln^{34}\alpha$ between HS^- and S^{2-} is on the order of 1.7‰ ($^{33/34}\theta$ = 0.51573 and $^{36/34}\theta$ = 1.8894).

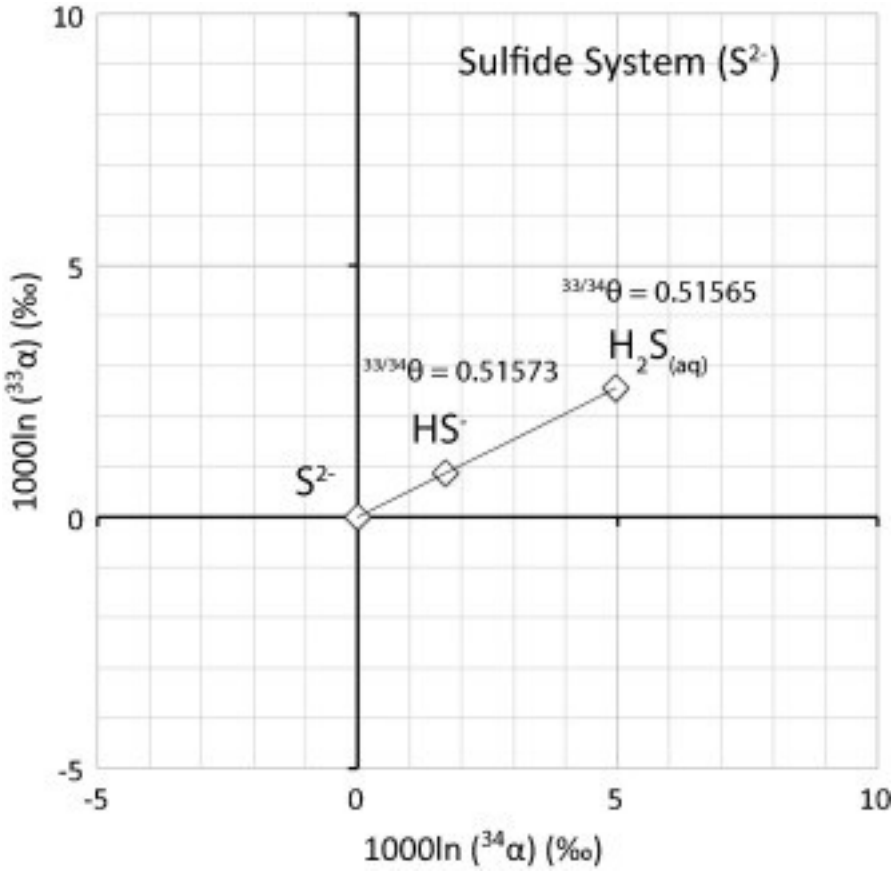

1. Download high-res image (136KB)
2. Download full-size image

Fig. 10. Triple isotope plot of theoretical fractionation factors for aqueous sulfide species relative to the atomic sulfide ion, S^{2-}, at 25 °C. The exponents of mass dependence for individual fractionation factors ($^{33/34}\theta$) are noted.

4.6. Fractionations between sulfate and the sulfide species

Fractionations between the two end-member oxidation states of sulfur (S^{2-} and S^{6+}) yield the largest equilibrium isotope fractionations in the aqueous sulfur system. The fractionation factor between SO_4^{2-} and H_2S is ($1000\ln(^{34}\alpha_{sulfate\text{-}H2S})$) is predicted to be 63.4‰ with corresponding $^{33/34}\theta = 0.51475$ and $^{36/34}\theta = 1.8981$ at 25 °C. The fractionation factor between SO_4^{2-} and HS^- ($1000\ln(^{34}\alpha_{sulfate\text{-}HS^-})$) is predicted to be 66.7‰ with corresponding $^{33/34}\theta = 0.51480$ and $^{36/34}\theta = 1.8978$ at 25 °C. Similarly, the fractionation factor between sulfate and the atomic sulfide dianion, S^{2-}, ($1000\ln(^{34}\alpha_{sulfate\text{-}sulfide})$) is predicted to be 68.4‰ with corresponding $^{33/34}\theta = 0.51482$ and $^{36/34}\theta = 1.8976$ at 25 °C.

4.7. Fractionations within and between thiosulfate and the major sulfide species

The intramolecular fractionation factor between the outer (“sulfanyl”) and inner (“sulfonate”) sulfur atoms in thiosulfate ($S_2O_3^{2-}$) ($1000\ln{}^{34}\alpha_{outer\text{-}inner}$) is predicted to be on the order of −53.8‰ at 25 °C, with corresponding ${}^{33/34}\theta = 0.51489$ and ${}^{36/34}\theta = 1.8972$. The fractionation factor between the outer (“sulfanyl”) sulfur atom in thiosulfate and H_2S ($1000\ln{}^{34}\alpha_{outer\text{-}H2S}$) is predicted to be small and on the order of −1.0‰ at 25 °C, where the magnitude of the major isotope fractionation factor increases with temperature (inverse temperature dependence) over the approximate temperature range of ≈ −15 to 180 °C to a maximum approaching $1000\ln{}^{34}\alpha_{outer\text{-}H2S} \approx -2‰$ at ≈ 180 °C. This inverse temperature dependence is the consequence of a crossover in the direction of the ${}^{34}\alpha_{outer\text{-}H2S}$ fractionation factor at sub-0 °C temperature ($T_{34/32\text{-}crossover} \approx -15$ °C). The fractionation factor between the outer sulfur (“sulfanyl”) atom in thiosulfate and the HS^- ion ($1000\ln{}^{34}\alpha_{outer\text{-}HS^-}$) is predicted to be 2.3‰ at 25 °C (opposite in direction to the similar H_2S-based fractionation factor at 25 °C), and also exhibits a crossover in proximity to ≈ 270 °C. The exponents of mass dependence (${}^{33/34}\theta$ and ${}^{36/34}\theta$) associated with both $\alpha_{outer\text{-}H2S}$ and $\alpha_{outer\text{-}HS^-}$ exhibit characteristic asymptotic behavior at their respective crossover temperatures (*cf.* Deines, 2003, Otake et al., 2008) (not shown) that lead to unusual exponents in proximity to the crossover temperature. For example, at 0 °C, the ${}^{33/34}\theta$ and ${}^{36/34}\theta$ associated with $\alpha_{outer\text{-}H2S}$ are computed to be 0.5197 and 1.857, respectively. Despite the unusual exponents associated with these crossovers, the capital delta values associated with these fractionation factors are very near zero at all relevant temperatures: e.g., at $T \geqslant 0$ °C, $\Delta^{33}S_{outer\text{-}H2S} \leqslant -0.002‰$ and $\Delta^{36}S_{outer\text{-}H2S} \leqslant -0.02‰$, and $\Delta^{33}S_{outer\text{-}HS^-} \approx 0.000‰$ and $\Delta^{36}S_{outer\text{-}HS^-} \leqslant 0.01‰$.

5. Discussion

5.1. Uncertainties in estimated fractionation factors

Uncertainties in our theoretically estimated fractionation factors can derive from three main sources: (1) errors arising from the harmonic and other approximations in the derivation of the Bigeleisen and Mayer equation (requiring higher-order corrections, e.g., for anharmonicity), (2) inadequacies in the theoretical method (choice of theoretical method and basis set), and (3) variability arising from the water cluster geometry. To quantitatively evaluate these uncertainties, we adopt a similar approach to Li and Liu (2011), where a similar water cluster model was used to calculate the equilibrium isotope fractionations among aqueous selenium compounds and anions.

5.1.1. Harmonic approximation

The BM-equation requires that harmonic frequencies be used to justify the various approximations used in its derivation (*cf.* Rustad and Bylaska, 2007, Rustad et al., 2010, Liu et al., 2010). We therefore use the calculated harmonic frequencies to calculate RPFRs/β-values and isotope fractionation factors. An appropriate comparison of theoretically computed vibrational frequencies to those derived from experiments is not possible at this time, because the conversion of our computed harmonic frequencies to fundamental frequencies requires computation of anharmonic constants (*cf.* Liu et al., 2010). The computation of anharmonic constants for large molecular clusters is computationally laborious and is beyond our computational resources. We therefore considered these computations beyond the scope of this study. Instead, we focus on calculations of anharmonic corrections to the BM-equation (RPFR) for simple gaseous molecules to gain insight into the magnitude of these corrections for more complex systems.

Liu et al. (2010) reviewed and applied a variety of anharmonic and higher-order corrections to the BM-equation for simple gaseous molecules at the MP2/aug-cc-pVTZ level. They show that many of these corrections are only significant when dealing with hydrogen–deuterium exchange reactions. For example, the total $^{34}S/^{32}S$-based corrected partition function ratios (CPFR) for $H_2S_{(g)}$ and $SO_{2(g)}$ are shifted by 0.3 and 0.6‰ at 300 K from their uncorrected RPFR counterparts, respectively, where the entirety of the correction for both compounds arises from the anharmonic contribution to the zero point energy (AnZPE; Liu et al., 2010). We have computed the anharmonic corrections to the ZPE (AnZPE) for a handful of gaseous sulfur molecules (H_2S, $S(OH)_2$, $(HS)O_2H$, SO_2, SO_3) at the B3LYP/6-31+G(d,p) level and find that they are of a similar magnitude (H_2S, $S(OH)_2$, $(HS)O_2H$, SO_2:∼−0.5‰, SO_3:∼−0.9‰; 25 °C) (Fig. S.2). Due to the low magnitude of these corrections and the inability to apply appropriate anharmonic corrections to our cluster calculations at this time, all RPFR/β values and fractionation factors in this study are reported in the harmonic approximation.

5.1.2. Theoretical level

The theoretical method and basis set employed can lead to significant error in the computed RPFRs and fractionation factors (*cf.* Rustad et al., 2008, Rustad et al., 2010). We evaluated the potential error introduced by any inadequacies in our theoretical approach via harmonic frequency scaling using high-level computations of simple neutral molecules modeled in the gas phase (*cf.* Li and Liu, 2011). Note that this is not the same practice as scaling theoretical harmonic frequencies to fit experimental

fundamental frequencies that introduce anharmonic contributions to the theoretical frequencies.

We computed harmonic frequencies for H_2S, S_2, SO_2, and SO at the CCSD/aug-cc-pVTZ level and derived a first-order harmonic scaling factor for the B3LYP/6-31+G(d,p) level employed for our water clusters on the order of 1.01–1.02 (i.e., a uniform 1–2% positive shift in the harmonic frequencies; Fig. S.3). The influence of this scaling factor on $^{34}\beta$ values and the computed fractionation factors varies depending on the compound(s) and temperature considered, but is generally magnified at lower temperatures. The effect of harmonic scaling is often negligible but can be on the permil level for some computed fractionation factors that involve compounds with higher magnitude $^{34}\beta$. For example, for the $SO_4^{2-}{}_{(30H2O)}/H_2S_{(30H2O)}$equilibrium fractionation factor, applying a harmonic frequency scaling factor of 1.02 results in a ~2‰ increase in the $^{34}\alpha$ fractionation factor at 25 °C from 1.0655 to 1.0677, but smaller shifts at higher temperatures (e.g. 1.1 and 0.6‰ positive shift at 200 °C and 400 °C, respectively). In some cases (but not all), the small shifts arising from harmonic frequency scaling places our theoretical fractionations factors in slightly better agreement with experimental constraints (explored further for individual systems in Section 5.4).

The practice of harmonic frequency scaling may not be ideal because different vibrational modes appear to scale slightly differently between computational methods (*cf.* Li and Liu, 2011). Furthermore, gaseous molecules may not capture the full range of error introduced by the level of theory and basis set employed in our aqueous cluster calculations, especially for the anions of more varied geometric and electronic structure computed in our study. From our own calculations, it appears that SO_2 may have a systematically higher scaling factor than the other compounds investigated that may be on the order of 1.065, which is why when SO_2 is included in the regression the net scaling factor increases from ~1.01 to ~1.02 (we show later that application of this higher SO_2-specific scaling factor places estimates of the $SO_{2(aq)}/SO_{2(g)}$ fractionation factor in slightly better agreement with experimental constraints, although overall the effect of the scaling is still only on the ~0.2‰ magnitude at 25 °C in the estimated fractionation factor). Due to these potential issues, we have chosen to not apply a harmonic scaling factor in the computations of our reported β values but we do discuss the effects of harmonic scaling on fractionation factors for individual systems (Section 5.4).

5.1.3. Cluster geometry

Variability in the water cluster geometry surrounding the solute of interest is another potential source of error/uncertainty in computed β values and fractionation factors.

From previous studies utilizing clusters manually constructed as in the present study (e.g., Li et al., 2009, Li and Liu, 2011) and clusters derived from molecular dynamics simulations (Rustad et al., 2008, Rustad et al., 2010), it is generally understood that error/uncertainty arising from cluster geometries is relatively small, and likely much lower than those associated with the theoretical approach (e.g., Rustad et al., 2010). Most theoretical studies of compounds in water clusters where the centrally coordinated element in the solute is undergoing isotope substitution have found that the variability in computed β is generally at the 0.1–1‰ level (1 s.d.) from one cluster geometry to another for multiple element systems (e.g., oxy-anions and compounds of C, Se, Ge, B; Rustad et al., 2008, Rustad et al., 2010, Li et al., 2009, Li and Liu, 2011). We performed a series of at least duplicate constructions and optimizations of water clusters (i.e., repeating the procedure of Section 3.4) for a select set of 30–40H_2O clusters in the sulfite system: SO_3^{2-}, $(HS)O_3^-$, $(HO)SO_2^-$, and the bisulfite dimer pyrosulfite, $S_2O_5^{2-}$. Duplicate constructions and optimizations of $SO_3^{2-}\cdot 30H_2O$, $(HS)O_3^-\cdot 30H_2O$, and $(HO)SO_2^-\cdot 34H_2O$ reveal that variability due to cluster geometry for aqueous sulfur compounds may also be small: $(HS)O_3^-\cdot 30H_2O$: $^{34}\beta = 1.0721 \pm 0.0001$, $SO_3^{2-}\cdot 30H_2O$: $^{34}\beta = 1.0510 \pm 0.0003$, $(HO)SO_2^-\cdot 34H_2O$: $^{34}\beta = 1.0487 \pm 0.0003$ (all at 25 °C and 1 s.d.). The two sulfur atoms in the bisulfite dimer, labeled here as 'A' and 'B': $(O_2\text{-}^{A}S\text{-}^{B}S\text{-}O_3)^{2-}$, have similar reproducibility in their $^{34}\beta$ values between four separate conformers ranging from 30 to 40H_2O clusters: ^{A}S: $^{34}\beta = 1.0438 \pm 0.0003$ and ^{B}S: $^{34}\beta = 1.0622 \pm 0.0011$ (25 °C, 1 s.e.), where the $^{34}\beta$ of the latter, higher-coordination site seems to vary systematically with the computed S—S bond-length, and may be a special case (Section 4.1). Considering all of the uncertainties derived from the above sources, we estimate the overall uncertainties associated with our theoretically computed fractionation factors ($^{34}\alpha$) for aqueous sulfur systems to be on the order of ~0.1 to 1–2‰, depending on temperature and the compounds/system considered. The major source of uncertainty is believed to be from the potential inadequacy of our theoretical approach (*cf.* Rustad et al., 2008, Rustad et al., 2010) and could potentially be better constrained with more sophisticated computational methods. A major aim of the present study is to explain the available experimental constraints for equilibrium fractionations in the sulfite system in the context of the complex speciation of sulfite. Much of the uncertainty in this analysis is dominated by uncertainties in experimental determinations of equilibrium quotients (e.g. bisulfite isomerization) and experimental fractionation factors (e.g. approaching a few permil in magnitude). Much of the uncertainties in the theoretically calculated fractionation factors discussed above are either comparable to, or within this range.

Therefore, we do not think the uncertainties in the calculations will affect the main conclusions of the present study.

5.2. General trends in the calculated $^{34}\beta$

The general relationships in the computed $^{34}\beta$ for the hydrated sulfur species can be explained by the general principles of stable isotope fractionation. The two primary factors influencing the magnitude of $^{34}\beta$ (Fig. 6) are: (1) the oxidation state of sulfur, and (2) the coordination of sulfur, i.e., the number of bonds formed with other atoms. Both of these exert first order controls on the bonding environment around sulfur, particularly on the bond stiffness/strength, and are the primary factors in influencing the relative magnitudes of $^{34}\beta$ that we have computed.

The oxidation state of the sulfur atom will affect the electron distribution throughout the molecule and therefore the strength and nature of the bonds with the other atoms. The force constants that describe the potential wells associated with the bonds (derived from the computation of the multidimensional electronic potential energy surface) will generally be higher for bonds associated with sulfur in higher oxidation states, meaning simply that the bonds will be more stiff. Thus, species with higher oxidation state will generally have higher $^{34}\beta$ than those with lower oxidation state in similarly coordinated structures. This is reflected in the significantly lower $^{34}\beta$ of the sulfoxylate ion (SO_2^{2-}; S^{2+}) as compared to sulfur dioxide(SO_2; S^{4+}), which have similar bent triatomic structures and two-fold coordination of the sulfur atom with bonds to oxygen atoms.

For a given oxidation state, the coordination of the sulfur exerts another first order control on $^{34}\beta$. The Bigeleisen and Mayer equation describes the relationship between isotope partitioning among molecules, zero point energies (ZPE), and molecular vibrations. The ZPE portion of the RPFR reflects the contribution from all vibrational modes and scales with the sum of the frequency shifts. Unless the bonds are weakened so much with increasing coordination that the adjusted sum of the frequency shifts decreases, the RPFR may increase with coordination. From a simple vibrational analysis of our solutes in vacuum, isotope substitution of the central sulfur atom in a bent (or linear tri-atomic), pyramidal, or tetrahedral molecular structure generally affects the asymmetric stretching and bending modes of the ground state vibrations the most and, therefore, contribute the most to the overall magnitude of the RPFR/β-values of the molecule. The number of these stretching and bending modes increases with increasing coordination of the central atom, and so all else being equal, the RPFR/β-values (and therefore, preference for the heavy isotope) may increase with increasing coordination. For example, the 2-fold coordinated $SO_{2(aq)}$ has a lower $^{34}\beta$ than the 3-fold coordinated SO_3^{2-} and $(HO)SO_2^-$ molecules, which have lower $^{34}\beta$ than the 4-fold coordinated

$(HS)O_3^-$ isomer of bisulfite (all S^{4+}). Variations from these relationships may be expected depending on the elemental composition of the bonded atoms/groups that may affect bonding environment and the manner in which frequency shifts are scaled.
Protonation of oxygen atoms has a smaller secondary effect on $^{34}\beta$ with respect to the centrally coordinated sulfur. These small secondary effects are due to how protonation of the oxygen atom affects its electron distribution and its bond to the sulfur atom. For example, the $^{34}\beta$ of the $(HO)SO_2^-$ isomer of bisulfite differs by only ~−2‰ from that of the non-protonated sulfite (SO_3^{2-}) at 25 °C. The slightly higher $^{34}\beta$ for the sulfite anion relative to the $(HO)SO_2^-$isomer of bisulfite is likely due to the slight weakening of the S—O bond corresponding to the protonated oxygen. This is consistent with the slightly longer S—O bond length for the protonated oxygen atom (Fig. 3; Table S.2). Similarly, in the sulfoxylate system, the $^{34}\beta$ for $(HO)SO^-$ and $S(OH)_2$ are both lower than that for SO_2^{2-} and the corresponding S—OH bond lengths are longer than S—O bond lengths (Fig. 4; Table S.2). The $^{34}\beta$ for $(HO)SO^-$and $S(OH)_2$ are nearly identical to one another (at 25 °C: $^{34}\beta$ = 1.0240 and $^{34}\beta$ = 1.0243, respectfully) and are likely within the uncertainties of the calculations. Multiple rotamers of these types yielding different orientations of the protons and OH-bonds with respect to the rest of the molecule are possible that will depend in large part on the water cluster geometry (direct coordination with water molecules) in the case of these computed structures. Such variability in structure would be expected to have small second order effects on the magnitude of $^{34}\beta$. For example, our two optimized $34H_2O$ conformers of $(HO)SO_2^-$ do not have exactly the same structure (slightly different orientations of the O—H bond relative to the rest of the molecule, i.e., O—S—O—H dihedral ~49–71°) and yield highly reproducible $^{34}\beta$ ($^{34}\beta$ = 1.0487 ± 0.0003 at 25 °C, 1 s.d.).

5.3. Exponents of mass-dependence: κ and θ

We compute exponents of mass dependence for β values ($^{33/34}\kappa$ and $^{36/34}\kappa$) over a wide range of temperature that conform to tight ranges (0.5148–0.5159 and 1.89–1.90, respectively; Fig. 7). The $^{33/34}\kappa$ for a given species is on a lower end of this range at low temperature and approaches the high range at high temperature, and *vice versa* for $^{36/34}\kappa$. The relationships in $^{33/34}\kappa$ and $^{36/34}\kappa$ we compute as a function of temperature for the diversity of aqueous sulfur compounds investigated herein are straightforward consequences of ZPE differences among isotopomers varying as a function of sulfur bonding environment (redox state, coordination, etc.).
The exponent of mass dependence computed for a fractionation factor between two compounds (A and B; $^{33/34}\theta_{A\text{-}B}$ or $^{36/34}\theta_{A\text{-}B}$) generally follows:

(9)n/34θA-B=n/34κAln(34βA)-n/34κBln(34βB)ln(34βA)-ln(34βB)
where n = 33 or 36 (we will focus on 33). Only when $^{33/34}K_{(A)} = {}^{33/34}K_{(B)}$ will $^{33/34}\theta_{A\text{-}B}$ be identical. When $^{33/34}K_{(A)} \neq {}^{33/34}K_{(B)}$, the magnitude of $^{33/34}\theta_{A\text{-}B}$ will be slightly shifted to either higher or lower values than either $^{33/34}K_{(A)}$ or $^{33/34}K_{(B)}$ depending on the relationships among the RPFRs/β-values (*cf.* Matsuhisa et al., 1978). In the latter case, there are two primary examples to consider: (1) When $^{34}\beta_A > {}^{34}\beta_B$ and the $^{33/34}K_A < {}^{33/34}K_B$, the computed $^{33/34}\theta_{A\text{-}B}$ will generally be slightly lower than either $^{33/34}K_A$ or $^{33/34}K_B$; and (2) when $^{34}\beta_A > {}^{34}\beta_B$ and the $^{33/34}K_A > {}^{33/34}K_B$, the computed $^{33/34}\theta_{A\text{-}B}$ will generally be slightly higher than either $^{33/34}K_A$ or $^{33/34}K_B$. The magnitudes of the shifts between $^{33/34}K$ values and the $^{33/34}\theta$ corresponding to a fractionation factor between compounds are magnified at lower temperature where differences in the magnitudes of β-values are largest (in the general case). The shifts are additionally magnified under hypothetical conditions where the differences between $^{33/34}K_A$ and $^{33/34}K_B$ are relatively large and differences between $^{34}\beta_A$ and $^{34}\beta_B$ are relatively small. For most fractionation factors computed among compounds of different oxidation state at low/ambient temperature, our calculations generally follow case (1). For example, at 0 °C the fractionation factor between sulfate (SO_4^{2-}; $^{34}\beta$ = 1.0910, $^{33/34}K$ = 0.5148) and sulfide (H_2S; $^{34}\beta$ = 1.0142, $^{33/34}K$ = 0.5157) yields $^{33/34}\theta$ = 0.5146, slightly lower than either compound's respective $^{33/34}K$ values. An example of case (2) is the fractionation factor between (HO)SO_2^- isomer of bisulfite ($^{34}\beta$ = 1.0487, $^{33/34}K$ = 0.51521; avg. of duplicate conformers, 25 °C) and $SO_{2(aq)}$ ($^{34}\beta$ = 1.0454, $^{33/34}K$ = 0.51511; 25 °C), where $^{33/34}\theta$ = 0.51652. Due to the tight range in $^{33/34}K$ and $^{36/34}K$ that we compute over a relatively large range in $^{34}\beta$ for various aqueous sulfur compounds, it may be generally concluded that our calculations would not predict exponents of mass dependence associated with equilibrium isotope fractionation factors significantly outside of the range of ca. $^{33/34}\theta \approx 0.514–0.516$ and $^{36/34}\theta \approx 1.89–1.90$ over a wide range of temperature (0 °C → ∞).

The major exception to this generality is for equilibrium isotope exchange reactions that are predicted to have crossovers, i.e., a shift in the direction of an isotope effect where preference for heavy isotopes undergoes inversion from one compound (or bonding environment) to the other at a particular temperature. Our calculations predict crossovers in the isotope exchange reactions between the outer ("sulfanyl") sulfur atom in thiosulfate and the two principle sulfide species (H_2S, HS^-). Crossovers and their effects on the exponents of mass dependence have been described previously in gas phase reactions for the sulfur isotope system (Deines, 2003, Otake et al., 2008). Briefly, these effects relate to crossover temperatures being slightly different for exchange

reactions involving isotopes of different mass, i.e., $T_{33/32\text{-crossover}} \neq T_{34/32\text{-crossover}} \neq T_{36/32\text{-crossover}}$. As a crossover temperature is approached, the exponents of mass dependence show asymptotic relationships where the exponent can take any value between +∞ and −∞ (Deines, 2003, Otake et al., 2008). Crossovers have been predicted in isotope exchange reactions involving H_2S and other reduced sulfur compounds containing S—S bonds (S_2/H_2S, S_8/H_2S; Deines, 2003, Otake et al., 2008), and presumably arise fundamentally from the competition between contributions from low frequency vibrational modes (like those associated with S—S bonds) and high frequency modes in H_2S (and HS^-) to the overall RPFRs as a function of temperature. Due to the small magnitude of the isotope effects in the asymptotic crossover range, these effects are not substantially expressed (i.e., $\Delta^{33}S \approx 0$, $\Delta^{36}S \approx 0$, as we have computed) without subsequent amplification via non-equilibrium isotope exchange processes (e.g., a Rayleigh distillation process; Deines, 2003, Otake et al., 2008).

In a previous study, Otake et al. (2008) emphasized computations utilizing a non-exponential formulation based on the approximation $^{33/34}\theta_{A-B} \approx (^{33}\alpha_{A-B} - 1)/(^{34}\alpha_{A-B} - 1)$ to argue that their theoretical calculations of select sulfur compounds (modeled as either gas phase or in PCM solvation models) predict a range of $^{33/34}\theta = 0.505–0.516$ for equilibrium fractionation factors (including SO_4^{2-}-H_2S), where the reference exponent of 0.515 is approached at high temperature. Computations of the mass dependence as $^{33/34}\theta_{A-B} = \ln(^{33}\alpha_{A-B})/\ln(^{34}\alpha_{A-B})$ calculated from the same fractionation factors yields a much more narrow range of $^{33/34}\theta \approx 0.514–0.516$ over the same temperature range. In other words, the so-called ‘band of mass dependence’ that Otake et al. (2008) argued for as $^{33/34}\theta \approx 0.505–0.516$ for simple equilibrium isotope exchange reactions lowers to 0.514–0.516 when the exponential definition of mass dependence is used. Note also that the computation of the mass dependence as $(^{33}\alpha - 1)/(^{34}\alpha - 1)$ is valid to characterize effects associated with a Rayleigh distillation process and not the condition of equilibrium isotope exchange.

5.4. Comparisons to available experiments, and predictions

The validity of the theoretical fractionation factors can be assessed by comparison with available experimental constraints, with particular focus on the sulfite system. Very little is known about the behavior of sulfoxylate species in aqueous solutions (particularly the isomerization quotients for the protonated species) and so we are only able to discuss the estimated ranges of fractionations possible in this system. Calculations of the other sulfur compounds (sulfide, sulfate, and thiosulfate) can also be compared to the available experimental datasets, including: fractionations among sulfide species,

fractionations between sulfate and sulfide species, the intramolecular fractionation factor for thiosulfate, and fractionations between the sulfide species and thiosulfate. We highlight potential experimental issues and include recommendations for future experimental determinations where they may be needed.

5.4.1. Sulfite system

Experimental constraints for the equilibrium sulfur isotope partitioning in the aqueous sulfite system are provided by Eriksen, 1972a, Eriksen, 1972b, and Eriksen (1972c). Eriksen (1972a) explored fractionations between bulk bisulfite and gaseous SO_2($HSO_3^-{}_{TOTAL}/SO_{2(g)}$) at pH = 4.5 where bisulfite dominates, Eriksen (1972b) explored the fractionation between gaseous SO_2 and aqueous SO_2 ($SO_{2(aq)}/SO_{2(g)}$) in acidic solutions (pH < 0.3), and Eriksen (1972c) explored fractionations between bulk bisulfite and gaseous SO_2 as a function of the ratio of total bisulfite: $SO_{2(aq)}$ (up to 10 M [HSO_3^-]; pH = < 0.3 or 4.5), which was a study of the effect of dimerization on isotope fractionations. With additional interpretation, the experiments presented in Eriksen (1972c) yield constraints on both the $SO_{2(aq)}/SO_{2(g)}$ and $HSO_3^-{}_{TOTAL}/SO_{2(g)}$ fractionation factors. Additional experimental constraints on the $SO_{2(aq)}/SO_{2(g)}$ fractionation factor are found in Chmielewski et al. (2002).

5.4.1.1. Bulk bisulfite in solution vs. $SO_{2(g)}$: highlighting the role of bisulfite isomers

In Fig. 11, our calculated fractionation factors for bisulfite species vs. $SO_{2(g)}$ are plotted with those from the experiments of Eriksen (1972a) and Eriksen (1972c) as a function of temperature. Eriksen (1972a) chose experimental conditions to minimize the presence of dimers and other sulfite species (pH = 4.5), so the experimentally determined fractionations should mostly reflect those of the two bisulfite isomers and gaseous sulfur dioxide. The ${}^{34}\alpha_{bisulfite(bulk)\text{-}SO2(g)}$ of Eriksen (1972a) appear to show a non-resolvable temperature dependence over the temperature range of 25–45 °C. The constraints from Eriksen (1972c)were regressed from multiple experiments performed over a range of χ_{HSO3T}:$\chi_{SO2(aq)}$ and seem to indicate a slight normal temperature dependence (these are discussed in more detail in Section 5.4.1.2).

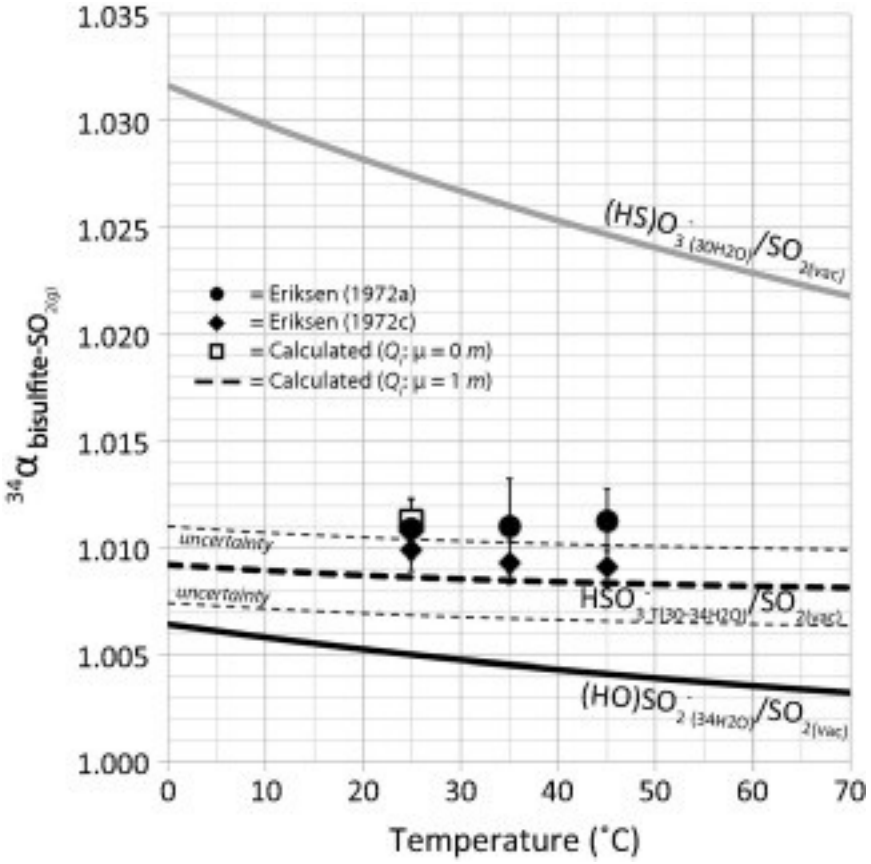

1. Download high-res image (225KB)
2. Download full-size image

Fig. 11. Comparison of theoretical fractionation factors to experimental constraints in the bisulfite-$SO_{2(g)}$system as a function of temperature, highlighting the influence of bisulfite isomerization on fractionation behavior. Black data points (circles and diamonds) are from the experimental studies of Eriksen (1972a)and Eriksen (1972c). The open (white) square is our theoretical estimate for the bulk fractionation factor using the isomerization quotient at 0 *m* ionic strength from Risberg et al. (2007) following Eq. (10) in the text. The thick dashed curve represents our theoretical estimate (Eq. (10) in the text) using the isomerization quotients as a function of temperature at 1 *m* ionic strength (Horner and Connick, 1986, Littlejohn et al., 1992; Fig. 2). The lighter dashed lines represent the uncertainty envelope derived solely from the propagation of the uncertainty of the isomerization quotient as a function of temperature that is based on the least squares linear regression in Fig. 2.

Using our theoretical calculations, we suggest that the experimental data can be explained in terms of the isomerization of bisulfite. Using the experimental constraints for the isomerization quotient for bisulfite as a function of temperature at 1 *m* ionic

strength (Horner and Connick, 1986, Littlejohn et al., 1992), we predict the $^{34}\alpha_{bisulfite(bulk)\text{-}SO2(g)}$ as the dashed curve in the figure via the following relationship:
(10)34αbisulfite(bulk)/SO2(g)=Qi(1+Qi)34β(HO)bisulfite+1(1+Qi)34β(HS)bisulfite34βSO2(g)
where Q_i as a function of temperature is computed via the relationship:
$\ln Q_i$ = 1413(±119)/T-3.1(±0.4) (valid over ∼ 2–67 °C, 1 *m* ionic strength; regressed from the combined datasets of Horner and Connick, 1986, Littlejohn et al., 1992). The corresponding uncertainty envelope plotted in Fig. 11 includes only the propagated uncertainty of the temperature dependence of the isomerization quotient. The predicted $^{34}\alpha_{bisulfite(bulk)\text{-}SO2(g)}$ at μ = 1 *m* has a temperature dependence that becomes more shallow with increasing temperature, reflecting the higher proportion of the HS-isomer with increasing temperature. This relationship is roughly consistent with the non-resolvable temperature dependence of Eriksen (1972a) and Eriksen (1972c). When we apply an isomerization quotient to our calculated fractionations performed in a low ionic strength medium (μ = 0 *m*, *T* = 25 °C; Risberg et al., 2007), we obtain a fractionation factor that is ∼2.4‰ higher than that obtained from application of the μ = 1 *m* isomerization quotient (open square data point in Fig. 11) and is indistinguishable from the experimental constraint of Eriksen (1972a) at this temperature.
The experimental data fall within the range of our calculated theoretical estimates that utilize the available experimental constraints of the relative mole fractions of bisulfite isomers present in solution in media of 0 and 1 *m* ionic strength. The experiments of Eriksen (1972a, c) were based on a distillation technique that required the solution to be constantly flushed (at an unspecified, “slow” rate) with N_2 gas to strip SO_2 out of solution while simultaneously adding HCl to keep pH constant. Such changes in ionic strength throughout experimental runs are a plausible source of at least some of the variability in the experimentally determined fractionation factors. The constant stripping of SO_2 from solution also requires that the rates of isotope exchange among the aqueous sulfite species be sufficiently rapid at all times, and disequilibria among species and the SO_2 stripped from solution may be another source of variability in the experimental fractionation factors. The complete effect of ionic strength on isomerization and isotope fractionations in this system cannot be evaluated in full until the isomerization quotient is determined as a function of ionic strength over a wide range of temperatures.
Despite the large uncertainties, it is clear from Fig. 11 that: (1) we are able to reproduce the general fractionation behavior in this system that has been determined

experimentally, and (2) isotope partitioning in this system is strongly influenced by the isomerization of bisulfite. Furthermore, fractionations in the sulfite system involving bisulfite may be especially dependent on ionic strength due to isomerization.

5.4.1.2. Bisulfite dimer: bulk bisulfite in solution vs. $SO_{2(g)}$ as a function of pH and $[HSO_3^-]_T$

Eriksen (1972c) measured the fractionation between gaseous SO_2 and bulk bisulfite as a function of the molar ratio of aqueous SO_2 and total bisulfite by varying $[HSO_3^-]_T$ (1.5–10 M) and pH (0.3 or 4.5). One of the primary aims of these experiments was to determine the effect of dimer formation on the observable fractionations. Assuming full isotopic equilibration throughout experimental runs, the experiments of Eriksen (1972c) should follow the simple mass balance relationship:

(11)34αS(IV)T(aq)/SO2(g)=34αSO2(aq)/SO2(g)χSO2(aq) +34αHSO3(T)-/SO2(g)χHSO3(T)-+34αdimer/SO2(g)χdimer

where χ and $^{34}\alpha$ refer to the mole fraction and fractionation factor (based on $^{34}S/^{32}S$) of or between the denoted species, respectively, and $HSO_{3\ (T)}^-$ = $(HO)SO_2^-$ + $(HS)O_3^-$. In the absence of a dimer (or significant influence thereof), measured fractionation factors between total S(IV) species in solution and $SO_{2(g)}$ plotted against the mole fraction of total bisulfite species present should form a linear array, i.e.:

(12)34αS(IV)T(aq)/SO2(g)=34αSO2(aq)/SO2(g)χSO2(aq)+34αHSO3(T)-/SO2(g)(1-χSO2(aq))

where $\chi_{HSO3(T)} = 1 - \chi_{SO2(aq)}$ due to the negligible presence of SO_3^{2-} at a pH of <4.5.

As Eriksen (1972c) originally noted, this relationship can deviate from linear due to the power of two dependence on $[HSO_{3\ (T)}^-]$ in the dimerization quotient if the system is driven to large conversion to the dimer (i.e., high $[HSO_{3\ (T)}^-]$) and if the fractionation between the dimer and bisulfite (total of both isomers) is relatively large.

Using the bisulfite dimer conformer computed to have the lowest S–S bond length, we compute a theoretical fractionation factor at 25 °C between the site-averaged dimer and bulk bisulfite (considering both isomers) of $1000\ln{}^{34}\alpha_{dimer/HSO3\text{-}(T)} = -1.6‰$ (μ = 0 *m*; Q_i = 2.57 ± 0.5; Risberg et al., 2007) and $1000\ln{}^{34}\alpha_{dimer/HSO3\text{-}(T)} = 0.9‰$ (μ = 1 *m*; Q_i = 4.9 ± 0.1; Horner and Connick, 1986). This indicates that the fractionation between the dimer and bulk bisulfite may be relatively small and perhaps within the uncertainty of the theoretical calculations. The directionality of this overall fractionation may additionally depend on the effects of ionic strength on the relative distribution of bisulfite isomers.

We illustrate worked examples of the relationship between the $^{34}\alpha_{S(IV)(aq)/SO2(g)}$ and $\chi_{SO2(aq)}$using our theoretical $^{34}\beta$ values and equilibrium quotients from the literature (μ = 0 *m* and 1 *m*)

and compare them with the experimental data of Eriksen (1972c) in Fig. 12 under comparable conditions. The smooth curves are based on our theoretical calculations where solid curves are the linear arrays ignoring the dimer and the dashed curves are estimates with the dimer included. For the calculations including the dimer (dashed), we assumed a pH range of 0–4.5 and we additionally assume $[S(IV)]_T$ = 10 M (the highest of the Eriksen range) to examine the maximum possible influence of the dimer. The thinnest dashed curves represent the same calculations as the thicker dashed curves (pH = 0–4.5, $[S(IV)]_T$ = 10 M) except with an artificially increased site-averaged $^{34}\beta$ of the dimer (equivalent to 5‰) for illustrative purposes due to the possibility that our theoretical calculations are underestimating this value due to a poorly constrained structure for the dimer. Ionic strength was not held constant in the experiments of Eriksen (1972c) and so the 0 *m* and 1 *m* are shown for comparison, as these are the only conditions for which all equilibrium quotients (dissociation, isomerization, dimerization) have been experimentally determined for computing mole fractions.

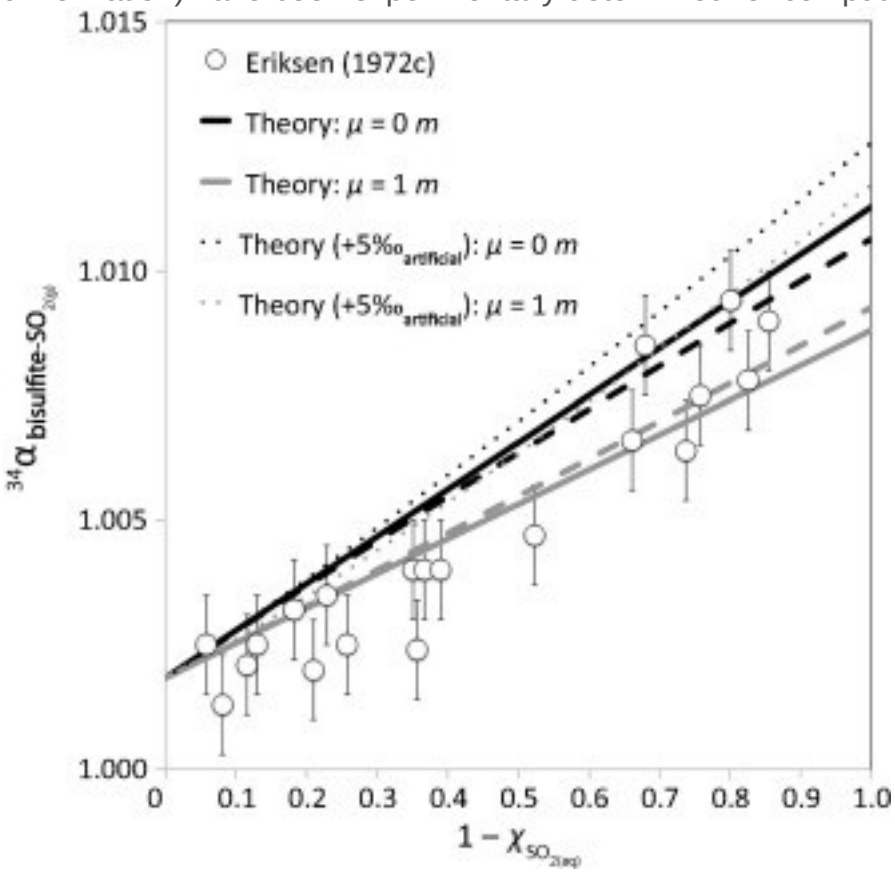

1. Download high-res image (146KB)
2. Download full-size image

Fig. 12. Fractionations at 25 °C in the sulfite system from Eriksen (1972c) (white circles) and a modeled system based on our theoretical fractionation factors and mass balance

calculations (solid or dashed curves). Solid curves ignore the bisulfite dimer and the thick dashed curves include the dimer assuming a total bisulfite concentration of 10 M (highest in the Eriksen experimental range) and a pH range of 0.5–4.5. The lightest dashed curves are identical to the thick dashed curves but include an artificially increased $^{34}\beta$ for the site-averaged dimer equivalent to 5‰ for illustration purposes.

The calculated fractionation trends in Fig. 12 are generally consistent with the experimental data of Eriksen (1972c), where the experimental data at relatively low $\chi_{SO2(aq)}$ appear to plot in between our estimates using equilibrium quotients performed at 0 and 1 *m* ionic strength. The presence of the dimer under conditions of $[S(IV)]_T$ = 10 M (thick dashed curves) affects the overall fractionations between bulk bisulfite in solution and gaseous SO_2 at the sub-permil level, which is well within the uncertainty of the experimental determinations. Eriksen (1972c) originally noted that the effect of the dimer is either non-resolvable or insignificant given the seeming linearity in the experimental dataset. Eriksen concluded that the fractionation factor between disulfite and bisulfite might not be significantly higher than non-dimer bisulfite, which is generally consistent with our theoretical calculations that take into consideration both isomers and the dimer.

Our theoretical calculations highlight the sensitivity of the fractionation trends in Fig. 12 to the relative distributions of the bisulfite isomers. Depending on the ratio of the two isomers in solution as a function of ionic strength, the dimer is computed to either dampen or enhance fractionations between bulk aqueous S(IV) and $SO_{2(g)}$ in the modeled system. It is important to reiterate, however, that our calculations of the dimer may overestimate the S–S bond length. From the standpoint of our calculations, shortening the dimer S–S bond (all else being equal) may increase the site-averaged $^{34}\beta$ for disulfite and change these calculated relationships depending on the magnitude of the $^{34}\alpha$ between the dimer and the pooled isomers. Our calculations based on an artificial increase in the site-averaged $^{34}\beta$ of the dimer (equivalent to 5‰) illustrate how computed fractionation relationships may be influenced due to a potential overestimation of the dimer S–S bond length. In this case, the fractionation factor $^{34}\alpha_{dimer/HSO3-(T)}$ is >1 for both ionic strength conditions and the overall influence of the dimer is to enhance fractionations between aqueous S(IV) and gaseous SO_2. We cannot presently confirm the validity of our dimer calculations due to potentially poor constraints on structure, and so it is possible that the dimer plays a different role than we have computed.

Based on the seeming linearity of his dataset, Eriksen (1972c) reasoned that the dimer could be ignored and he regressed his data presented in Fig. 12 to obtain constraints

for the $^{34}\alpha_{SO2(aq)\text{-}SO2(g)}$ and $^{34}\alpha_{HSO3(T)\text{-}SO2(g)}$ fractionation factors from the end member cases of $\chi_{SO2(aq)} = 0$ and $\chi_{SO2(aq)} = 1$. This yields $1000\ln{}^{34}\alpha_{SO2(aq)\text{-}SO2(g)} = 0.9 \pm 0.4‰$ and $1000\ln{}^{34}\alpha_{HSO3(T)\text{-}SO2(g)} = 9.9 \pm 1‰$ (1 s.e., note: the latter fractionation determined this way at 25, 35, and 45 °C are those that are plotted in Fig. 11), where the latter is slightly lower in magnitude but unresolvable from the experiments reported in Eriksen (1972a). These are highly comparable to our theoretical fractionation factors of $1000\ln{}^{34}\alpha_{SO2(aq)\text{-}SO2(g)} = 1.8‰$ and $1000\ln{}^{34}\alpha_{HSO3(T)\text{-}SO2(g)}$ of 11.2 and 8.8‰ (±1‰, 1 s.e.) using isomerization quotients determined at ionic strength of 0 and 1 *m*, respectively (see Section 5.4.1.3 for detailed discussion of the $SO_{2(aq)}/SO_{2(g)}$ fractionation factor). Although the estimates of Eriksen (1972c) are within the uncertainty of the determinations from Eriksen (1972a), the slightly lower magnitudes of Eriksen (1972c) may reflect the slight influence of the dimer on the bulk fractionation behavior of the system. Further experimentation in this system may allow this hypothesis to be tested.

5.4.1.3. Solvated vs. gaseous sulfur dioxide: $SO_{2(aq)}/SO_{2(g)}$

Eriksen, 1972b, Eriksen, 1972c, and Chmielewski et al. (2002) provide estimates of the $^{34}\alpha$ fractionation factor between gaseous and solvated sulfur dioxide. These determinations are plotted in Fig. 13 with our computed $^{34}\alpha$ fractionation factor based on the $SO_{2(30H2O)}$ and $SO_{2(vacuum)}$ calculations. The experiments of Eriksen (1972b) overlap with our calculated fractionation factors within experimental uncertainty but it is clear that the uncertainties in the experimental fractionation factors (reflecting experimental reproducibility) may be as large or larger than the magnitude of the fractionation factor itself and so make the comparison difficult. Estimates from the Eriksen (1972c) experiments are reported to be more precise and seem to record an inverse fractionation relationship with temperature, which is neither predicted from the theoretical calculations nor is observed in the more recent and detailed experiments of Chmielewski et al. (2002). Our calculations appear to agree with the experiments of Chmielewski et al. (2002) in terms of both temperature dependence and magnitude, where the experiments are within ca. $\leqslant$ 0.5‰ of the calculations. The ca. $\leqslant$0.5‰ offset between the Chmielewski et al. (2002) experiments and our calculations is systematic and could be within the uncertainties/error of both determinations. Application of the CCSD/aug-cc-pVTZ-derived harmonic scaling factor of 1.02 does not decrease the offset with the experiments substantially (~0.1‰ at 25 °C). Using only the SO_2 calculations in the gas phase at the CCSD/aug-cc-pVTZ and B3LYP/6-31+G(d,p) level, we can derive a scaling factor on the order of 1.065 for SO_2 alone that may be more appropriate to use in this case. When applied to our harmonic frequencies, the

estimated $SO_{2(aq)}/SO_{2(g)}$ fractionation factor shifts to better agreement with the Chmielewski et al. (2002) experiments: $1000\ln(^{34}\alpha_{SO2\cdot30H2O/SO2(vacuum)}) = 2.1‰$ at 25 °C.

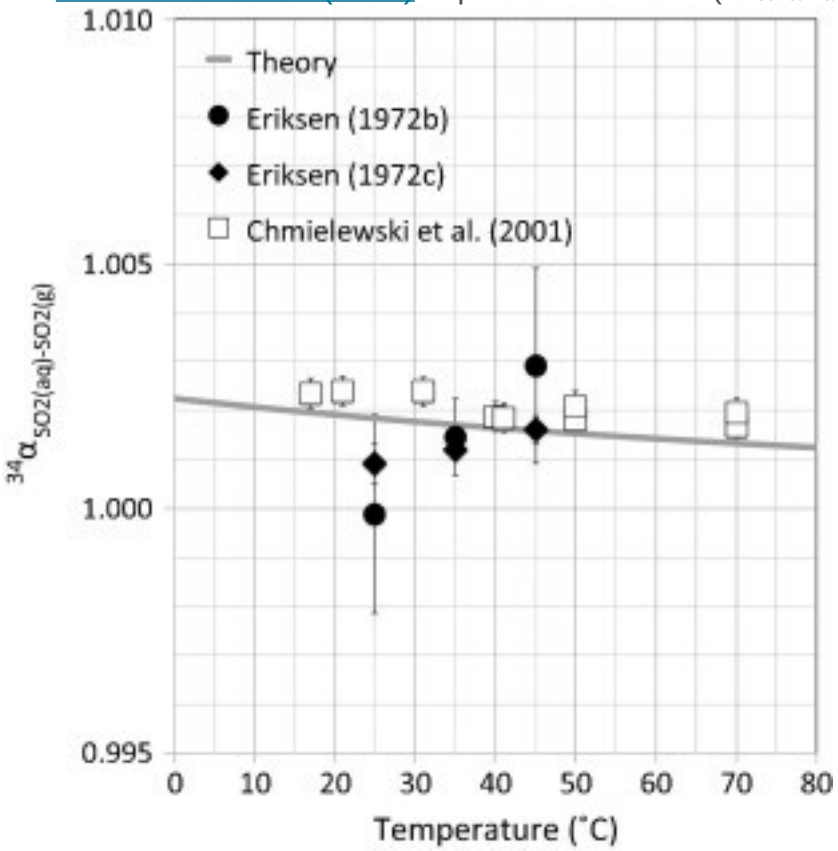

1. Download high-res image (141KB)
2. Download full-size image

Fig. 13. The major isotope fractionation factor between aqueous and gaseous sulfur dioxide. The curves represent our theoretical values and the data points represent experimental values from Eriksen (1972b)(black circles), Eriksen (1972c) (black diamonds), and Chmielewski et al. (2002) (white squares).

An additional consideration is the pH of the experiments of Chmielewski et al. (2002) (not reported) and whether or not any bisulfite may have been present in the experimental solutions that may have biased the fractionation between aqueous S(IV) and gaseous SO_2towards higher values. Even between a pH of 0.5 and 1, bisulfite (sum of both isomers) comprises between ca. 4 and 12% of the total S(IV) in solution at low ionic strength (μ = 0 *m*; Beyad et al., 2014). With ca. 4 % of bisulfite present in solution (corresponding to a pH ~ 0.5 at low ionic strength) and the remaining being $SO_{2(aq)}$, we calculate a fractionation factor between S(IV) in solution and gaseous SO_2 of ~2.2‰ at 25 °C based on our calculated $^{34}\beta$ values and assuming the isomerization quotient at low ionic strength (Q_i = 2.57 ± 0.5; Risberg et al., 2007), which is ~0.4‰ higher than our

computed $SO_{2(aq)}/SO_{2(g)}$ fractionation factor and can account for much of the apparent offset between theory and experiment. We cannot uniquely attribute the offset between theory and experiment in this case to either pH/speciation or error in the theoretical calculations but our analysis nevertheless further highlights the strong role of speciation in influencing fractionation behavior in aqueous S(IV) systems.

5.4.1.4. Predicted fractionations: $[HSO_3^-]_T/[SO_3^{2-}]$

The isomerization of bisulfite appears to exert a strong influence on the observable fractionations between bulk bisulfite and sulfur dioxide in the gas phase and there are similar consequences for fractionation behavior between bulk bisulfite and sulfite in solution. Presently, there do not appear to be any experimental constraints for fractionations among sulfite species in solution and, thus, our theoretical estimates appear to represent the first constraints on these fractionations. Fig. 14 plots the calculated fractionation factors between bisulfite species and sulfite as a function of temperature.

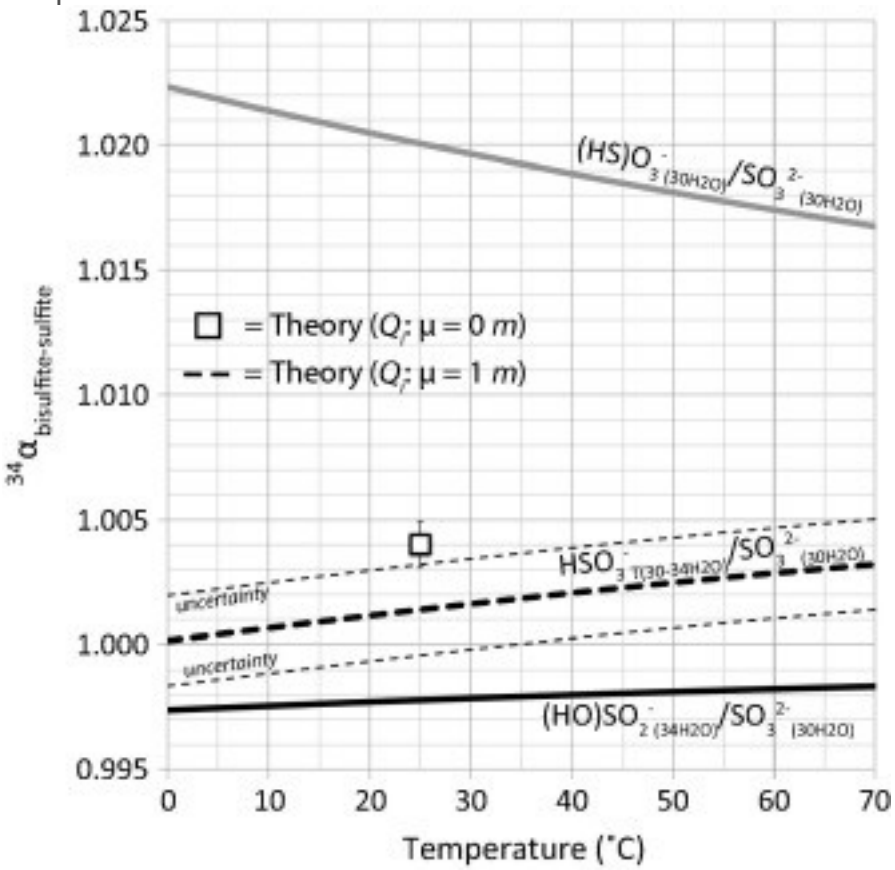

1. Download high-res image (212KB)
2. Download full-size image

Fig. 14. Theoretical estimates/predictions of the major isotope fractionation factors among the anions in the sulfite system: sulfite *sensu stricto* (SO_3^{2-}) and the

two isomers of bisulfite. The open (white) square and the thick dashed curve are the predicted bulk fractionation factors between bisulfite and sulfite using the isomerization quotients at ionic strengths of 0 *m* (Risberg et al., 2007) and 1 *m* (Horner and Connick, 1986, Littlejohn et al., 1992), respectively, following Eq. (13) in the text.

Using the isomerization quotients as a function of temperature at μ = 1 *m* (Horner and Connick, 1986, Littlejohn et al., 1992), we predict the $HSO_{3\ T}^{-}$-SO_3^{2-} fractionation factor following a similar relationship to that of Eq. (10) (Section 5.4.1.1):

(13)34αbisulfite(bulk)/sulfite=Qi(1+Qi)34β(HO)bisulfite+1(1+Qi)34β(HS)bisulfite34βsulfite

With the similarly derived uncertainty envelope estimated only from the uncertainty of the temperature dependence of the isomerization quotient. This prediction yields an apparent *increase* in the bulk bisulfite-sulfite fractionation with increasing temperature. This apparent inverse-fractionation with increasing temperature relationship is due to the combined effects of the small magnitude of the $(HO)SO_2^{-}$-SO_3^{2-} fractionation factor relative to the $(HS)O_3^{-}$-SO_3^{2-} fractionation factor and the increasing proportion of the $(HS)O_3^{-}$ isomer with increasing temperature. In this case, the presence of the minor $(HS)O_3^{-}$ isomer is controlling: (1) the magnitude and potentially the direction of the $HSO_{3\ T}^{-}$-SO_3^{2-} fractionation factor, and (2) the apparent inverse-fractionation-temperature relationship. It is expected that similar relationships would be observed under low-ionic strength conditions, where the absolute magnitude of the fractionation may be slightly higher at any given temperature due to an increase in the proportion of the $(HS)O_3^{-}$ isomer at low ionic strength (see open square data point in Fig. 14; Risberg et al., 2007). Table 2 contains a summary of computed theoretical fractionations vs. the experiments of Eriksen (1972c) and Chmielewski et al. (2002) at 25 °C.

Table 2. Summary of $^{34}S/^{32}S$ based fractionation factors in the sulfite system from experiments and theoretical calculations at 25 °C.

1000ln^{34}α	**Experiment (‰)**	**Theoretical[a] (‰)**
$SO_{2(aq)}$–$SO_{2(g)}$	0 ± 2[a]	1.8
	0.9 ± 0.4[b]	
	∼2.2[c]	
$HSO_{3\ T}^{-}$–$SO_{2(aq)}$	9 ± 1[b]	9.4 ± 0.9 (μ = 0 *m*)
		6.9 ± 0.1 (μ = 1 *m*)
$HSO_{3\ T}^{-}$–SO_3^{2-}	N/A	4.0 ± 0.9 (μ = 0 *m*)
		1.5 ± 0.1 (μ = 1 *m*)

The calculated values involving bisulfite were computed using isomer proportions from quotients determined at ionic strength of 0 *m* (Risberg et al., 2007) and 1 *m* ionic strength (Horner and Connick, 1986). Uncertainties on the calculated values solely represent the propagated uncertainties on the isomerization quotients reported at 25 °C in the references.

a

Eriksen (1972b).

b

Eriksen (1972c).

c

Chmielewski et al. (2002).

*

Computed at the B3LYP/6-31+G(d,p) level.

5.4.2. Sulfoxylate system: general predictions

As in the sulfite system, isotope partitioning in the sulfoxylate system will depend on the isomerization of sulfoxylic acid and the bisulfoxylate species (the dominant forms of sulfoxylate under most environmentally relevant conditions; Makarov et al., 2010), which is presently not constrained in aqueous solutions. The 3-fold coordinated HS-bonded isomers in the sulfoxylate system are computed to be highly fractionated (∼14–15‰ at 25 °C) relative to their respective two-fold coordinated HO-bonded isomers (Fig. 9). Depending on the relative stabilities of these isomers, equilibrium isotope partitioning in the sulfoxylate system could be as equally (or more) complex as the sulfite system. Similar effects relating to the relative distributions of isomers as a function of temperature and ionic strength could come into play, leading to complex isotope fractionations as a function of solution conditions. Research directed at determining the distribution of these isomers in solution over a wide range of environmental conditions is needed before any detailed assessment of isotope partitioning in this system can be made. The further detection and quantification of unbound sulfoxylate species associated with chemical and enzymatic transformations (e.g., dissimilatory sulfite reductase) would also allow an assessment of the importance of these aqueous species in widespread sulfur cycling processes like dissimilatory sulfate reduction.

5.4.3. Sulfide system

The major isotope fractionation factor ($^{34}\alpha$) between aqueous and gaseous H_2S ($H_2S_{(aq)}$-$H_2S_{(g)}$) at low temperature (ca. 0–100 °C) has been previously determined experimentally (Fry et al., 1986, Geßler and Gehlen, 1986, Szaran, 1996) and estimated theoretically

by Czarnacki and Hałas (2012). A summary of these determinations and our own estimate from the H_2S_{30H2O}-H_2S_{vacuum} calculations is presented in Fig. 15. Our calculated $H_2S_{(aq)}$-$H_2S_{(g)}$fractionation factor based on our H_2S_{30H2O}-H_2S_{vacuum} calculations at the B3LYP/6-31+G(d,p) level of theory is indistinguishable from the previous theoretical constraints based on the H_2S_{5H2O}− H_2S_{vacuum} calculations of Czarnacki and Hałas (2012) at both the B3LYP/6-311++G(d,p) and MP2/6-311++G(d,p) levels of theory, which represent the largest basis set and explicit solvation ($5H_2O$) applied in their study. Their calculations utilized a larger basis set (and a higher-level theoretical method in the case of the MP2 calculations)—implementing the triple zeta basis set, rather than double zeta, with diffuse functions added to the hydrogen atoms—but much smaller H_2O clusters than what we have computed. Their H_2O computations coordinated the H_2S molecule in ring structures ranging from 2 to $5H_2O$ molecules that did not approximate a complete solvation shell. Their theoretical estimates are effectively identical to our own and, taken together, broadly agree with the available experimental constraints, although the experimental constraints exhibit considerable variability from study to study.

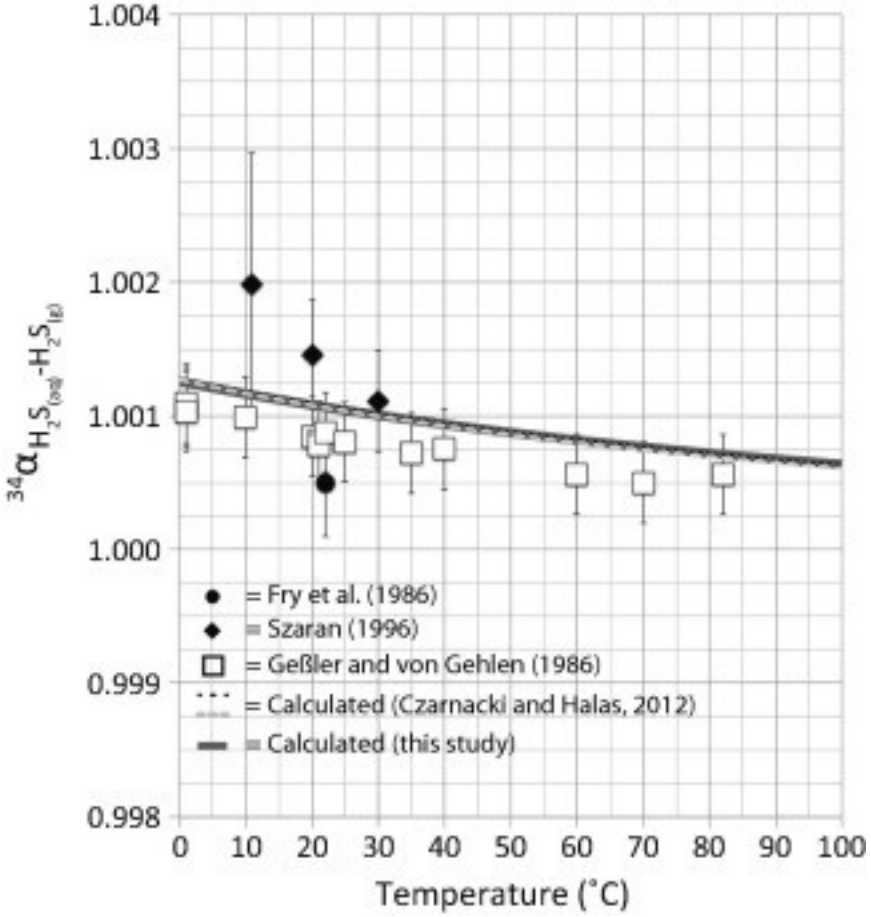

1. Download high-res image (211KB)

2. Download full-size image

Fig. 15. The major isotope fractionation factor between aqueous and gaseous hydrogen sulfide (H_2S). The curves represent our theoretical values and those of Czarnacki and Hałas (2012) and the data points represent experimental values from the literature.

The most detailed experimental constraints as a function of temperature come from Geßler and Gehlen (1986) and display a very similar temperature dependence to the theoretical constraints and quantitatively agree with the theoretical estimates within about ~0.3‰ at all determined temperatures. The slight ~0.3‰ offset is systematic and may be reasonably assumed to be within the uncertainties of the respective experimental and theoretical approaches. The determinations of Szaran (1996) are typically higher in magnitude and appear to display a steeper temperature dependence than either the theoretical estimates or Geßler and Gehlen (1986); because of this disagreement (especially with respect to the temperature dependence), it may be reasonably assumed that the experiments of Szaran (1996) do not represent true equilibrium values. The singular determination of Fry et al. (1986) at 22 °C is slightly lower than the Geßler and Gehlen (1986) but is still within the uncertainty of their data. Fry et al. (1986) and Geßler and Gehlen (1986) also provided constraints on the $H_2S_{(aq)}$-$HS^-_{(aq)}$ fractionation factor by measuring the isotopic fractionation between gaseous H_2S and dissolved sulfide in solution as a function of pH at ca. room temperature (22 °C and 20 °C, respectively). Their determinations are plotted with our theoretical estimate from our H_2S_{30H2O}-HS^-_{30H2O} calculations in Fig. 16. In either experimental case, the fractionation factor was estimated by coupling the determinations of the fractionation factor $H_2S_{(aq)}$-$H_2S_{(g)}$at low pH, then measuring the same fractionation in solutions of higher pH where both $H_2S_{(aq)}$ and $HS^-_{(aq)}$ are present in solution, utilizing information about the dissociation quotient ($H_2S_{(aq)} \rightleftharpoons HS^-_{(aq)} + H^+$, estimated as $\log Q_{d1} \sim 7$ in either case) to back out an estimate for the $H_2S_{(aq)}$-$HS^-_{(aq)}$ fractionation factor by either simple mass balance calculations (Fry et al., 1986) or graphically in the case of Geßler and Gehlen (1986). These two experimental investigations yield slightly different estimates for the $H_2S_{(aq)}$-$HS^-_{(aq)}$fractionation factor at ca. room temperature in solution: Fry et al. (1986) obtain a $^{34}\alpha$ for $H_2S_{(aq)}$-$HS^-_{(aq)}$ of 1.0026 ± 0.0002 (1 s.d., two experiments) at 22 °C and Geßler and Gehlen (1986) estimate a value of ~1.0046 at 20 °C. Our theoretical value falls in between these estimates ($^{34}\alpha$ = 1.0033 at 20 °C).

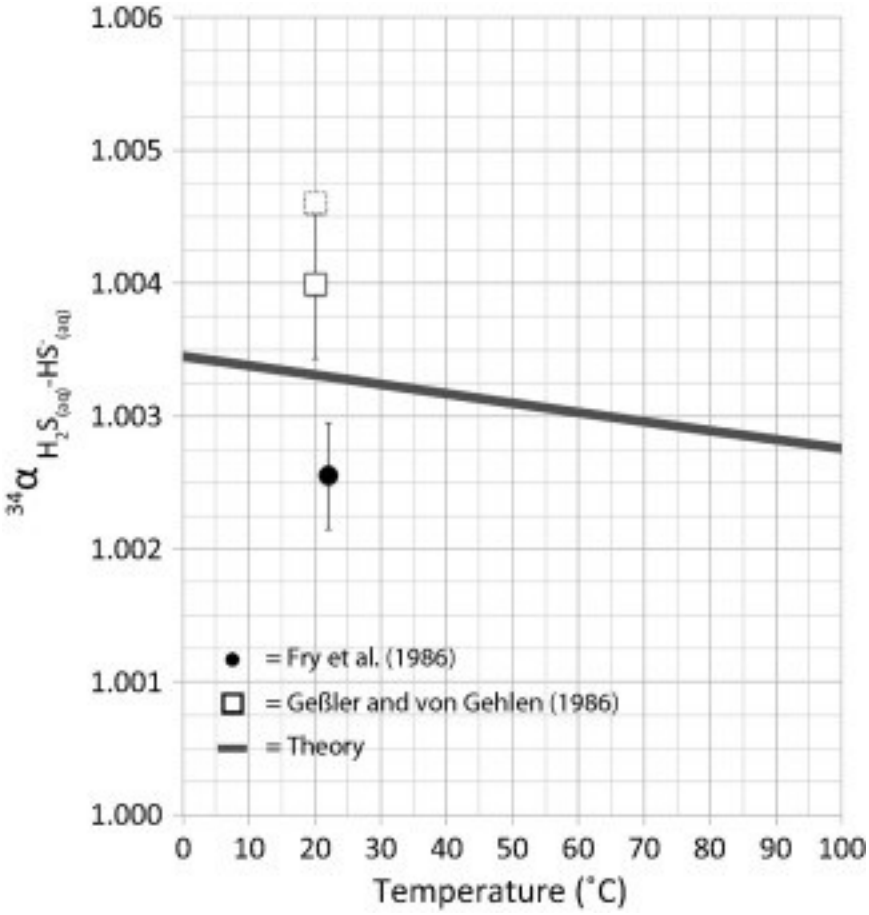

1. Download high-res image (169KB)
2. Download full-size image

Fig. 16. The major isotope fractionation factor between the two predominate aqueous sulfide species, $H_2S_{(aq)}$ and $HS^-_{(aq)}$, where curves represent our theoretical values and the data points are experimental constraints. The dashed white square is the estimate from Geßler and Gehlen (1986) and the solid white square is our own re-estimate using their data and the dissociation quotients as a function of ionic strength from Hershey et al. (1988) (see Section 5.4.3 for further explanation).

A primary difference between the experimental approaches of Fry et al. (1986) and Geßler and Gehlen (1986) is in how pH was adjusted and the resulting changes in ionic strength that ensued. We hypothesize that changes in the dissociation quotient due to ionic strength could have lead to an overestimation of the $H_2S_{(aq)}$-$HS^-_{(aq)}$ fractionation factor by Geßler and Gehlen (1986) and may also have influenced the determination in Fry et al. (1986). Fry et al. (1986) did not completely describe the ionic strength conditions of their experiments, only that they worked from stock sulfide solutions (very basic when prepared from Na_2S crystals) and adjusted to the desired pH using phosphoric acid. They computed their $H_2S_{(aq)}$-$HS^-_{(aq)}$ fractionation factor using a

dissociation quotient for low ionic strength media ($\log Q_{d1}$ = 7.04; consistent with the thermodynamic value of 7.02 at 22 °C and μ = 0 *m;*Hershey et al., 1988). From the description of the Fry et al. (1986) experiments, it is difficult to assess how ionic strength may have influenced their results, but because much more detail is provided in the Geßler and Gehlen (1986) study, we can make quantitative reinterpretations of their data.

Geßler and Gehlen (1986) measured fractionations between $H_2S_{(g)}$ and $H_2S_{(aq)T}$($H_2S_{(aq)T}$ = $H_2S_{(aq)}$ + $HS^-_{(aq)}$) at 20 °C as a function of pH utilizing different concentrations of NaOH (up to 2 M NaOH for the highest pH measurements), significantly changing ionic strength from experiment to experiment. At 20 °C, the first dissociation quotient of $H_2S_{(aq)}$(Q_{d1}) varies as a function of ionic strength from pQ_{d1} = 7.05 at μ = 0 *m* to 6.72 at μ = 1 *m*(Hershey et al., 1988; NaCl media) and it appears Geßler and Gehlen (1986) assumed a constant $\log Q_{d1} \sim 7$ for their graphical estimation. We re-estimate the $H_2S_{(ag)}$/$HS^-_{(aq)}$fractionation factor at 20 °C from their data using the following simple mass balance relationship (solving for $^{34}\alpha_{HS\text{-}/H2S(aq)}$):

(14)34αS(II)T(aq)/H2S(g)=34αH2S(aq)/H2S(g)[χH2S(aq)+34αHS-/H2S(aq)χHS-]

where $\chi_{H2S(aq)}$ and $\chi_{HS\text{-}(aq)}$ are the mole fractions of H_2S and HS^- in solution, which we estimated here by utilizing the Q_{d1} as function of ionic strength from Hershey et al. (1988), and estimating the ionic strength from the reported NaOH concentration (ignoring the slight difference between molarity and molality) and the reported pH. The $^{34}\alpha_{TOTAL(aq)–H2S(g)}$ is the measured fractionation between total aqueous sulfide and $H_2S_{(g)}$ at a given pH and [NaOH] and $^{34}\alpha_{H2S(aq)\text{-}H2S(g)}$ = 1.0008 (approximately invariant over the ionic strength range ∼0–2 M; Geßler and Gehlen, 1986). These data are not tabulated in the original publication and, thus, the $^{34}\alpha_{TOTAL(aq)–H2S(g)}$, pH, and [NaOH] were estimated from the published figures (corresponding to the experiments performed at [NaOH] = 0.05, 0.2, 0.5, 1.0, 1.5, and 2.0 M). This procedure yields a re-estimated $^{34}\alpha$ between $H_2S_{(aq)}$/$HS^-_{(aq)}$ of about 1.0040 ± 0.0003 (1 s.d. of 6 experiments), slightly lower than their estimated value of 1.0046, and consistent with our interpretation that their usage of a constant Q_{d1} over an ionic strength range of ∼0–2 M lead to an overestimation of the fractionation factor. This re-estimated fractionation factor is plotted Fig. 16 in addition to their original estimate. Our theoretical estimation based on the HS^-_{30H2O} and H_2S_{30H2O} calculations plots directly in between the Fry et al. (1986) determination and our re-estimated value from Geßler and Gehlen (1986) and is within ∼0.7‰ of each. Future experimental investigations of these fractionation factors as a function of temperature and ionic strength will allow for a more detailed comparison to our theoretical constraints.

5.4.4. Equilibrium isotope effect between sulfate and sulfide

Our calculations of the $^{34}\beta$ of sulfide species (principally H_2S_{30H2O} and HS^-_{30H2O}) and the sulfate anion ($SO_4^{2-}{}_{30H2O}$) can be used to provide new constraints on the equilibrium isotope effect between the two end-member oxidation states of sulfur for use in both high-temperature and low-temperature (principally biological) applications. Fig. 17 plots the computed $^{33}\alpha$ and $^{34}\alpha$ for $SO_4^{2-}{}_{30H2O}$-H_2S_{30H2O} (solid grey curves) and $SO_4^{2-}{}_{30H2O}$-HS^-_{30H2O} (dashed grey curves) along with the empirical relation derived from experimental data compiled in Ohmoto and Lasaga (1982) (solid black line, ~200–400 °C) and the recent experiments of Syverson et al. (2015), which were the first to measure $^{33}\alpha$ fractionations in this system. (Calculations of the S^{2-} ion are not included due to its likely negligible abundance over a wide range of pH and T conditions; Ellis and Giggenbach, 1971, Schoonen and Barnes, 1988, Migdisov et al., 2002). Due to the extremely low rates of isotope exchange between sulfide species and sulfate at low temperature (*cf.*Ohmoto and Lasaga, 1982), the experimental constraints all fall within the 200–400 °C temperature range. Ohmoto and Lasaga (1982) reported an experiment performed at 100 °C but it did not come at all close to equilibrating; the measured fractionation between sulfate and sulfide after 240 h of reaction time only approached ~4‰. The reported fractionation factor for 100 °C in their paper ($^{34}\alpha_{\text{sulfate-sulfide}}$ ~1.048) is simply the value calculated from their extrapolated empirical temperature dependence over the 200–400 °C range, from with they estimated a rate for isotopic exchange at this temperature based on how far the experimental fractionation was from the extrapolated value.

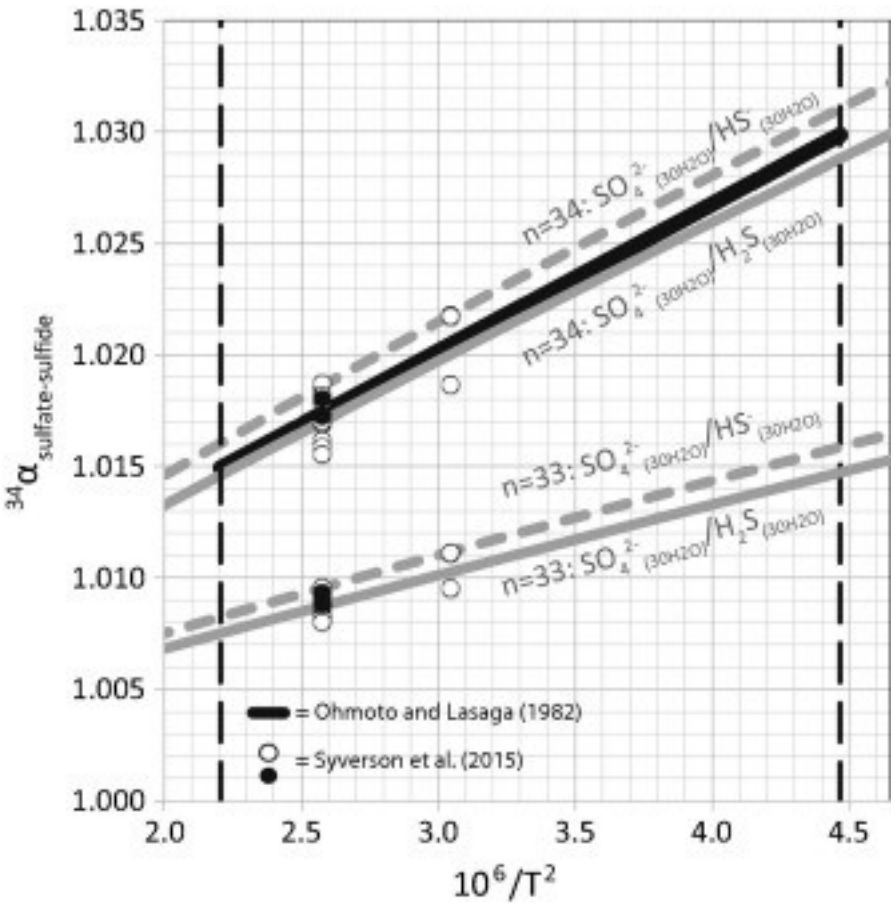

1. Download high-res image (247KB)
2. Download full-size image

Fig. 17. Comparison of our theoretical estimations of fractionations between sulfate and sulfide (gray curves; solid and dashed indicate H_2S and HS^-, respectively) and the available experimental constraints at high temperature (200–400 °C, indicated by dashed vertical lines). The black curve is derived from a compilation of experimental data by Ohmoto and Lasaga (1982). The data points (circles) are the recent experimental values derived from the $FeS_{2pyrite}$-H_2S-SO_4^{2-} system, where black circles indicate demonstrably equilibrated experiments via mass dependent relationships (see Section 5.4.4 for further explanation).

The estimate from our $SO_4^{2-}{}_{30H2O}$-H_2S_{30H2O} calculations is consistent with the empirical relationship of Ohmoto and Lasaga (1982) over the 200–400 °C temperature range, where the maximum displacement of the two curves approaches ~1‰ at the lowest temperature in this range (200 °C). Additionally, the Ohmoto and Lasaga (1982) curve plots in between the computed fractionation factors for $SO_4^{2-}{}_{30H2O}$-H_2S_{30H2O} and $SO_4^{2-}{}_{30H2O}$-HS^-_{30H2O}. As inferred from their tabulated data, the experiments from which Ohmoto and Lasaga (1982)derived this empirical relation were mostly performed at low *in situ* pH

conditions (where H_2S is dominant) but some of the experiments were performed at higher pH where the HS^- ion may have been present in appreciable amounts; the $SO_4^{2-}{}_{30H2O}$-$HS^-{}_{30H2O}$ curves are presented mostly for reference and to illustrate the effects of simple speciation. The experiments from which this relation is derived may also have exhibited more complex *in situ* speciation than we have calculated (e.g., ion pairs of HS^- and SO_4^{2-} with Na^+ and protonated forms of sulfate, principally HSO_4^-). We would expect the differences in the SO_4^{2-}-H_2S and the HSO_4^--H_2S fractionation factor to be minimal (especially over 200–400 °C) because protonation is on one of the oxygen atoms in sulfate (*cf.* sulfite and sulfoxylate species as computed here) and perhaps similarly small for ion pairs forming with sulfate for similar reasons. The formation of ion pairs that involve direct interactions with sulfur, such as $NaSH^0$, may have greater effects. Complications due to our relatively simplified treatment of speciation may account for some of the small displacement between the theoretical and empirical curves. Errors in the empirically derived relationship may also be present (e.g., biased high due to quenching effects, disequilibrium, etc.)—noting that Ohmoto and Lasaga (1982) had only the major isotope ratio, $^{34}S/^{32}S$, with which to judge equilibrium from the available experiments.

The small, apparent divergence of the Ohmoto and Lasaga (1982)-derived sulfate/sulfide fractionation factor and our own based on the $SO_4^{2-}{}_{30H2O}$-H_2S_{30H2O} calculations at the low temperature end (~200 °C) may also be within the uncertainty of the theoretical calculations. The combination of effects related to anharmonicity, inadequacies in the theoretical method, and cluster geometry variability may contribute permil level error/uncertainty in computed fractionation factors. To explore this more quantitatively, we will focus on errors arising from inadequacies in the theoretical method that may represent the major source of error in the calculations. When we apply our CCSD/aug-cc-pVTZ-derived harmonic scaling factor of 1.01–1.02 to the harmonic frequencies for the SO_4^{2-} and H_2S $30H_2O$ clusters, the resulting fractionation factors appear to come into more quantitative agreement with the Ohmoto and Lasaga (1982) curve over the entire experimental temperature range (Fig. S.4), which might suggest much of the apparent discrepancy results from inadequacies in the theoretical method employed in the present study. Since the discrepancy is small (sub-permil), we cannot rule out contributions from the other factors discussed above.

For comparison, we also plot in Fig. S.4 other theoretical estimates based on our own calculations of $H_2S_{(vacuum)}$ and $SO_4^{2-}{}_{(vacuum)}$ using the IEF-PCM solvation model (without any form of frequency scaling) and previous theoretical calculations utilizing experimentally-derived fundamental frequencies and frequency shifts for the minor isotopes (Ono et al.,

2007), both of which are several permil displaced from the experimental constraints and our 30H_2O cluster calculations. Comparison to our IEF-PCM calculations further emphasizes the long-understood need for explicit solvation models in placing theoretical fractionation factors more quantitatively in-line with experimental fractionation factors in aqueous systems.

Our theoretical predictions also appear to be in reasonably good agreement with the recent experimental constraints of Syverson et al. (2015) who investigated equilibrium isotope fractionations ($^{33}\alpha$ and $^{34}\alpha$) in the H_2S-SO_4^{2-}-FeS_2 system at 300 °C and 350 °C. Their constraints at 350 °C are perhaps more quantitatively robust as these experiments were pursued at longer run times than the lower temperature experiments, and also in greater numbers. The starting solutions were comprised of sodium thiosulfate in acidic ferrous solutions. Upon ramping up the temperature to experimental conditions, thiosulfate undergoes quantitative hydrolytic disproportionation to sulfate and sulfide in 1:1 M ratios. Since the sulfate and sulfide produced this way tended to have resolvable $\Delta^{33}S$ values as judged from the shortest experimental runs (a mass-conservation disequilibrium effect), this approach allowed for the direct monitoring of equilibrium. Fig. 17 shows all of their reported fractionations between sulfate and sulfide, which represent a wide range of experimental run times (ranging from <1 h up to 4,297 h as the longest experimental run). The lowest fractionations measured were typically those that were run for the shortest times and had not achieved isotopic equilibrium. The data points plotted as black circles are from end-run experimental analyses that indicated isotopic equilibrium between sulfate and sulfide by way of identical $\Delta^{33}S$ values between sulfate and sulfide within analytical uncertainty (their experiments labeled: 2–4, 4–4). When taken as an average for the 350 °C determination, the demonstrably equilibrated experiments yield fractionation factors of $^{33}\alpha_{\text{sulfate-sulfide}}$ = 1.0091 ± 0.0003 and $^{34}\alpha_{\text{sulfate-sulfide}}$ = 1.0176 ± 0.0006 (1 s.d.), which agree well with our estimated $^{33}\alpha_{\text{sulfate-sulfide}}$ = 1.0087 and $^{34}\alpha_{\text{sulfate-sulfide}}$ = 1.0170 from the $SO_4^{2-}{}_{30H2O}$-H_2S_{30H2O} calculations. We note that application of the CCSD/aug-cc-pVTZ-derived 1.01–1.02 harmonic scaling factors puts the theoretical fractionation factors at $^{33}\alpha_{\text{sulfate-sulfide}}$ = 1.0089–1.0091 and $^{34}\alpha_{\text{sulfate-sulfide}}$ = 1.0173–1.0177 from the $SO_4^{2-}{}_{30H2O}$-H_2S_{30H2O}calculations at 350 °C.

The apparent agreement with high temperature experiments suggest that our calculations may yield reasonable estimations of these fractionations at low-temperature conditions as well (*cf.*Schauble, 2004), although it is important to note that any systematic errors in the calculations will scale inversely with temperature. Due to the extremely low rates of isotope exchange between sulfate and sulfide at low temperature, the only other low temperature constraints have relied either on BM

calculations utilizing experimental vibrational spectra(fundamental frequencies) and frequency shifts for the minor isotopes via force field models (e.g., Sakai, 1968, Farquhar et al., 2003, Ono et al., 2007) or, in perhaps the least ideal case, extrapolating the empirical temperature dependence of high-temperature constraints to low temperatures (from Ohmoto and Lasaga, 1982). Neither approach is strictly valid—for example, computing RPFRs from experimental fundamental frequencies via the BM-equation violates the harmonic oscillator approximations used in its derivation (*cf.*Liu et al., 2010)—and so our calculations may provide some of the most reliable estimates to date at low-temperature within the harmonic approximation. The low temperature fractionations computed via our calculations will likely have the most applicability to network models of isotope partitioning for sulfate reducing organisms (*cf.*Wing and Halevy, 2014), as well as the estimation of sulfate-sulfide equilibration rates from non-equilibrated low-temperature experiments (*cf.* approach of Ohmoto and Lasaga, 1982). Fig. 18 presents the data of Fig. 17 with an expanded temperature range (down to the equivalent of 0 °C) and includes data from recent experiments from sulfate reducing organisms that have produced the largest fractionations between sulfate and sulfide that have been measured to date (Canfield et al., 2010, Sim et al., 2011a, Leavitt et al., 2013). It has been postulated that the maximum isotope fractionations possible in a sulfate reducing organism approach the equilibrium fractionation factor between sulfate and sulfide species at the given growth temperature (*cf.*, Sim et al., 2011a, Wing and Halevy, 2014), which is based on the consistency between some of the largest fractionations observed in certain cultures of sulfate reducers and the available constraints on equilibrium fractionations. Using the Sim et al. (2011a) and Sim et al. (2011b) pure culture (*Desulfovibrio* sp., DMSS-1) dataset as an example (also, see Leavitt et al., 2013 and Wing and Halevy, 2014), as cell specific sulfate reduction rates approach extremely low values, the magnitude of the observed $^{33}S/^{32}S$- and $^{34}S/^{32}S$-based fractionation factors between sulfate and sulfide appear to approach near their expected equilibrium values (Fig. 18; see also Fig. S.5). The largest fractionation reported between sulfate and sulfide from the Sim et al. dataset is $^{34}\alpha_{sulfate\text{-}sulfide}$ ~1.0656 ± 0.0003 with a corresponding observed $^{33}S/^{32}S$- and $^{34}S/^{32}S$-based exponent of 0.5142 ± 0.0002 (~20 °C; Sim et al., 2011a). From this perspective, at 20 °C our calculations would predict a $^{34}\alpha_{sulfate\text{-}sulfide}$ for $SO_4^{2-}{}_{30H2O}$-H_2S_{30H2O} of 1.0674 and a $SO_4^{2-}{}_{30H2O}$-$HS^-{}_{30H2O}$ 1.0709, with corresponding $^{33/34}\theta_{sulfate\text{-}sulfide}$ of 0.5147 and 0.5148, respectively. We note that applying our CCSD/aug-cc-pVTZ-derived harmonic scaling factors of 1.01–1.02 will increase the $^{34}S/^{32}S$-based fractionation factor estimates slightly: for $SO_4 2-_{30H2O}$-H_2S_{30H2O} = 1.0685–1.0696 and $SO_4^{2-}{}_{30H2O}$-$HS^-{}_{30H2O}$ = 1.0720–1.0732 at 20 °C, which may be

appropriate in this case due to the enhanced agreement with Ohmoto and Lasaga (1982) at high temperature. Our calculations do not confirm or sufficiently test any hypotheses regarding the controls on fractionation magnitudes in sulfate reducing organisms, but may provide end-member constraints for isotope fractionation network models that use equilibrium fractionation factors (e.g., Wing and Halevy, 2014).

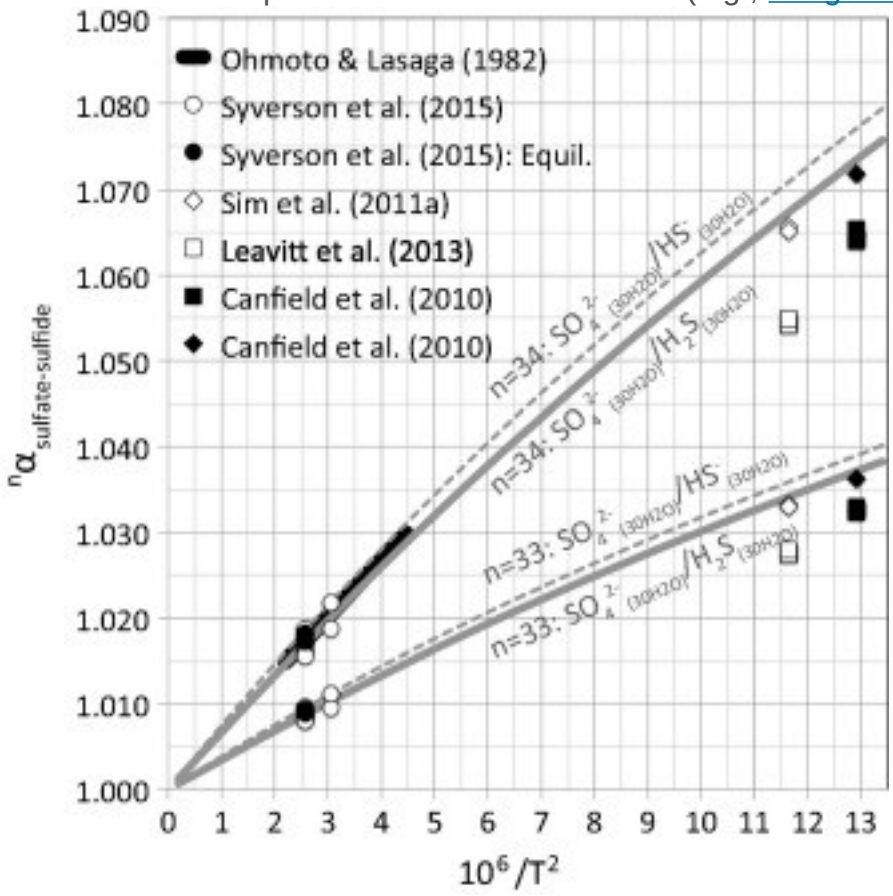

1. Download high-res image (275KB)
2. Download full-size image

Fig. 18. Comparison of our theoretical estimations of fractionations between sulfate and sulfide (gray curves; solid and dashed indicate H_2S and HS^-, respectively) and the available experimental constraints plotted from ambient to high temperature (0–2000 °C). Labeling is same as in Fig. 17. Also included for reference are the largest fractionations reported in microbial sulfate reduction experiments at ambient T: (1) Pure culture experiments: white squares (Leavitt et al., 2013) and white diamonds (Sim et al., 2011a) and (2) experiments with natural populations (Canfield et al., 2010): water incubations = black squares and sediment incubations = black diamonds.

5.4.5. Fractionations within and between thiosulfate and the major sulfide species

The isotope fractionations associated with isotope exchange between the “outer” (**S**-SO_3^{2-}; “sulfane”) and “inner” (S-**S**O_3^{2-}; “sulfonate”) sulfur atoms in thiosulfate ($S_2O_3^{2-}$), as well as those between these two sites and aqueous sulfide (i.e., $H_2S_{(aq)}$/$HS^-_{(aq)}$) have been studied experimentally (Uyama et al., 1985) and reinterpreted in terms of exchange rates and slightly revised equilibrium fractionation factors in follow up studies (Chu and Ohmoto, 1991, Chu et al., 2004). Fig. 19 plots the experimentally derived fractionation factors ($^{34}\alpha$) for S-**S**O_3^{2-}/**S**-SO_3^{2-}, S-**S**O_3^{2-}/H_2S, and **S**-SO_3^{2-}/H_2S (100–170 °C, as compiled/evaluated in Chu et al., 2004; bold and underline emphasizes the sulfur site undergoing exchange in thiosulfate) along with the same fractionation factors computed from our $S_2O_3^{2-}{}_{(30H2O)}$ and $H_2S_{(30H2O)}$ cluster calculations (the same calculations involving $HS^-_{(30H2O)}$ have been omitted for simplicity of graphical presentation, but see discussion below). In terms of fractionation magnitude, the fractionation between the intramolecular sites of thiosulfate appear to be in the most agreement between the experimental dataset and our own calculations, where a slightly steeper temperature dependence is predicted from our calculations than appears to be represented in the experimental dataset.

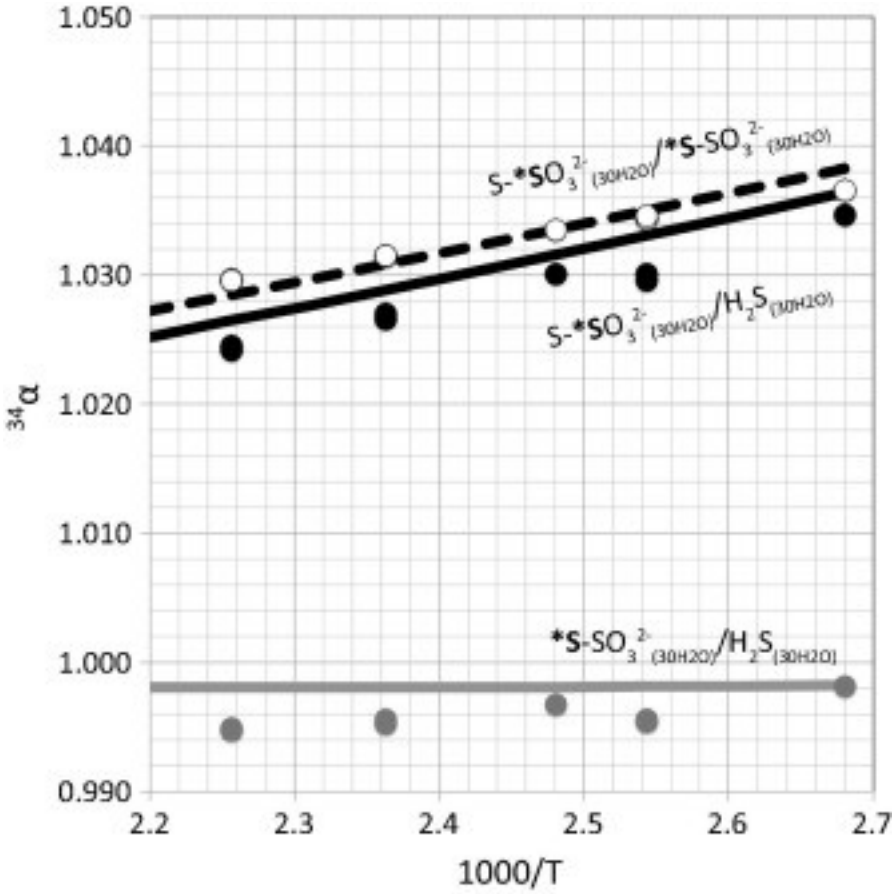

1. Download high-res image (188KB)

2. Download full-size image

Fig. 19. The major isotope fractionation factor for the intramolecular isotope fractionation in thiosulfate(experimental: white circles, our theoretical: dashed black curve), fractionations between the outer ("sulfanyl") sulfur in thiosulfate and $H_2S_{(aq)}$ (experimental: gray circles, our theoretical: gray curve), and the inner ("sulfonate") sulfur in thiosulfate and $H_2S_{(aq)}$ (experimental: black circles, our theoretical: black curve). Experimental data have been derived by Chu et al. (2004) from the experiments of Uyama et al. (1985).

The fractionations predicted from our calculations and the experiments between the two sulfur sites in thiosulfate and H_2S appear to be systematically shifted by a few permil but agree in their temperature dependence. The experimental dataset of Uyama et al. (1985)seems to indicate that the **S**-SO_3^{2-}/H_2S fractionation factor increases in magnitude with increasing temperature over the 100–170 °C range, which the calculations also predict; we find this to be related to a crossover at sub-0 °C temperature. These offsets in the magnitude of the fractionation factors between theory and experiment appear to be the largest we have observed in our overall study and may be on the high end of the estimated uncertainties in the calculations.

The relatively large offset (few permil) between theory and experiment in the thiosulfate/sulfide system may reflect speciation. The experiments were done under *in situ*pH conditions that were circumneutral (ca. 5.4–7.2) where HS^- may be present at appreciable levels at the experimental temperatures (*cf.*Ellis and Giggenbach, 1971, Hershey et al., 1988). However, the computed fractionations between the two sulfur sites in thiosulfate and HS^- do not bring the calculated fractionation factors in better agreement with the experiments. Due to the HS^- ion having a lower $^{34}\beta$ than H_2S, predicted fractionations between S-**S**O_3^{2-}/HS^-, and **S**-SO_3^{2-}/HS^- are shifted upward relative to the H_2S counterparts in Fig. 19, in the opposite direction needed to agree with the experimental datasets. The formation of $NaSH^0$ ion pairs could, in principle, explain some of the offset, but we have not computed this species. In order for the $NaSH^0$ ion pair to account for the several permil offset alone, it would need to be a major species under the experimental conditions and/or have a comparable (or higher) $^{34}\beta$ than H_2S. Applying the harmonic frequency scaling factor of 1.01–1.02 to the frequencies of the sulfide and thiosulfate $30H_2O$ clusters also shifts the predicted fractionation factors in the opposite direction of the experimental constraints on the order of 1–2‰ for the S-**S**O_3^{2-}/H_2S and S-**S**O_3^{2-}/**S**-SO_3^{2-} fractionation factors, and has negligible effect on the smaller **S**-SO_3^{2-}/H_2S fractionation factor. Based on our simple treatment, error arising from the employed theoretical method alone may not be able to explain the systematic

offset between theory and experiment. Based on the present constraints, we cannot rule out contributions from experimental error (e.g., the influence of other sulfur compounds being present, either under experimental conditions or produced/decomposed upon quenching or processing), complex speciation effects, and other errors arising from the calculations (e.g., anharmonic effects and cluster geometry variability) in describing the apparent offset between theory and experiment. The offset is somewhat puzzling given the relatively good agreement between our theoretical calculations and the experiments of the intramolecular fractionation factor for thiosulfate, as well as the H_2S/HS^- fractionation factor (Section 5.4.3), and may indicate further experimentation is warranted in these systems.

5.5. Further implications of isomerization: relative reactivity of $(HO)SO_2^-$ and $(HS)O_3^-$

On the molecular and mechanistic level, the two isomers of bisulfite have been hypothesized to have different reactivity towards oxidants due to the absence of the lone pair of electrons on sulfur in the tetrahedral $(HS)O_3^-$ form, where the pyramidal $(HO)SO_2^-$ containing the lone electron pair on the sulfur atom might be expected to be more reactive (e.g., Yiin et al., 1987, Brandt and van Eldik, 1995). In other words, the $(HS)O_3^-$ isomer is hypothesized to be sterically hindered in terms of reactions requiring access to the sulfur atom, which could be relevant for all redox reactions involving sulfite and bisulfite species (noting that, from this perspective, $(HO)SO_2^-$ and SO_3^{2-} would be expected to behave more similarly in reactions, at least relative to $(HS)O_3^-$). This hypothesis can be extended to the relative reactivity of the isomers towards the active binding sites of intracellular enzymes in biological redox processes (e.g., the heme sites in reductases like dissimilatory sulfite reductase and MccA where binding occurs directly to the sulfur atom; Parey et al., 2010, Hermann et al., 2015), because the lone pair of electrons would be necessary for bond formation to the Fe in the heme groups.

To our knowledge, this hypothesis has yet to be tested rigorously and would be expected to depend on the energetics and rates of tautomerization (i.e., the intramolecular transfer of the proton from the sulfur atom to the oxygen atom):

(15)(HS)O3-→(HO)SO2-Ktautomerization

where $k_{tautomerization}$ represents the rate constant in the direction as indicated. If tautomerization occurs rapidly, perhaps the $(HS)O_3^-$ isomer could tautomerize prior to (or during) a reaction to expose the sulfur atom and its lone pair of electrons for binding or electron transfer in a way that led to minimal discrimination between $(HS)O_3^-$ and $(HO)SO_2^-$during chemical reactions. Alternatively, if tautomerization was slow, the rates

of tautomerization might inhibit reactions involving $(HS)O_3^-$ and lead to an overall discrimination between $(HS)O_3^-$ and $(HO)SO_2^-$.

There are several consequences of the hypothesis that relatively slow tautomerization could lead to a discrimination between the bisulfite isomers during chemical reactions and, in particular, inhibit the reactivity for the $(HS)O_3^-$ isomer. From the standpoint of isotope mass balance, assuming that the bisulfite pool is at isotopic equilibrium prior to reaction, a preference for the $(HO)SO_2^-$ isomer (or SO_3^{2-}) upon reaction would mean that the chemical reaction preferentially samples a fractionated portion of the total sulfite pool, which our calculations predict to be due almost exclusively to the presence of the $(HS)O_3^-$ isomer that has a high $^{34}\beta$ and shifts the other sulfite species towards isotopically lighter values (relative to the total S^{4+} composition). If the isotope effect associated with the chemical reaction is a so-called *normal* kinetic isotope effect (i.e., the typical case in which the light isotopomers react more readily than heavy isotopomers due to the predominating influence of weakly bound transition state(s)), slow tautomerization could lead to an apparent boost in the magnitude of the instantaneous fractionation between the bulk bisulfite pool and the pooled product. However, should the reaction be associated with a so-called *inverse* isotope effect (i.e., the atypical case of the heavy isotopomer reacting more readily than the light isotopomer), the effect of sluggish tautomerization would be less-straightforward: it could either lead to a dampening of magnitude of the apparent fractionation, or could possibly even lead to an apparent reversal in the direction of the fractionation (from inverse to normal) depending on the relative magnitudes of the fractionation associated with the KIE vs. that associated with the EIEs among the sulfite species. The complex speciation of sulfite species in solution may contribute to considerable ambiguity in the meaning of measured isotope effects associated with unidirectional reactions involving sulfite under solution conditions of mixed-species, potentially obscuring any observation of primary kinetic isotope effects.

We consider a simple qualitative example to illustrate hypothetical effects associated with bisulfite isomerization within the basic framework of sulfate reduction. For the sake of this exercise, we first assume that equilibration rates between the sulfite and bisulfite isomers are sufficiently fast that they are in chemical and isotopic equilibrium at all times over all respiration rates and residence times of sulfite species within the cell. We consider a pool of sulfite species being generated via the reduction of APS. Upon the cleavage of the S—O bonds, the sulfite species would enter solution as inorganic anions and immediately undergo hydrolysis reactions to form the different bisulfite isomers, the relative equilibrium distribution of which would depend on the pH,

temperature, and ionic strength conditions of the intracellular aqueous environment. Once equilibrated chemically and isotopically, this pool would be characterized by an isotopically light pool of sulfite *sensu stricto* and $(HO)SO_2^-$ and a relatively heavy pool of $(HS)O_3^-$. The magnitude of the bulk fractionation would depend on the relative distribution of these species and therefore depend on the temperature, ionic strength, and pH of the intracellular environment. If the active siroheme site of dissimilatory sulfite reductase discriminated between the aqueous sulfite species and showed a preference for sulfite *sensu stricto* and/or $(HO)SO_2^-$, the unidirectional reduction of this sulfite could introduce an apparent amplification in the instantaneous fractionation that eventually forms sulfide (all else being equal), which considering mass balance could amount to an amplification on the level of several permil depending on conditions. In this simple case of hypothetical species discrimination, the $(HS)O_3^-$ isomer would effectively be acting as a relative dynamic 'sink' for heavy isotopes within the metabolism. An effect of this kind would be sensitive to temperature due to the increasing proportion of the $(HS)O_3^-$isomer with increasing temperature, which would be significant for sulfate reducers that grow at higher temperatures.

Even given little to no species discrimination with respect to enzymatic redox transformations involving the sulfite species, the presence of the $(HS)O_3^-$ isomer would be predicted to cause shifts in the isotopic mass balance between the bulk intracellular sulfite pool and other downstream and upstream pools in the metabolism. In this case, the magnitudes of these effects would likely depend on the rates of isotopic equilibrium among the sulfite species, especially in how these rates compare to the residence time of total sulfite in the cell. Since the residence time of sulfite species will vary as a function of cell specific reduction rate (which, in turn, is controlled by a wide variety of extra- and intra-cellular environmental and metabolic conditions; *cf.* Wing and Halevy, 2014), the magnitudes of any of the hypothetical effects associated with the $(HS)O_3^-$ isomer could vary over wide ranges of growth conditions.

6. Conclusion

The calculations presented here provide some of the most detailed constraints on sulfur isotope partitioning in the sulfite system available to date, and provide new constraints on fractionation factors involving many of the major aqueous sulfur compounds relevant to hydrothermal and (bio)geochemical cycles. From a detailed comparison to the experimental datasets of Eriksen, the calculations reveal that the isomerization of bisulfite is a major control on isotope partitioning in this system. However, much uncertainty still exists in the isomerization quotient as a function of temperature over a

wide range of ionic strength. Future research should be directed at constraining this quotient over a wide range of conditions (temperature and ionic strength) to more precisely determine its influence in the sulfur cycle. Further detailed experimentation of the equilibrium isotope effects in the sulfite system as a function of temperature and ionic strength could test the predictions made by our theoretical calculations. Due to the complexity of sulfite solutions, precise and species-specific determinations of isotope partitioning in the sulfite system will be reliant upon the combination of experimental and theoretical techniques.

The pH and ionic strength dependency of sulfur isotope partitioning in the sulfite system is predicted to be significant due to the complex speciation of sulfite. Treating the sulfite system in isotope partitioning models strictly as the pyramidal sulfite anion (SO_3^{2-}) (e.g., network models of sulfate reducing metabolisms) is clearly invalid for most conditions relevant to natural systems, particularly intracellular conditions where pH is typically circum-neutral. Future treatment and applications should include all relevant species. Assumptions about similarity in structure between sulfite species and their isotope partitioning behavior should be avoided in any future experimental approaches. It remains to be shown whether or not the two structural isomers of bisulfite behave differently during chemical reactions, but if they do, there could be consequences in isotope fractionations associated with chemical reactions in sulfite media where both isomers are present.

Calculations of the isotope partitioning behavior of the sulfoxylate species have been included here in the hopes of igniting research towards their further characterization in aqueous solutions. As in the sulfite system, isotope partitioning among sulfoxylate species will strongly depend on the isomerization of the protonated species, principally H_2SO_2(sulfoxylic and sulfinic acid) and bisulfoxylate species. Techniques exist for producing these compounds via the decomposition of organic precursors (e.g., thiourea dioxide; Svarovsky et al., 2001, Makarov et al., 2002, Makarov et al., 2010) and so their characterization in aqueous solutions should be possible, in principle. If such species do indeed exist within the MSR framework, their characterization could allow for an even more elaborate understanding of sulfate reduction metabolisms. The role these compounds play in other redox processes (e.g., sulfide oxidation) could further be illuminated and allow for detailed understandings of their mechanisms as well.

Acknowledgements

This work was supported by a NASA Earth and Space Sciences Fellowship (NESSF) granted to D.L. Eldridge (NNX12AL77H), NSF grant 1361945: Sulfur isotope studies of sulfide oxidation (J. Farquhar), and the Investment in Science Fund at WHOI (W. Guo). We thank the late John (“Jack”) Tossell for early discussions of aqueous cluster calculations. We additionally thank E.A. Schauble for editorial handling, and three anonymous reviewers for comments and suggestions that greatly improved the presentation in this manuscript.

Appendix A. Supplementary data

Download Word document (1MB)Help with docx files

Supplementary data 1.

Download spreadsheet (289KB)Help with xlsx files

Supplementary data 2.

References

Becke, 1993

A.D. Becke**Density functional thermochemistry: the role of exact exchange**

J. Chem. Phys., 98 (1993), pp. 5648-5652

CrossRefView Record in Scopus

Beyad et al., 2014

Y. Beyad, R. Burns, G. Puxty, M. Maeder**A speciation study of sulfur(iv) in aqueous solution**

Dalton Trans., 43 (2014), pp. 2147-2152

CrossRefView Record in Scopus

Bigeleisen and Mayer, 1947

J. Bigeleisen, M.G. Mayer**Calculation of equilibrium constants for isotopic exchange reactions**

J. Chem. Phys., 15 (1947), pp. 261-267

CrossRefView Record in Scopus

Bowles et al., 2014

M.W. Bowles, J.M. Mogollón, S. Kasten, M. Zabel, K.-U. Hinrichs**Global rates of marine sulfate reduction and implications for sub-sea-floor metabolic activities**

Science, 344 (2014), pp. 889-891

CrossRefView Record in Scopus

Bradley et al., 2011

A.S. Bradley, W.D. Leavitt, D.T. Johnston**Revisiting the dissimilatory sulfate reduction pathway**

Geobiology, 9 (2011), pp. 446-457

CrossRefView Record in Scopus

Brandt and van Eldik, 1995

C. Brandt, R. van Eldik**Transition metal-catalyzed oxidation of sulfur(IV) oxides. Atmospheric-relevant processes and mechanisms**

Chem. Rev., 95 (1995), pp. 119-190

CrossRefView Record in Scopus

Canfield and Teske, 1996

D.E. Canfield, A. Teske**Late Proterozoic rise in atmospheric oxygen concentration inferred from phylogenetic and sulphur-isotope studies**

Nature, 382 (1996), pp. 127-132

CrossRefView Record in Scopus

Canfield et al., 2010

D.E. Canfield, J. Farquhar, A.L. Zerkle**High isotope fractionations during sulfate reduction in a low-sulfate euxinic ocean analog**

Geology, 38 (2010), pp. 415-418

CrossRefView Record in Scopus

Cao and Liu, 2011

X. Cao, Y. Liu**Equilibrium mass-dependent fractionation relationships for triple oxygen isotopes**

Geochim. Cosmochim. Acta, 75 (2011), pp. 7435-7445

ArticleDownload PDFView Record in Scopus

Cao and Liu, 2012

X. Cao, Y. Liu**Theoretical estimation of the equilibrium distribution of clumped isotopes in nature**

Geochim. Cosmochim. Acta, 77 (2012), pp. 292-303

ArticleDownload PDFView Record in Scopus

Chacko et al., 2001

T. Chacko, D.R. Cole, J. Horita**Equilibrium oxygen, hydrogen and carbon isotope fractionation factors applicable to geologic systems**

Rev. Mineral. Geochem., 43 (2001), pp. 1-81

CrossRefView Record in Scopus

Chen and Morris, 1972

K. Chen, J. Morris**Kinetics of oxidation of aqueous sulfide by O_2**

Environ. Sci. Technol., 6 (1972), pp. 529-537

CrossRefView Record in Scopus

Chmielewski et al., 2002

A.G. Chmielewski, M. Derda, R. Wierzchnicki, A. Mikolajczuk**Sulfur isotope effects for the SO_2(g)-SO_2(aq) system**
Nukleonika, 47 (2002), pp. S69-S70
View Record in Scopus

Chu and Ohmoto, 1991

X.-L. Chu, H. Ohmoto**Kinetics of isotope exchange reactions involving intra- and intermolecular reactions: I. Rate law for a system with two chemical compounds and three exchangeable atoms**
Geochim. Cosmochim. Acta, 55 (1991), pp. 1953-1961
View Record in Scopus

Chu et al., 2004

X. Chu, H. Ohmoto, D.R. Cole**Kinetics of sulfur isotope exchange between aqueous sulfide and thiosulfate involving intra- and intermolecular reactions at hydrothermal conditions**
Chem. Geol., 211 (2004), pp. 217-235
ArticleDownload PDFView Record in Scopus

Clayton and Mayeda, 1996

R.N. Clayton, T.K. Mayeda**Oxygen isotope studies of achondrites**

Geochim. Cosmochim. Acta, 60 (1996), pp. 1999-2017
ArticleDownload PDFView Record in Scopus

Cline and Richar
1969

J. Cline, F. Richards**Oxygenation of hydrogen sulfide in seawater at constant salinity, temperature and pH**
Environ. Sci. Technol., 3 (1969), pp. 838-843
CrossRefView Record in Scopus

Connick et al., 19

R.E. Connick, T.M. Tam, E. Von Deuster**Equilibrium constant for the dimerization of bisulfite ion to form disulfite(2-) ion**
Inorg. Chem., 21 (1982), pp. 103-107
CrossRefView Record in Scopus

Crabtree et al., 2

K.N. Crabtree, O. Martinez, L. Barreau, S. Thorwirth, M.C. McCarthy**Microwave detection of sulfoxylic acid (HOSOH)**
J. Phys. Chem. A, 117 (2013), pp. 3608-3613
CrossRefView Record in Scopus

Craig, 1957

H. Craig**Isotopic standards for carbon and oxygen and correction factors for mass-spectrometric analysis of carbon dioxide**
Geochim. Cosmochim. Acta, 12 (1957), pp. 133-149
ArticleDownload PDFView Record in Scopus

Czarnacki and H

M. Czarnacki, S. Hałas**Ab initio calculations of sulfur isotope fractionation factor for H_2S in aqua–gas system**
Chem. Geol., 318–319 (2012), pp. 1-5
ArticleDownload PDFView Record in Scopus

Deines, 2003

P. Deines**A note on intra-elemental isotope effects and the interpretation of non-mass-dependent isotope variations**
Chem. Geol., 199 (2003), pp. 179-182
ArticleDownload PDFView Record in Scopus

Ellis and Giggen

A.J. Ellis, W. Giggenbach**Hydrogen sulphide ionization and sulphur hydrolysis in high temperature solution**
Geochim. Cosmochim. Acta, 35 (1971), pp. 247-260
ArticleDownload PDFView Record in Scopus

Eriksen, 1972a

T.E. Eriksen**Sulfur isotope effects. I. The isotopic exchange coefficient for the sulfur isotopes ^{34}S–^{32}S in the system SO_2g-HSO_3-aq at 25, 35, and 45 °C**
Acta Chem. Scand., 26 (1972), pp. 573-580
CrossRefView Record in Scopus

Eriksen, 1972b

T.E. Eriksen**Sulfur isotope effects. II. The isotopic exchange coefficient for the sulfur isotopes ^{34}S–^{32}S in the system SO_2g-aqueous solutions of SO_2**
Acta Chem. Scand., 26 (1972), pp. 581-584
CrossRef

Eriksen, 1972c

T.E. Eriksen**Sulfur isotope effects. III. Enrichment of ^{34}S by chemical exchange between SO_2g and aqueous solutions of SO_2**
Acta Chem. Scand., 26 (1972), pp. 975-979
CrossRefView Record in Scopus

Falk and Giguere

M. Falk, P.A. Giguere**On the nature of sulphurous acid**
Can. J. Chem., 36 (1958), pp. 1121-1125
CrossRef

Farquhar et al., 2

J. Farquhar, D.T. Johnston, B.A. Wing, K.S. Habicht, D.E. Canfield, S. Airieau, M.H.Thiemens**Multiple sulphur isotopic interpretations of biosynthetic pathways: implications for biological signatures in the sulphur isotope record**
Geobiology, 1 (2003), pp. 27-36
CrossRefView Record in Scopus

Foresman and F

J.B. Foresman, Æ. Frisch**Exploring Chemistry with Electronic Structure Methods**
(second ed.), Gaussian, Inc,, Wallingford, CT (1996)

Frisch et al., 201

M.J. Frisch, G.W. Trucks, H.B. Schlegel, G.E. Scuseria, M.A. Robb, J.R. Cheeseman, G.Scalmani, V. Barone, B. Mennucci, G.A. Petersson, H. Nakatsuji, M. Caricato, X. Li, H.P. Hratchian, A.F.Izmaylov, J. Bloino, G. Zheng, J.L. Sonnenberg, M. Hada, M. Ehara, K. Toyota, R. Fukuda, J. Hasegawa, M. Ishida, T. Nakajima, Y. Honda, O. Kitao, H. Nakai, T. Vreven, J.A. Montgomery Jr., J.E. Peralta, F.Ogliaro, M. Bearpark, J.J. Heyd, E. Brothers, K.N. Kudin, V.N. Staroverov, T. Keith, R. Kobayashi, J.Normand, K. Raghavachari, A. Rendell, J.C. Burant, S.S. Iyengar, J. Tomasi, M. Cossi, N. Rega, J.M.Millam, M. Klene, J.E. Knox, J.B. Cross, V. Bakken, C. Adamo, J. Jaramillo, R. Gomperts, R.E.Stratmann, O. Yazyev, A.J. Austin, R. Cammi, C. Pomelli, J.W. Ochterski, R.L. Martin, K. Morokuma, V.G.Zakrzewski, G.A. Voth, P. Salvador, J.J. Dannenberg, S. Dapprich, A.D. Daniels, Ö. Farkas, J.B.Foresman, J.V. Ortiz, J. Cioslowski, D.J. Fox**Gaussian 09, Revision B.01**
Gaussian Inc., Wallingford, CT (2010)

Fry et al., 1986

B. Fry, H. Gest, J.M. Hayes**Sulfur isotope effects associated with protonation of HS- and volatilization of H2S**

Chem. Geol., 58 (1986), pp. 253-258

ArticleDownload PDFView Record in Scopus

Gerding and Nijv

H. Gerding, W.J. Nijveld**Raman Spectrum of Gaseous and Liquid Sulphur Dioxide and its Solutions in Water**

Nature, 137 (1936)

1070–1070

Geßler and Gehl

R. Geßler, K.V. Gehlen**Investigation of sulfur isotope fractionation between H2S gas and aqueous solutions**

Fresenius' Zeitschrift für Anal. Chem., 324 (1986), pp. 130-136

CrossRefView Record in Scopus

Golding, 1960

R.M. Golding**741. Ultraviolet absorption studies of the bisulphite-pyrosulphite equilibrium**

J. Chem. Soc. (1960), pp. 3711-3716

CrossRefView Record in Scopus

Hermann et al., 2

B. Hermann, M. Kern, L. La Pietra, J. Simon, O. Einsle**The octahaem MccA is a haem c-copper sulfite reductase**

Nature, 520 (2015), pp. 706-709

CrossRefView Record in Scopus

Hershey et al., 1

J.P. Hershey, T. Plese, F.J. Millero**The pK_1* for the dissociation of H_2S in various ionic media**

Geochim. Cosmochim. Acta, 52 (1988), pp. 2047-2051

ArticleDownload PDFView Record in Scopus

Hoffmann and Li

M.R. Hoffmann, B.C. Lim**Kinetics and mechanism of the oxidation of sulfide by oxygen: catalysis by homogeneous metal-phthalocyanine complexes**

Environ. Sci. Technol., 13 (1979), pp. 1406-1414

CrossRefView Record in Scopus

Horner and Conn

D.A. Horner, R.E. Connick**Equilibrium quotient for the isomerization of bisulfite ion from HSO3- to SO3H-**

Inorg. Chem., 25 (1986), pp. 2414-2417

CrossRefView Record in Scopus

Jørgensen, 1977

B.B. Jørgensen**The sulfur cycle of a coastal marine sediment (Limfjorden, Denmark)**
Limnol. Oceanogr., 22 (1977), pp. 814-832
CrossRefView Record in Scopus

Jørgensen, 1982

B.B. Jørgensen**Mineralization of organic matter in the sea bed – the role of sulphate reduction**
Nature, 296 (1982), pp. 643-645
CrossRefView Record in Scopus

Jørgensen, 1990

B.B. Jørgensen**A thiosulfate shunt in the sulfur cycle of marine sediments**
Science, 249 (1990), pp. 152-154
View Record in Scopus

Jørgensen and N

B.B. Jørgensen, D.C. Nelson**Sulfide oxidation in marine sediments: geochemistry meets microbiology**
J.P. Amend, K.J. Edwards, T.W. Lyons (Eds.), Sulfur Biogeochemistry – Past and Present, GSA Special Papers 379 (2004), pp. 63-81
CrossRefView Record in Scopus

Jørgensen et al.,

B.B. Jørgensen, M. Bang, T.H. Blackburn**Anaerobic mineralization in marine-sediments from the Baltic-Sea-North-Sea transition**
Mar. Ecol. Ser., 59 (1990), pp. 39-54
CrossRefView Record in Scopus

Leavitt et al., 201

W.D. Leavitt, I. Halevy, A.S. Bradley, D.T. Johnston**Influence of sulfate reduction rates on the Phanerozoic sulfur isotope record**
Proc. Natl. Acad. Sci. U.S.A., 110 (2013), pp. 11244-11249
CrossRefView Record in Scopus

Lee et al., 1988

C. Lee, W. Yang, R.G. Parr**Development of the Colle–Salvetti correlation-energy formula into a functional of the electron-density**
Phys. Rev. B, 37 (1988), pp. 785-789
CrossRefView Record in Scopus

Li and Liu, 2011

X. Li, Y. Liu**Equilibrium Se isotope fractionation parameters: a first-principles study**
Earth Planet. Sci. Lett., 304 (2011), pp. 113-120
ArticleDownload PDFCrossRefView Record in Scopus

Li et al., 2009

X. Li, H. Zhao, M. Tang, Y. Liu**Theoretical prediction for several important equilibrium Ge isotope fractionation factors and geological implications**
Earth Planet. Sci. Lett., 287 (2009), pp. 1-11
ArticleDownload PDFCrossRefView Record in Scopus

Littlejohn et al., 1992
D. Littlejohn, S.A. Walton, S.-G. Chang**A raman study of the isomers and dimer of hydrogen sulfite ion**
Appl. Spec., 46 (1992), pp. 848-851
CrossRef

Liu et al., 2010
Q. Liu, J.A. Tossell, Y. Liu**On the proper use of the Bigeleisen-Mayer equation and corrections to it in the calculation of isotopic fractionation equilibrium constants**
Geochim. Cosmochim. Acta, 74 (2010), pp. 6965-6983
ArticleDownload PDFView Record in Scopus

Lyons and Nickless, 1968
D. Lyons, G. Nickless**The lower oxy-acids of sulphur**
G. Nickless (Ed.), Inorganic Sulfur Chemistry, Elsevier, New York (1968), pp. 509-534
View Record in Scopus

Makarov et al., 2002
S.V. Makarov, E.V. Kudrik, R. van Eldik, E.V. Naidenko**Reactions of methyl viologen and nitrite with thiourea dioxide. New opportunities for an old reductant**
J. Chem. Soc. Dalton Trans. (2002), pp. 4074-4076
CrossRefView Record in Scopus

Makarov et al., 2010
S.V. Makarov, D.S. Sal'nikov, A.S. Pogorelova**Acid-base properties and stability of sulfoxylic acid in aqueous solutions**
Russ. J. Inorg. Chem., 55 (2010), pp. 301-304
CrossRefView Record in Scopus

Martell and Smith, 1982
A.E. Martell, R.M. Smith**Critical Stability Constants, Volume 5: First Supplement**
Springer Science+Business Media, New York (1982)

Matsuhisa et al., 1978
Y. Matsuhisa, J.R. Goldsmith, R.N. Clayton**Mechanisms of hydrothermal crystallization of quartz at 250 °C and 15 kbar**
Geochim. Cosmochim. Acta, 42 (1978), pp. 173-182
ArticleDownload PDFView Record in Scopus

Migdisov et al., 2002
A.A. Migdisov, A.E. Williams-Jones, L.Z. Lakshtanov, Y.V. Alekhin**Estimates of the second dissociation constant of H2S from the surface sulfidation of crystalline sulfur**

Geochim. Cosmochim. Acta, 66 (2002), pp. 1713-1725
ArticleDownload PDFView Record in Scopus

Miller, 2002

M.F. Miller**Isotopic fractionation and the quantification of 17O anomalies in the oxygen three-isotope system: an appraisal and geochemical significance**
Geochim. Cosmochim. Acta, 66 (2002), pp. 1881-1889
ArticleDownload PDFView Record in Scopus

Millero et al., 1989

F.J. Millero, J.P. Hershey, G. Johnson, J.-Z. Zhang**The solubility of SO_2 and the dissociation of H_2S0_3 in NaC1 solutions**
J. Atmos. Chem., 8 (1989), pp. 377-389
CrossRefView Record in Scopus

Napolion et al., 2008

B. Napolion, M.J. Huang, J.D. Watts**Coupled-cluster study of isomers of H_2SO_2**
J. Phys. Chem. A, 112 (2008), pp. 4158-4164
CrossRefView Record in Scopus

Ohmoto and Lasaga, 1982

H. Ohmoto, A.C. Lasaga**Kinetics of reactions between aqueous sulfates and sulfides in hydrothermal systems**
Geochim. Cosmochim. Acta, 46 (1982), pp. 1727-1745
ArticleDownload PDFView Record in Scopus

Oliveira et al., 2008

T.F. Oliveira, C. Vonrhein, P.M. Matias, S.S. Venceslau, I.A.C. Pereira, M. Archer**The crystal structure of Desulfovibrio vulgaris dissimilatory sulfite reductase bound to DsrC provides novel insights into the mechanism of sulfate respiration**
J. Biol. Chem., 283 (2008), pp. 34141-34149
CrossRefView Record in Scopus

Ono et al., 2007

S. Ono, W.C. Shanks III, O.J. Rouxel, D. Rumble**S-33 constraints on the seawater sulfate contribution in modern seafloor hydrothermal vent sulfides**
Geochim. Cosmochim. Acta, 71 (2007), pp. 1170-1182
ArticleDownload PDFView Record in Scopus

Otake et al., 2008

T. Otake, A.C. Lasaga, H. Ohmoto**Ab initio calculations for equilibrium fractionations in multiple sulfur isotope systems**
Chem. Geol., 249 (2008), pp. 357-376
ArticleDownload PDFView Record in Scopus

Parey et al., 2010

K. Parey, E. Warkentin, P.M.H. Kroneck, U. Ermler**Reaction cycle of the dissimilatory sulfite reductase from archaeoglobus fulgidus**
Biochemistry, 49 (2010), pp. 8912-8921
CrossRefView Record in Scopus

Richet et al., 1977

P. Richet, Y. Bottinga, M. Javoy**A review of hydrogen, carbon, nitrogen, oxygen, sulphur, and chlorine stable isotope fractionation among gaseous molecules**
Ann. Rev. Earth Planet. Sci., 5 (1977), pp. 65-110
CrossRef

Risberg et al., 2007

E.D. Risberg, L. Eriksson, J. Mink, L.G.M. Pettersson, M.Y. Skripkin, M. Sandström**Sulfur X-ray absorption and vibrational spectroscopic study of sulfur dioxide, sulfite, and sulfonate solutions and of the substituted sulfonate ions X3CSO3- (X = H, Cl, F)**
Inorg. Chem., 46 (2007), pp. 8332-8348
View Record in Scopus

Rustad and Bylaska, 2007

J.R. Rustad, E.J. Bylaska**Ab initio calculation of isotopic fractionation in $B(OH)_3$(aq) and BOH_4-(aq)**
J. Am. Chem. Soc., 129 (2007), pp. 2222-2223
CrossRefView Record in Scopus

Rustad et al., 2008

J.R. Rustad, S.L. Nelmes, V.E. Jackson, D.A. Dixon**Quantum-chemical calculations of carbon-isotope fractionation in CO_2(g) aqueous carbonate species, and carbonate minerals**
J. Phys. Chem., 2 (2008), pp. 542-555
CrossRefView Record in Scopus

Rustad et al., 2010

J.R. Rustad, E.J. Bylaska, V.E. Jackson, D.A. Dixon**Calculation of boron-isotope fractionation between B(OH)3(aq) and $B(OH)_4$-(aq)**
Geochim. Cosmochim. Acta, 74 (2010), pp. 2843-2850
ArticleDownload PDFView Record in Scopus

Sakai, 1968

H. Sakai**Isotopic properties of sulfur compounds in hydrothermal processes**
Geochem. J., 2 (1968), pp. 29-49
CrossRefView Record in Scopus

Santos et al., 2015

A.A. Santos, S.S. Venceslau, F. Grein, W.D. Leavitt, C. Dahl, D.T. Johnston, I.A.C. Pereira**A protein trisulfide couples dissimilatory sulfate reduction to energy conservation**
Science, 350 (2015), pp. 1541-1545
CrossRefView Record in Scopus

Schauble, 2004

E.A. Schauble**Applying Stable Isotope Fractionation Theory to New Systems**

Rev. Mineral. Geochem., 55 (2004), pp. 65-111

CrossRefView Record in Scopus

Schoonen and Barnes, 1988

M.A.A. Schoonen, H.L. Barnes**An approximation of the second dissociation constant for hydrogen sulfide**

Geochim. Cosmochim. Acta, 52 (1988), pp. 649-654

ArticleDownload PDFView Record in Scopus

Sim et al., 2011a

M.S. Sim, T. Bosak, S. Ono**Large sulfur isotope fractionation does not require disproportionation**

Science, 333 (2011), pp. 74-77

CrossRefView Record in Scopus

Sim et al., 2011b

M.S. Sim, S. Ono, K. Donovan, S.P. Templer, T. Bosak**Effect of electron donors on the fractionation of sulfur isotopes by a marine *Desulfovibrio* sp.**

Geochim. Cosmochim. Acta, 75 (2011), pp. 4244-4259

ArticleDownload PDFView Record in Scopus

Steiger and Steudel, 1992

T. Steiger, R. Steudel**Sulfur-compounds. 149. Structures, relative stabilities and vibrational-spectra of several isomeric forms of sulphoxylic acid (H_2SO_2) and its anion (HSO_{2^-})- An ab initio study**

J. Mol. Struct. Thermochem., 257 (1992), pp. 313-323

ArticleDownload PDFView Record in Scopus

Steudel and Prenzel, 1989

R. Steudel, A. Prenzel**Raman spectroscopic discovery of the hydrogenthiosulphate anion, $HSSO_3$-, in solid $NH_4HS_2O_3$**

Z. Naturforsch., B: Chem., 44 (1989), pp. 1499-1502

View Record in Scopus

Steudel and Steudel, 2009

R. Steudel, Y. Steudel**Microsolvation of thiosulfuric acid and its tautomeric anions [HSSO 3]- and [SSO2(OH)]- studied by B3LYP-PCM and G3X(MP2) calculations**

J. Phys. Chem. A, 113 (2009), pp. 9920-9933

CrossRefView Record in Scopus

Svarovsky et al., 2001

S.A. Svarovsky, R.H. Simoyi, S.V. Makarov**A possible mechanism for thiourea-based toxicities: kinetics and mechanism of decomposition of thiourea dioxides in alkaline solutions**

J. Phys. Chem. B, 105 (2001), pp. 12634-12643
CrossRefView Record in Scopus

Syverson et al., 2015
D.D. Syverson, S. Ono, W.C. Shanks, W.E. Seyfried**Multiple sulfur isotope fractionation and mass transfer processes during pyrite precipitation and recrystallization: an experimental study at 300 and 350°C**
Geochim. Cosmochim. Acta, 165 (2015), pp. 418-434
ArticleDownload PDFView Record in Scopus

Szaran, 1996
J. Szaran**Experimental investigation of sulphur isotopic fractionation between dissolved and gaseous H_2S**
Chem. Geol., 127 (1996), pp. 223-228
ArticleDownload PDFView Record in Scopus

Tossell, 1997
J.A. Tossell**Theoretical studies on possible sulfur oxides with +2 oxidation states in aqueous solution**
Chem. Geol., 141 (1997), pp. 93-103
ArticleDownload PDFView Record in Scopus

Urey, 1947
H.C. Urey**The thermodynamic properties of isotopic substances**
J. Chem. Soc. (Lond.) (1947), pp. 562-581
CrossRefView Record in Scopus

Uyama et al., 1985
F. Uyama, H. Chiba, M. Kusakabe, H. Sakai**Sulfur isotope exchange reactions in the aqueous system: thiosulfate-sulfide-sulfate at hydrothermal temperature**
Geochem. J., 19 (1985), pp. 301-315
CrossRefView Record in Scopus

Vairavamurthy and Zhou, 1995
M.A. Vairavamurthy, W. Zhou**Characterization of a transient +2 sulfur oxidation state intermediate from the oxidation of aqueous sulfide**
M.A. Vairavamurthy, M.A.A. Schoonen (Eds.), Geochemical Transformations of Sedimentary Sulfur, American Chemical Society, Washington, DC (1995), pp. 280-292
CrossRef

Vairavamurthy et al., 1993
A. Vairavamurthy, B. Manowitz, G.W. Luther, Y. Jeon**Oxidation-state of sulfur in thiosulfate and implications for anaerobic energy-metabolism**
Geochim. Cosmochim. Acta, 57 (1993), pp. 1619-1623
ArticleDownload PDFView Record in Scopus

Voegele et al., 2004

A.F. Voegele, C.S. Tautermann, T. Loerting, K.R. Liedl**On the formation of the sulfonate ion from hydrated sulfur dioxide**
J. Phys. Chem., 108 (2004), pp. 3859-3864
CrossRefView Record in Scopus

Williamson and Rimstidt, 1992

M.A. Williamson, J.D. Rimstidt**Correlation between structure and thermodynamic properties of aqueous sulfur species**
Geochim. Cosmochim. Acta, 56 (1992), pp. 3867-3880
ArticleDownload PDFView Record in Scopus

Wing and Halevy, 2014

B.A. Wing, I. Halevy**Intracellular metabolite levels shape sulfur isotope fractionation during microbial sulfate respiration**
Proc. Natl. Acad. Sci. U.S.A., 111 (2014), pp. 18116-18125
CrossRefView Record in Scopus

Wolfsberg et al., 2010

M. Wolfsberg, W.A. Van Hook, P. Paneth, L.P.N. Rebelo**Isotope Effects in the Chemical, Geological, and Bio Sciences**
Springer, New York (2010)

Yiin et al., 1987

B.S. Yiin, D.M. Walker, D.W. Margerum**Non-metal redox kinetics general-acid-assisted reactions of chloramine with sulfite and hydrogen sulfite**
Inorg. Chem., 26 (1987), pp. 3435-3441
CrossRefView Record in Scopus

Young et al., 2002

E.D. Young, A. Galy, H. Nagahara**Kinetic and equilibrium mass-dependent isotope fractionation laws in nature and their geochemical and cosmochemical significance**
Geochim. Cosmochim. Acta, 66 (2002), pp. 1095-1104
ArticleDownload PDFView Record in Scopus

Zachariasen, 1932

W.H. Zachariasen**The crystal lattice of potassium pyrosulphite, $K_2S_2O_5$, and the structure of the pyrosulphite group**
Phys. Rev., 40 (1932), p. 923
CrossRef

Zeebe, 2009

R.E. Zeebe**Hydration in solution is critical for stable oxygen isotope fractionation between carbonate ion and water**
Geochim. Cosmochim. Acta, 73 (2009), pp. 5283-5291
ArticleDownload PDFView Record in Scopus

Zhang and Ewing, 2002

Z. Zhang, G.E. Ewing**Infrared spectroscopy of SO2 aqueous solutions**
Spectrochim. Acta, Part A, 58 (2002), pp. 2105-2113
ArticleDownload PDFView Record in Scopus

Zhang and Millero, 1993

J.-Z. Zhang, F.J. Millero**The products from the oxidation of H2S in seawater**
Geochim. Cosmochim. Acta, 57 (1993), pp. 1705-1718
ArticleDownload PDFView Record in Scopus

Zopfi et al., 2004

J. Zopfi, T.G. Ferdelman, H. Fossing**Distribution and fate of sulfur intermediates-sulfite, tetrathionate, thiosulfate, and elemental sulfur-in marine sediments**
J.P. Amend, K.J. Edwards, T.W. Lyons (Eds.), Sulfur Biogeochemistry – Past and Present, GSA Special Papers 379 (2004), pp. 97-116
CrossRefView Record in Scopus